PROCESS NMR ASSOCIATES, LLC

Technical White Paper Series

Quantitative ^{1}H NMR of Beer

A Single-Experiment Chemical Fingerprint for Component Quantification, Residual Dextrin Architecture, and Process Understanding

John C. Edwards, Ph.D.

Process NMR Associates, LLC

84 Patrick Lane, Suite 115, Poughkeepsie, NY 12603

www.process-nmr.com

Document Details

Field	Entry
Filename	PNA_White_Paper_qNMR_of_Beer_v1.1.docx
Version	1.1 — AI-assisted framework prepared for author augmentation with primary PNA data. This revision adds the traditional brewing-parameter formalism (Section 5.7), the expanded sour beer, barrel aging, and glycerol conversion chemistry (Sections 7.2 and 7.3), and the systematic preservative and additive treatment with the flavored-malt-beverage survey data (Section 7.5)
Generation date	August 20, 2026 (v1.0); August 23, 2026 (v1.1)
Drafting model	claude-opus-5 (v1.0) and claude-fable-5 (v1.1 revision), as configured for the generating sessions; the model actually serving a given turn may differ and is not independently observable
Reasoning effort	Not declared by the author for this document; not observable by the drafting system and therefore not asserted
Primary source material	Four Process NMR Associates presentations supplied by the author: World Brewing Congress 2016 poster No. 77 (Denver, CO); Bell's Brewery technical seminar, Comstock, MI, October 12, 2018; American Chemical Society Mid-Hudson Section meeting, Vassar College, Poughkeepsie, NY, February 11, 2019; Master Brewers Certificate Program, University of California, Davis, April 28, 2022
Tools engaged	CrossRef REST and OpenURL metadata services (reference verification); Anthropic web search and retrieval (literature discovery); poppler-utils (source-deck text and image extraction); ImageMagick (figure preparation); Node.js with docx 9.6.1 (document assembly); LibreOffice (PDF rendering and pagination check)
Reference status	Seventy-one references, each resolved against CrossRef prior to drafting; the six references added for v1.1 were verified by the same protocol. Three DOIs carried in earlier Process NMR Associates material were found to be incorrect and have been corrected here (see Section 10.4)
AI-assistance statement	The narrative background, literature synthesis, spectral-region organization, tabulated assignment and response-factor data, algebraic development of the quantitation and dextrin-structure formalisms, arithmetic worked examples, and document architecture were drafted with AI assistance and verified against the cited primary literature. All experimental spectra, chromatograms, concentration data, hop assays, mash trials, and commercial-beer survey results reproduced herein were generated at Process NMR Associates, LLC by the author. Interpretive conclusions, brewing-process judgments, and any recommendation offered to a client remain the responsibility of the author.

Abstract

A single quantitative ^{1}H NMR experiment performed on a degassed beer sample resolves and quantifies, without compound-specific calibration, the ethanol and higher alcohols, the fermentation-derived organic acids, the free amino acids and nucleotides, the esters and diols, the Maillard and polyphenolic aromatics, the aldehydic staling markers, and — uniquely among routine brewery methods — the structural distribution of the residual α-glucan dextrins that survive mashing and fermentation. The present white paper develops that proposition in full, using data acquired at Process NMR Associates on commercial beers, worts, mashes, malt extracts, hops, and non-alcoholic products over roughly a decade of method development. The quantitation scheme is presented in complete algebraic form, including the dual-aliquot design in which a 175 µL native-beer sample carries the volatile inventory while a lyophilized 1000 µL aliquot carries the non-volatile inventory at reduced water and ethanol background; the maleic acid internal standard formalism is reduced to two simple response factors, and a worked example is carried through to a verified ethanol concentration. Regions of the spectrum are treated in sequence, with tabulated chemical shifts, multiplicities, coupling constants, proton counts, and per-integral response factors supplied in a form suitable for direct transcription into a laboratory integration template. The residual dextrin section forms the core of the document: the anomeric window between δ 4.4 and 5.5 is dissected into the α-(1→4) linear envelope, the near-branch envelope, the α-(1→6) branch-point signal, the reducing-end α and β pair, and the free-glucose anomers, and the four-window integral scheme used at Process NMR Associates is compared point by point against degrees of polymerization determined independently by diffusion-ordered spectroscopy in the published literature, with which it agrees in ordering and at its high-frequency anchor while remaining uncalibrated at its branch-proximal end. From these integrals, expressions for number-average degree of polymerization, α-(1→6) branch fraction, dextrose equivalent, and the fermentable-to-non-fermentable ratio are derived and worked through numerically. Two internal consistency checks not previously exploited in this laboratory are introduced. Because the α and β anomers of a reducing terminus are held at a fixed mutarotation equilibrium, the measured α:β ratio at the reducing end and at free glucose provides a direct, sample-by-sample audit of integration accuracy across the anomeric window, and its application to the mash series reported here identifies a systematic bias in every sample and an outright integration fault in one. Separately, the requirement that the residue count equal the chain count plus the linkage count supplies a mass-balance closure that any correct set of anomeric integrals must satisfy. A further finding of the methodological work is that the ten milligrams of maleic acid used as internal standard amounts to 133 millimolar in the analytical solution and fixes every preparation near pH 1.5, so that the organic acids are observed at their fully protonated limits and at positions independent of the pH of the beer — an effect that explains the observed chemical shifts, makes fixed integration windows safe across styles, and simultaneously rules out any attempt to infer concentration from peak position. The measured composition is translated into the traditional vocabulary of the brewhouse through the Balling mass balance: original extract, apparent and real extract, original and final gravity, and the apparent and real degrees of fermentation are recovered from the ethanol and dissolved-solids determinations alone, worked through to 11.94 °P, 77.1 percent, and 63.2 percent for a representative lager, and a wort-side fermentability prediction is shown to reproduce the information content of the forced-fermentation attenuation-limit test. Process case studies follow: the temperature dependence of biological mash acidification, in which the traditional 49 °C sour-mash hold is shown to optimize the lactic-to-acetic acid balance rather than the absolute lactic acid yield; the carbohydrate consequences of turbid mashing in a New England India pale ale; mixed-culture and Brettanomyces fermentations, developed through the phase structure of spontaneous lambic

fermentation, the mannitol–acetate redox coupling of heterofermentative metabolism, and the chemistry of the barrel, where oxygen ingress, the slow esterification clock of ethyl lactate, and wood-derived cellobiose each leave a spectroscopic record; the glycerol conversion pathway in full, from the coenzyme-B_{12}-dependent dehydration through 1,3-propanediol and 3-hydroxypropionic acid to the acrolein chemistry that underlies the amertume defect and the distillation hazard of degraded substrates; non-alcoholic and low-alcohol products, for which ethanol was quantified down to 0.01 % v/v and total calorie and carbohydrate declarations reproduced to better than one unit; hop α-acid, β-acid, and terpene assay by ^{1}H NMR against a modified American Society of Brewing Chemists chromatographic reference; and a systematic treatment of preservatives, additives, and sweeteners, in which sorbate, benzoate, citrate, propylene glycol, and back-sweetening sugars are quantified and steviol glycosides identified across a flavored-malt-beverage survey, and the internal consistency of a product formulation is tested from a single spectrum. A candid assessment of systematic error is given, in which the interaction of the 60° excitation pulse, the 15 s recycle period, and the spin–lattice relaxation times of the internal standard and of slowly relaxing analytes such as formate is quantified explicitly and shown to be the dominant uncorrected bias in the present protocol. The document closes with the design of the spectral library, preprocessing chain, and validation discipline required to carry this data set into the chemometric and machine-learning treatment for which it is intended.

Table of Contents

Abstract **3**
1. Introduction **10**
1.1 The Analytical Problem in a Brewery Laboratory 10
1.2 What a Single Proton Spectrum Contains 10
1.3 Scope and Provenance of the Data Presented 11
2. Why Quantitative NMR Differs from the Rest of the Brewery Laboratory **12**
2.1 The Primary-Ratio Argument 12
2.2 Linearity, Dynamic Range, and the Absence of Response Factors 12
2.3 What Is Given Up in Exchange 13
3. The Process NMR Associates Beer qNMR Method **14**
3.1 Degassing and the Dual-Aliquot Design 14
3.2 The Native-Beer Aliquot 14
3.3 The Lyophilized Aliquot 15
3.4 The Internal Standard 15
3.4.1 A Consequence Not Previously Recognized: the Standard Fixes the pH 15
3.5 Acquisition 16
3.6 The Quantitation Expressions 17
3.7 A Worked Example 18
3.8 Relaxation, Flip Angle, and the Principal Systematic Risk 18
3.9 The Ethanol ^{13}C Satellite Problem 21
3.10 Uncertainty Budget 21
4. Reading the Spectrum: Region by Region **23**
4.1 The Global View 23
4.2 Pure-Component Spectra as the Basis of Assignment 25
4.3 The High-Field Region: δ 0.8 to 1.8 28
4.4 The Mid-Field Region: δ 1.8 to 3.2 31
4.5 The Carbohydrate Bulk Region: δ 3.2 to 4.4 32
4.6 The Anomeric Region: δ 4.4 to 5.5 33
4.7 The Aromatic, Nucleoside, and Maillard Region: δ 5.5 to 9.8 33
4.8 Two-Dimensional Support 36
4.9 The Working Response-Factor Table 37
5. What the Numbers Say: A Survey of Commercial Beers **39**
5.1 Ethanol 40
5.2 Organic Acids 41
5.3 Amino Acids and Yeast-Assimilable Nitrogen 43
5.4 Higher Alcohols, Esters, and Diols 45
5.5 Nutritional Bookkeeping 46
5.6 Other Nuclei 48

5.7 Traditional Brewing Parameters from the NMR Composition 48
6. Residual Dextrin Chemistry **51**
6.1 Where Limit Dextrins Come From 51
6.2 The Anomeric Fingerprint of Finished Beer 52
6.3 The Four-Window Integral Scheme 55
6.4 Independent Corroboration of the Chain-Length Assignments 58
6.5 Reducing-End Bookkeeping and the Anomeric-Ratio Internal Check 59
6.6 Structural Parameters 61
6.7 A Worked Example 62
6.8 The Commercial Survey 63
6.9 Malt and Hot-Water Extract Survey 64
6.10 Turbid Mashing: a New England India Pale Ale Case Study 65
6.11 Interferents and Look-Alikes 68
6.12 What the Present Data Cannot Yet Support 69
6.13 Extensions: Heteronuclear, Homodecoupled, and Diffusion Methods 70
7. Process and Product Case Studies **70**
7.1 Biological Acidification of the Mash 71
7.2 Sour Beer, Mixed-Culture Fermentation, and Barrel Aging 73
7.3 The Glycerol Conversion Pathway: 1,3-Propanediol, 3-Hydroxypropionic Acid, and the Acrolein Question 76
7.4 Non-Alcoholic and Low-Alcohol Products 78
7.5 Preservatives, Additives, Sweeteners, and Label Chemistry 81
7.6 Hops: α-Acids, β-Acids, and Terpenes 86
7.7 Diastatic Contamination and Package Stability 90
7.8 Benchtop and At-Line Implementation 90
8. From Spectra to Models: the Chemometric and Machine-Learning Roadmap **91**
8.1 Two Data Matrices, Not One 91
8.2 Preprocessing 91
8.3 Unsupervised Structure First 93
8.4 Supervised Models and the Validation Discipline 93
8.5 Where Machine Learning Earns Its Place — and Where It Does Not 93
8.6 Designing the Library 94
9. Limitations and What the Method Does Not See **94**
10. Conclusions **95**
10.1 What the Method Delivers 95
10.2 What This Study Adds 96
10.3 The Immediate Experimental Priorities 96
10.4 Corrections to Reference Material 96
References **98**
Summary **103**

Figures

Figure 1. Superimposed ^{1}H spectra of thirty commercial beers — the global view 24
Figure 2. Pure-component spectra of fermented-beverage constituents 26
Figure 3. Reporter chemical shifts for the principal quantified species 27
Figure 4. Organic acid, alcohol, and amino acid region — twenty-three beers 29
Figure 5. Aromatic amino acid, nucleotide, and Maillard region — thirty beers 34
Figure 6. Two-dimensional J-resolved spectrum of a lyophilized Scottish ale 37
Figure 7. Alcoholic strength by qNMR against label declaration 41
Figure 8. Organic acid distribution across twenty-three commercial beers 42
Figure 9. Free amino acid and nucleoside distribution 44
Figure 10. Pure-component amino acid spectra 45
Figure 11. Energy content per serving, resolved by contributing class 47
Figure 12. Amylolysis and the origin of branched limit dextrins 52
Figure 13. Anomeric region of twenty-three commercial beers — the dextrin atlas 53
Figure 14. Wort after cooling against finished beer — the anomeric region 58
Figure 15. α-(1→4) glucan distribution across twenty-three commercial beers 64
Figure 16. Hot-water extracts of a malt series 65
Figure 17. Standard mash against turbid mash — anomeric region 66
Figure 18. Carbohydrate quantities for the New England India pale ale mash trial 67
Figure 19. Sour mash spectra across the souring temperature series 71
Figure 20. Metabolite mass fraction against souring temperature 72
Figure 21. Effect of Brettanomyces and bacterial activity on sour beer 73
Figure 22. Barrel-aged, malolactic, dry, and back-sweetened ciders compared 76
Figure 23. The glycerol conversion pathway in sidra, with authentic standard 78
Figure 24. Non-alcoholic malt beverage — full analysis against declaration 79
Figure 25. Six non-alcoholic and low-alcohol products with qNMR strength 80
Figure 26. Preservative screening across nine flavored malt beverages 83
Figure 27. Fully annotated hard seltzer spectrum — additives and carriers 83
Figure 28. ^{1}H spectra of a hop series in $CDCl_3$ 87
Figure 29. Hop bitter acid analysis by chromatography and by NMR 88

Tables

Table 1. Quantitative ^{1}H NMR compared with the conventional analytical panel 13
Table 2. Acquisition and preparation parameters 17
Table 3. Relaxation response and bias at 60° flip angle and 15 s recycle 19
Table 4. Indicative uncertainty budget 21
Table 5. Constituent classes of beer and their NMR observability 24
Table 6. ^{1}H assignments, δ 0.8 to 1.8 29
Table 7. ^{1}H assignments, δ 1.8 to 3.2 31

Table 8. ^{1}H assignments, δ 5.5 to 9.8 35
Table 9. Response factors for the Process NMR Associates beer panel 38
Table 10. Energy factors and nutritional declaration values 39
Table 11. Traditional brewing parameters from the qNMR composition 50
Table 12. Assignments in the anomeric region of lyophilized beer 54
Table 13. The four-window α-(1→4) integration scheme 55
Table 14. Structural parameters for the four mash samples 62
Table 15. Interferents in the anomeric region and their discrimination 68
Table 16. Non-alcoholic and low-alcohol products against declaration 80
Table 17. Additives and sweeteners in eight flavored malt beverages 84
Table 18. Hop composition by ^{1}H NMR 88
Table 19. Recommended preprocessing chain for the beer spectral matrix 92

1. Introduction

1.1 The Analytical Problem in a Brewery Laboratory

Beer is, by any reasonable measure, one of the most compositionally intricate liquids that is subjected to routine industrial quality control. Beyond water and ethanol there remains a dissolved solute burden of roughly twenty to fifty grams per liter, distributed across carbohydrates of every degree of polymerization from glucose to the residual branched dextrins, the fermentation-derived organic acids, free amino acids and small peptides, nucleosides and nucleotides, glycerol and the vicinal diols, higher alcohols and their acetate esters, hop-derived bitter acids and their oxidation products, cereal β-glucans and arabinoxylans, polyphenols, and the Maillard products generated during kilning and boiling. Individual constituent concentrations span more than five orders of magnitude within a single sample.

The conventional response to that complexity has been to fragment it. Density measurement or near-infrared correlation supplies alcohol and real extract; high-performance liquid chromatography with refractive-index or pulsed-amperometric detection supplies the individual sugars; a second chromatographic configuration, usually with an ion-exclusion column and ultraviolet detection, supplies the organic acids; enzymatic kits supply individual metabolites one at a time; headspace gas chromatography supplies the volatiles; ninhydrin colorimetry supplies free amino nitrogen; and a dedicated iso-octane extraction with ultraviolet absorbance at 275 nm supplies bitterness units. Each determination answers a narrow question well. Each requires its own calibration curve, its own certified standards, its own column chemistry and mobile phase, its own aliquot, and its own analyst time, and the aggregate composition is then assembled from a dozen separate measurements made on a dozen separate portions of a sample that no longer exists in its original state.[19]

The cost of that fragmentation is not only economic. It is also epistemic. Because the determinations are independent, they cannot be reconciled against one another; there is no mass balance, no internal consistency check, and no way to notice that the carbohydrate result and the attenuation result are mutually incompatible. Nor does the fragmented approach record anything about the sample that was not asked for in advance. A beer that has gone wrong in an unanticipated way is invisible to a battery of targeted assays, because none of them was pointed at the compound responsible.

1.2 What a Single Proton Spectrum Contains

Nuclear magnetic resonance spectroscopy offers a fundamentally different proposition, and the difference is worth stating plainly rather than as a marketing claim. Every hydrogen nucleus in the sample that is not exchanged into the deuterium reservoir contributes to the spectrum, and it contributes an integrated area that is strictly proportional to the number of such nuclei present, with a proportionality constant that is identical for every proton in the sample regardless of its chemical environment. There is no response factor. There is no extinction coefficient, no detector-specific sensitivity, no ionization efficiency, and no need for an authentic standard of the analyte in order to determine how much of it is present. A single reference compound of known mass, added to the tube, calibrates the entire spectrum simultaneously.[18,30]

What follows from this is that one acquisition, lasting a quarter of an hour, yields a quantitative inventory of the sample rather than an answer to a question. The inventory is simultaneously targeted, in that named compounds may be integrated and reported in milligrams per liter, and untargeted, in that the entire digitized spectrum is retained and can be interrogated later for compounds that were of no interest at the time of

measurement. The spectrum is, in this sense, an archival object: a beer analyzed in 2016 can be re-examined in 2026 for a component whose significance was not recognized when the sample was run. That property is what makes the technique a natural substrate for multivariate and machine-learning treatment, and it is the reason the present document has been organized to feed that treatment. The claim is not rhetorical: molecular profiles have been recovered by NMR from beers brewed between one hundred and ten and one hundred and thirty years ago, and read for what they reveal about brewing practice in the late nineteenth century.[27]

The application of high-resolution NMR to beer was placed on a systematic footing in the early 2000s by Gil and co-workers at Aveiro, whose 500 MHz survey of ale and lager production combined ^{1}H spectroscopy with principal component analysis and established the assignment framework on which almost all subsequent work has rested,[1] and by the Carlsberg laboratory, which demonstrated that organic and amino acids in beer could be quantified by NMR with precision competitive against the enzymatic and chromatographic reference methods then in use.[3] The intervening two decades have produced validated quantitative protocols,[5] automated profiling platforms covering more than eighty beer metabolites,[6] a substantial style-discrimination and authentication literature,[7,12,13,14,15,16,21,24,25,26] and a specialized body of carbohydrate work centered on the Carlsberg and Technical University of Denmark groups that has resolved the beer oligosaccharide and limit-dextrin series in unprecedented structural detail.[38,39,40,41,42]

1.3 Scope and Provenance of the Data Presented

This white paper is broad by intention. It sets out to describe everything in beer that proton NMR can be made to report on, how each observation is converted into a number, what that number means in process terms, and where the method is weaker than its advocates usually admit. The experimental material reproduced here was generated at Process NMR Associates over roughly a decade and was presented in four venues: a poster at the World Brewing Congress in Denver in 2016, a technical seminar at Bell's Brewery in Comstock, Michigan, in October 2018, a lecture to the Mid-Hudson Section of the American Chemical Society at Vassar College in February 2019, and a lecture to the Master Brewers Certificate Program at the University of California, Davis, in April 2022. The commercial-beer survey, the mash and wort trials, the sour-mash temperature study, the non-alcoholic beer series, and the hop assays are all drawn from that body of work. One published account of the sour-mash study exists in the peer-reviewed literature.[28]

A deliberate emphasis has been placed on the residual dextrin fraction. That emphasis reflects both the author's current analytical interest and an objective judgment about where the technique is least replaceable: the branched α-limit dextrins are the majority of the non-volatile carbohydrate in most finished beers, they govern real extract, body, calorie content, and the risk posed by diastatic contamination, and they are effectively invisible to the sugar-by-sugar chromatographic methods used in most breweries, which resolve glucose through maltotetraose and then report everything beyond as an undifferentiated lump. Section 6 accordingly develops the anomeric region of the spectrum in detail, derives the structural parameters obtainable from it, and — equally importantly — states which of those parameters the present data can support and which cannot yet be defended.

The document is issued as a framework. Sections in which the author's primary concentration tables, replicate statistics, and additional dextrin data are to be inserted are marked as such. Reference numbers appear as superscripts in the body and correspond to the numbered list beginning on page 98; every entry

in that list was resolved against the CrossRef registry before drafting began, and the three errors found in earlier Process NMR Associates reference material are itemized in Section 10.4.

2. Why Quantitative NMR Differs from the Rest of the Brewery Laboratory

2.1 The Primary-Ratio Argument

The claim that quantitative NMR is a primary ratio method deserves to be unpacked, because it is frequently asserted and rarely justified. A primary method of measurement is one whose result is obtained directly in terms of base units without reference to a standard of the same quantity being measured. In quantitative ^{1}H NMR the measured quantity is an integrated signal area, and the relationship between that area and the amount of substance is

$$I = k \cdot N \cdot n \tag{1}$$

in which I is the integrated area, N the number of chemically equivalent protons giving rise to the signal, n the amount of substance in the active volume, and k a constant of the instrument and the acquisition. The crucial point is that k contains no molecular parameter. It depends on the magnetic field, the probe, the receiver gain, and the pulse sequence, but not on the identity of the molecule under observation. Taking the ratio of the analyte signal to that of a reference compound weighed into the same tube therefore eliminates k entirely, leaving

$$n_a / n_{ref} = (I_a / N_a) \cdot (N_{ref} / I_{ref}) \tag{2}$$

and the analyte amount follows from the reference mass, the reference molar mass, and the reference purity alone. No standard of the analyte is required, has ever been required, or would improve the result. This is what is meant when the technique is described as calibration-free, and it is why certified reference materials themselves are increasingly value-assigned by quantitative NMR rather than by chromatography.[30]

2.2 Linearity, Dynamic Range, and the Absence of Response Factors

Two practical consequences follow. The first is that the integrated area is proportional to concentration over the entire range for which signal can be observed, without the curvature and saturation familiar from ultraviolet absorbance at high optical density or from mass spectrometric ion sources at high analyte flux. The proportionality constant is not necessarily the ideal one — incomplete relaxation scales it, as Section 3.8 quantifies — but it is a constant, and a multiplicative scale error is a different and far more tractable defect than a nonlinear response. Ethanol has been quantified in the work reported here from 0.01 % v/v in a nominally alcohol-free lager to values above 10 % in barley wines and to far higher values in distillates, on the same calibration, in the same experiment, with no dilution series and no change of method. The second is that a compound never previously encountered can be quantified the moment its structure is recognized, because the only compound-specific information required is the molar mass and the number of protons contributing to the integrated multiplet. Both are known from the structure.

Against this must be set the honest limitation. NMR is an insensitive technique. The practical limit of detection for a well-resolved singlet at 300 MHz with sixty-four transients is of the order of one to a few milligrams per liter, which places the vicinal diketones, the sulfur volatiles, most of the trace esters, and the

individual iso-α-acids in finished beer below the threshold of one-dimensional quantitation. Higher field, cryogenically cooled probes, longer acquisition, sample concentration by lyophilization, or two-dimensional methods each recover part of that ground, but the fundamental sensitivity gap relative to mass spectrometry does not close. The correct posture is that NMR replaces the majority of the routine composition panel and complements rather than displaces gas chromatography with mass spectrometric or sulfur-selective detection for the trace volatiles.

2.3 What Is Given Up in Exchange

Three further trade-offs should be acknowledged before the method is described. Signal overlap, not sensitivity, is the dominant analytical constraint in beer, and it is most acute in the carbohydrate massif between δ 3.2 and 4.4 where every glucose ring proton in the sample contributes to a single unresolvable envelope. The chemical shifts of the organic acids move appreciably with pH, and beer sits on the steep portion of several titration curves, which means that peak positions are not fixed landmarks but composition-dependent variables — a nuisance for automated integration and, as will be seen, an opportunity for concentration determination by a different route.[8] And the instrument is expensive: a superconducting spectrometer represents a capital commitment that no small brewery will make, which is why the model that has proven workable in practice is a specialist service laboratory receiving samples from many producers rather than an instrument in every brewhouse.

Table 1. Comparison of quantitative ^{1}H NMR with the conventional analytical panel applied to beer.

Attribute	Quantitative ^{1}H NMR	Conventional panel (HPLC, GC, enzymatic, densitometric)
Calibration	One reference compound calibrates all analytes simultaneously; no analyte standards required	Separate multi-point calibration and certified standard for every analyte
Response factor	Identical for every proton; determined by structure alone	Analyte- and detector-specific; must be measured
Linearity	Strictly linear over the full observable range	Range-limited; dilution or re-calibration commonly required
Analytes per run	Entire soluble hydrogen-bearing inventory in one acquisition	One class per run; several instruments and configurations
Sample preparation	Degassing, addition of standard and D_2O; optional lyophilization	Filtration, extraction, derivatization, distillation depending on assay
Sample consumption	0.2–1.0 mL; sample recoverable	Consumed; multiple aliquots
Consumables and waste	D_2O and an NMR tube; no solvent stream	Mobile phases, columns, cartridges, reagent kits, solvent waste
Untargeted capability	Complete; full spectrum archived for later interrogation	None; only what was calibrated is seen
Structural information	Direct — connectivity, linkage, anomeric configuration, branching	Indirect, by retention time against a standard
Limit of detection	≈1–5 mg/L for a resolved singlet at 300 MHz, 64 transients	µg/L to ng/L depending on detector
Dominant limitation	Signal overlap and sensitivity	Scope — only pre-selected analytes are measured

Attribute	Quantitative ^{1}H NMR	Conventional panel (HPLC, GC, enzymatic, densitometric)
Capital cost	High (superconducting spectrometer)	Moderate per instrument, high in aggregate for full panel

Detection limits quoted for NMR refer to one-dimensional quantitation on the instrumentation described in Section 3.5; cryoprobe and higher-field configurations improve them by roughly an order of magnitude.

3. The Process NMR Associates Beer qNMR Method

3.1 Degassing and the Dual-Aliquot Design

Carbonation is the first obstacle. Beer at packaging carries of the order of five grams of dissolved carbon dioxide per liter, and the pressure release that accompanies transfer into a 5 mm tube nucleates bubbles that destroy the field homogeneity established by shimming and that continue to evolve throughout the acquisition. Decarbonation is therefore mandatory rather than optional, and in the work reported here it has been accomplished by repeated agitation on a vortex mixer until effervescence ceases.

The method as practiced does not analyze a single preparation. Two aliquots are taken from the same degassed sample and are analyzed separately, and the reason for the division is more interesting than the conventional statement of it. The stated rationale has been that lyophilization compromises the volatile inventory, so that ethanol, methanol, acetic acid, ethyl acetate, and the fusel alcohols must be measured on native beer. That is correct as far as it goes. The stronger argument, and the one that should be made explicitly in any method validation package, concerns dynamic range. Freeze-drying removes the water and the bulk of the ethanol before the sample is redissolved in deuterium oxide, which collapses the two largest signals in the spectrum and, with them, the two largest sources of interference. The anomeric region that carries the entire dextrin structural argument lies immediately beside the water resonance and is unusable when a proton reservoir of some thirty molar sits at δ 4.79 in the diluted native preparation, and of more than a hundred molar in beer itself; the lactate methyl doublet at δ 1.41 lies directly beneath the high-frequency ^{13}C satellite of the ethanol methyl triplet and cannot be integrated honestly in the presence of undiminished ethanol. The lyophilized aliquot exists in order to make the non-volatile inventory measurable, not merely in order to concentrate it.

A concentration factor is obtained as a by-product. One milliliter of degassed beer is lyophilized and the residue redissolved in a total of 750 µL, so that non-volatile analytes are presented to the receiver at roughly 1.33 times their concentration in the original beer while the water background has been reduced by more than two orders of magnitude. The arithmetic that converts the resulting integrals back to milligrams per liter of original beer is given in Section 3.6 and refers throughout to the one milliliter of beer taken, not to the volume of the reconstituted solution.

3.2 The Native-Beer Aliquot

For the volatile inventory, 175 µL of degassed beer is combined with 100 µL of maleic acid stock solution and 375 µL of deuterium oxide of 99.8 atom % D, giving 650 µL in a 5 mm tube. The tube is capped and agitated briefly. The deuterium oxide serves both as the field–frequency lock solvent and as a dilution that moderates the water signal. The dilution itself never enters the quantitation, because standard and analyte occupy the same solution and their integral ratio is preserved; only the volume of beer sampled appears in

the expressions of Section 3.6. No filtration, extraction, derivatization, or pH adjustment is performed, and the sample is recoverable.

3.3 The Lyophilized Aliquot

For the non-volatile inventory, 1000 µL of degassed beer is transferred to a two-dram vial and freeze-dried in a Virtis Benchtop K lyophilizer. The entire residue is redissolved in 650 µL of deuterium oxide, 100 µL of maleic acid stock is added, and the solution is agitated before transfer to a 5 mm tube. Exchangeable hydroxyl and carboxyl protons equilibrate with the deuterium reservoir during reconstitution, so the anomeric region contains carbon-bound protons only; the same is broadly true of the native aliquot, where the hydroxyl protons are exchange-averaged into the water resonance, and the decisive advantage of the lyophilized preparation is therefore the removal of the water and ethanol lines rather than the removal of hydroxyl signals.

3.4 The Internal Standard

Maleic acid is used as the internal quantitation standard, dispensed as 100 µL of a stock solution in deuterium oxide of 99.8 atom % D formulated to deliver 10.0 mg of the acid into each tube. The choice is a good one. The two vinyl protons of maleic acid are chemically equivalent and appear as a sharp two-proton singlet at δ 6.40, in a region of the beer spectrum that is otherwise almost empty — downfield of the anomeric envelope, upfield of the aromatic manifold, and free of overlap in every beer, wort, mash, and non-alcoholic product examined. The compound is non-volatile, is available at certified purity with content itself assigned by quantitative NMR and traceability to national standards, is soluble to well above the required concentration, and does not react with beer constituents on the timescale of an analysis.

Two cautions apply. The purity factor must be carried explicitly; the earlier Process NMR Associates material uses 0.99 in the 2016 poster and 0.995 in the later presentations, reflecting a change of lot, and the value used must be traceable to the certificate of the lot actually consumed. Second, the concentration of the stock solution is misprinted in all four source presentations, where it appears as ten milligrams per one hundred milliliters. That formulation would deliver ten micrograms of standard to the tube, three orders of magnitude below the value the quantitation expression assumes and far too little to serve as a reference against a beer containing forty grams per liter of ethanol. The stock is in fact approximately 100 mg mL^{-1}, such that 100 µL delivers 10.0 mg, which is consistent with the annotation "175 µL + 10.0 mg MA" carried on the spectra themselves and with the numerical agreement demonstrated in Section 3.7. The misprint should be corrected wherever the method is documented.

3.4.1 A Consequence Not Previously Recognized: the Standard Fixes the pH

Ten milligrams of maleic acid in a final volume of 650 µL is 86.2 µmol in 0.650 mL, or 133 mmol L^{-1}; in the 750 µL lyophilized preparation the concentration is 115 mmol L^{-1}. Maleic acid is a moderately strong diprotic acid with $pK_{a1} = 1.92$, and a 0.13 M solution of it has a hydrogen ion concentration near 0.034 M, corresponding to a pH close to 1.5. The buffering capacity of beer, which is of the order of thirty to fifty milliequivalents per liter per pH unit and is diluted almost fourfold in the native preparation, cannot resist that addition. Every sample analyzed by this protocol is therefore presented to the spectrometer not at its own pH of 3.9 to 4.6 but at a common pH in the region of 1.5 to 2.5, fixed by the internal standard.

The observation is not a criticism of the method; it explains the spectra and, properly stated, it is a strength. Every carboxylic acid in the sample is driven to its fully protonated form, which is why lactate is observed

at δ 1.41 rather than at the δ 1.33 of the free anion, why acetate appears at δ 2.08 rather than at δ 1.92, why succinate appears at δ 2.67 rather than at the δ 2.41 of the dianion, and why the citrate AB system is found near δ 2.9 to 3.05. Because the pH is set by the standard rather than by the sample, those positions are reproducible from beer to beer irrespective of style, so that a lager at pH 4.5 and a gose at pH 3.2 present their organic acid resonances at the same chemical shifts. The alignment problem that dominates the preprocessing of most beer NMR data sets, and that is normally addressed by buffering or by interval-wise alignment algorithms, is largely solved here as a by-product of the quantitation scheme.

Three consequences follow and should be recorded. Chemical shifts obtained under this protocol are not the chemical shifts of beer, and assignment tables imported from the buffered or native-pH literature will not match; the tables in Section 4 are stated for the present conditions and are internally consistent. The chemical-shift-based quantification approach demonstrated for beer, in which concentration is inferred from peak position rather than from area, cannot be applied to spectra acquired this way, because the position is fixed by the standard and no longer responds to the analyte. And the low pH is itself a chemical condition to which the sample is subjected: acid-catalyzed mutarotation is accelerated, which is favorable for the anomeric equilibrium relied upon in Section 6.5, while acid-catalyzed glycosidic hydrolysis, negligible over the sixteen minutes of an acquisition at ambient temperature, is not negligible if prepared samples are stored, and prepared tubes should therefore be run promptly rather than queued overnight.

3.5 Acquisition

Spectra were acquired on a Varian Mercury MVX-300 equipped with a 5 mm Varian ATB probe operating at a ^{1}H resonance frequency of 299.67 MHz. A π/3 excitation pulse was applied, the spectral width was 8 kHz, and 64k complex points were collected over an 8 s acquisition time, giving a digital resolution of 0.125 Hz per point before zero-filling — considerably finer than is customary in metabolomic profiling and well matched to the narrow linewidths of the small-molecule constituents. A 7 s relaxation delay followed each acquisition, so that the recycle period was 15 s. Sixty-four transients were averaged, and the total experiment time was approximately sixteen minutes. Water suppression was applied by presaturation. Where gradient hardware and a modern console are available, the one-dimensional nuclear Overhauser spectroscopy presaturation sequence whose suppression behavior and artifacts have been analyzed in detail by McKay,[34] or the gradient schemes known as WET[35] and excitation sculpting,[36] are the preferred implementations on newer instruments. The distinction between them matters for the work of Section 6: the one-dimensional nuclear Overhauser sequence uses the same presaturation element and bleaches exchanging and near-resonant signals to the same degree, its advantages being baseline flatness and lineshape, whereas only the gradient schemes genuinely reduce the perturbation of signals lying close to the water frequency — among them the β-anomeric reducing-end doublet at δ 4.65, which sits only some forty-five hertz from the suppressed line at 300 MHz. In processing, the maleic acid singlet was normalized to an integral of 100, corresponding to 50 units per proton, so that component concentrations follow directly from the expressions of Section 3.6.

The parameters are conservative and the choice of a long acquisition time in place of a longer relaxation delay is sound, since transverse signal decay during acquisition also permits longitudinal recovery. Analyses have been performed satisfactorily on instruments from 200 to 800 MHz, and the chemical-shift axis in parts per million is field-independent by construction, so that assignment tables and integral windows transfer between instruments without modification. What does not transfer is resolution:

multiplets that are baseline-separated at 600 MHz are strongly overlapped at 300 MHz, and integral windows defined for one field must be re-examined at another.

Table 2. Acquisition and preparation parameters for the Process NMR Associates beer qNMR method.

Parameter	Native-beer aliquot	Lyophilized aliquot
Sample taken	175 µL degassed beer	1000 µL degassed beer, lyophilized
Internal standard	100 µL maleic acid stock = 10.0 mg	100 µL maleic acid stock = 10.0 mg
Solvent	375 µL D_2O (99.8 atom % D)	650 µL D_2O (99.8 atom % D)
Final volume	650 µL	750 µL
Analyte classes	ethanol, methanol, fusel alcohols, acetic acid, ethyl acetate, acetaldehyde	organic acids, amino acids, sugars, dextrins, glycerol, diols, nucleosides, polyphenols
Spectrometer	Varian Mercury MVX-300, 5 mm ATB probe	Varian Mercury MVX-300, 5 mm ATB probe
^1H frequency	299.67 MHz	299.67 MHz
Excitation pulse	π/3 (60°)	π/3 (60°)
Spectral width	8 kHz (≈26.7 ppm)	8 kHz (≈26.7 ppm)
Data points / acquisition time	64k complex / 8.0 s	64k complex / 8.0 s
Relaxation delay / recycle period	7.0 s / 15.0 s	7.0 s / 15.0 s
Transients	64	64
Total experiment time	≈16 min	≈16 min
Solvent suppression	Presaturation of residual HDO	Presaturation of residual HDO
Normalization	Maleic acid singlet = 100 (50 per proton)	Maleic acid singlet = 100 (50 per proton)

3.6 The Quantitation Expressions

For a component observed in the native-beer aliquot, the concentration in the original beer is

$$C_i\ (\text{mg/L}) = 0.995 \times 10 \times [(I_i / N_i) / 50] \times (M_i / 116.07) \times (1\,000\,000 / 175) \quad (3)$$

and for a component observed in the lyophilized aliquot,

$$C_i\ (\text{mg/L}) = 0.995 \times 10 \times [(I_i / N_i) / 50] \times (M_i / 116.07) \times (1\,000\,000 / 1\,000) \quad (4)$$

in which I_i is the integrated area of the reporter signal on the scale that sets the maleic acid singlet to 100, N_i is the number of protons contributing to that signal, M_i is the molar mass of the component in g mol^{-1}, 116.07 g mol^{-1} is the molar mass of maleic acid, 10 is the mass of standard in milligrams, 0.995 is the certified purity of the standard lot, the divisor 50 is the maleic acid integral per proton, and the final factor converts the sampled volume in microliters to a per-liter basis.

Both expressions collapse usefully. Gathering the constants gives, for the native aliquot,

$$C_i\ (\text{mg/L}) = 9.797 \times (M_i / N_i) \times I_i \quad (5)$$

and for the lyophilized aliquot,

$$C_i\ (\text{mg/L}) = 1.714 \times (M_i / N_i) \times I_i \tag{6}$$

so that each component in the analytical panel carries a single scalar response factor, $k_i = 9.797\ M_i/N_i$ or $1.714\ M_i/N_i$, that converts its normalized integral directly to milligrams per liter. Tabulating those factors once, as in Table 9, removes all arithmetic from the routine analysis and makes the integration template auditable by inspection. The earlier Process NMR Associates material uses 116.1 g mol^{-1} for the standard; the accurate value of 116.07 has been adopted here, a change of 0.03 percent that alters no tabulated figure at the precision quoted. Ethanol is additionally reported on a volume basis, for which

$$\text{Ethanol (\% v/v)} = C_EtOH\ (\text{mg/L}) / 7890 \tag{7}$$

follows from the density of ethanol at 20 °C, 0.789 g mL^{-1}.

3.7 A Worked Example

The arithmetic is worth carrying through once in full, both as a check on the expressions and as a template. Consider a lager whose ethanol methyl triplet at δ 1.18 integrates to 261.0 on the scale that sets the maleic acid singlet to 100.0. The triplet arises from three protons and the molar mass of ethanol is 46.07 g mol^{-1}, so from equation (5),

$$C_EtOH = 9.797 \times (46.07 / 3) \times 261.0 = 9.797 \times 15.357 \times 261.0 = 39\ 270\ \text{mg/L} \tag{8}$$

and from equation (7) the alcoholic strength is 39 270 / 7890 = 4.98 % v/v.

The result may be verified from first principles without recourse to the collected constants. Ten milligrams of maleic acid, of molar mass 116.07 g mol^{-1}, is 86.16 µmol of the standard and therefore 172.3 µmol of standard protons, which is the quantity of protons represented by an integral of 100.0. One unit of integral accordingly corresponds to 1.723 µmol of protons. The ethanol methyl integral of 261.0 therefore represents 449.7 µmol of protons; divided by three protons per molecule this is 149.9 µmol of ethanol, and multiplied by the molar mass, 6.906 mg of ethanol, all of it contained in the 175 µL of beer that was taken. Scaled to a liter this is 39 470 mg L^{-1}, and after multiplication by the 0.995 purity factor, 39 270 mg L^{-1} — identical to equation (8) — corresponding to 4.98 % v/v. A beer declared at 5.0 % on the label would be reported by this method as 4.98 %. Note that the dilution into 650 µL never enters the arithmetic: the standard and the analyte occupy the same solution and the same active volume, so their ratio is preserved and only the volume of beer sampled matters. Insensitivity to the final volume, and to any transfer loss or evaporation that affects standard and analyte alike, is an underappreciated advantage of internal-standard qNMR over volumetric methods.

> *Author data placeholder — replicate precision. The repeatability of the ethanol determination, expressed as the relative standard deviation of n replicate preparations of a single beer, together with the corresponding figures for the principal organic acids and for the total anomeric integral, should be inserted here from the Process NMR Associates validation records. These figures are required for the ISO/IEC 17025 method validation file and are the natural anchor for the uncertainty budget of Section 3.10.*

3.8 Relaxation, Flip Angle, and the Principal Systematic Risk

The single largest uncorrected systematic error in the protocol as described is not integration, baseline, or phasing. It is incomplete longitudinal relaxation, and because the internal standard is one of the slowly

relaxing species in the tube, the error does not cancel. The point deserves quantitative treatment rather than a caution.

Under repetitive pulsing with flip angle θ and recycle period T_R, the steady-state signal of a spin with spin–lattice relaxation time T_1 is given by the relation established by Ernst and Anderson in their foundational treatment of Fourier transform magnetic resonance,[33]

$$S = S_0 \cdot \sin\theta \cdot (1 - E) / (1 - E\cos\theta), \quad E = \exp(-T_R / T_1) \tag{9}$$

so that the fractional response relative to a fully relaxed spin excited at the same flip angle is $f(T_1) = (1 - E)/(1 - E\cos\theta)$. With the parameters of Section 3.5 — θ = 60°, cos θ = 0.5, T_R = 15.0 s — this function is essentially unity for fast-relaxing spins and falls away for slow ones, as tabulated in Table 3. A component whose reporter signal relaxes with $T_1 \leq 3$ s recovers to better than four parts per thousand of its fully relaxed value. That does not mean it requires no correction, because the reported concentration is scaled by the ratio of the analyte response to the standard response, and if the standard relaxes slowly the error persists however fast the analyte is. The difficulty arises when the standard and the analyte relax at appreciably different rates, because the reported concentration is scaled by the ratio $f(T_1,\text{analyte})/f(T_1,\text{standard})$.

Maleic acid is the species at risk on the reference side. Its vinyl protons have no directly bonded neighbors other than each other, dipolar relaxation is correspondingly inefficient, and values in the range of five to eight seconds are typical for the olefinic proton of small unsaturated diacids in deuterium oxide at ambient temperature. If T_1 of the standard is 5.5 s while the ethanol methyl relaxes at 2 s, every reported concentration in the analysis is high by 3.5 %. If the standard relaxes at 8 s, the bias rises to 9.0 %. This is not a speculative concern: it is consistent with the tendency, visible in the comparison of NMR ethanol against declared label values in Figure 7, for the NMR result to sit slightly above the declaration across a majority of the products examined.

The converse error afflicts slowly relaxing analytes. Formate presents the extreme case. Its single formyl proton at δ 8.44 has no coupling partner and no adjacent protons; T_1 values in excess of ten seconds are routine for formate in aqueous solution, and at $T_1 = 12$ s the response is only 83 % of full. Measured against a standard relaxing at 5.5 s, formate would be under-reported by roughly fourteen percent. The acetate methyl singlet, and the aromatic protons of gallic acid and of the nucleotide bases warrant the same scrutiny, since isolated methine and aromatic protons in small molecules commonly relax more slowly than methyl groups. The anomeric protons of the dextrins are not at risk on this account and should not be assumed to be: they carry an adjacent H2 partner and belong to slowly tumbling oligomers, so dipolar relaxation is efficient and their T_1 values lie in the region of one to two seconds.

Table 3. Fractional steady-state response $f(T_1)$ at θ = 60° and T_R = 15.0 s, and the resulting bias when an analyte is referenced against a maleic acid standard relaxing at 5.5 s.

T_1 (s)	$E = \exp(-T_R/T_1)$	$f(T_1)$	Bias vs standard at T_1 = 5.5 s	Representative species
1.0	3.1×10^{-7}	1.0000	+3.5 %	anomeric and ring protons of oligosaccharides; amino acid CH
2.0	5.53×10^{-4}	0.9997	+3.5 %	ethanol CH_3; lactate CH_3; alanine CH_3
3.0	6.74×10^{-3}	0.9966	+3.1 %	fusel alcohol methyls; glycerol
4.0	2.35×10^{-2}	0.9881	+2.3 %	succinate CH_2; malate CH_2
5.5	6.54×10^{-2}	0.9662	0 (reference)	maleic acid vinyl CH (assumed)

T_1 (s)	$E = \exp(-T_R/T_1)$	$f(T_1)$	Bias vs standard at T_1 = 5.5 s	Representative species
8.0	1.534×10^{-1}	0.9169	−5.1 %	acetate CH_3; isolated methine CH
10.0	2.231×10^{-1}	0.8744	−9.5 %	isolated aromatic CH
12.0	2.865×10^{-1}	0.8328	−13.8 %	formate CH
15.0	3.679×10^{-1}	0.7746	−19.8 %	worst-case isolated singlet

The assumed 5.5 s relaxation time of the standard is illustrative and must be replaced by a measured value; the entire bias column scales with that measurement. Values of $f(T_1)$ computed from equation (9).

Three remedies are available and they are not equivalent. Lengthening the recycle period to five times the longest relevant T_1 removes the problem but would extend the experiment beyond an hour and is unattractive for a service laboratory. Measuring T_1 for the standard and for each reporter signal by inversion recovery in the actual matrix, and applying the computed correction factor $f(T_1,\text{std})/f(T_1,\text{analyte})$ to each response factor in Table 9, costs one additional experiment per matrix type and leaves the throughput untouched; this is the recommended course. Substituting an internal standard whose reporter signal relaxes faster reduces but does not eliminate the analyte-side error, and the candidates are less attractive than they appear: the trimethylsilyl protons of 3-(trimethylsilyl)propionate relax over several seconds in deuterium oxide and are not reliably faster than a maleate vinyl proton, and the reagent is in any case known to associate with proteins and polyphenols in beer and to be biased low in consequence. Any substitution should be preceded by a measured relaxation time, not assumed. Reducing the excitation flip angle is the remedy most easily overlooked and, in the short term, the most useful, because the differential-relaxation error vanishes as the flip angle approaches zero. Holding the recycle period at 15 s and moving from 60° to 30° reduces the bias against a standard relaxing at 5.5 s from +3.5 to +0.9 percent for a fast-relaxing analyte, from −5.1 to −1.5 percent at T_1 = 8 s, and from −13.8 to −4.2 percent for formate at T_1 = 12 s — a reduction by a factor of roughly three and a half, obtained at a cost of a 42 percent loss of signal per transient that is recovered by tripling the transient count. Finally, the internal standard may be dispensed with entirely and the calibration transferred from an external reference through the reciprocity relation of the probe, an approach validated specifically for beer and beer-based mixed beverages in an automated implementation and one that should be evaluated if the analysis is to be accredited.[20,31,32]

> *Action item. An inversion-recovery T_1 survey of the maleic acid singlet and of the twelve principal reporter signals, performed in a representative beer, a representative wort, and a representative lyophilized reconstitution, is the highest-value single experiment available for improving the accuracy of this method. Until it is performed, the concentrations reported by the protocol should be understood to carry an unquantified multiplicative bias of the order of a few percent, common to all analytes referenced against maleic acid.*

3.9 The Ethanol ^{13}C Satellite Problem

A second systematic interference, smaller in magnitude but sharply localized, arises from the natural-abundance carbon-13 satellites of the ethanol methyl resonance. One molecule in ninety of the ethanol present carries ^{13}C at the methyl carbon, and the resulting doublet is displaced by half of $^1J(^{13}C–^1H) \approx 125$ Hz to either side of the parent line. At 299.67 MHz that displacement is 0.209 ppm, placing satellites at δ 0.97 and δ 1.39, each carrying 0.55 % of the parent intensity.

In the native-beer aliquot of a five-percent lager the ethanol methyl integrates to roughly 261 on the maleic acid scale, so each satellite carries an integral of about 1.44. The lactate methyl doublet at δ 1.41 in a conventionally fermented beer containing 150 mg L^{-1} of lactic acid would integrate to approximately 0.5 on the same scale. The interfering satellite is thus three times the size of the analyte signal, and any lactate value obtained by integrating that region of a native-beer spectrum is dominated by ethanol. The high-field satellite at δ 0.97 sits among the valine, leucine, and isoleucine methyl doublets with the same consequence. This is the concrete, quantitative reason for the dual-aliquot design described in Section 3.1: the lyophilized aliquot, in which the great majority of the ethanol has been removed, is the only preparation in which the region between δ 0.9 and 1.5 can be integrated honestly.

Where residual ethanol persists after lyophilization the satellites persist with it in proportion, and two straightforward corrections are available. The satellite positions and relative intensity are deterministic — ±62.5 Hz and 0.55 % of the parent — so they can be inserted as constrained components in a global spectral deconvolution, which the Mestrelab global spectral deconvolution and simple mixture analysis tools used in this laboratory support directly. Alternatively, multiple-frequency presaturation may be applied at the two satellite positions in addition to the water frequency, at the cost of a small dead zone in the spectrum. Carbon-13 decoupling during acquisition would collapse the satellites into the parent line entirely, but is impractical here because an eight-second acquisition time produces an unacceptable decoupler duty cycle on a room-temperature probe.

3.10 Uncertainty Budget

The measurement uncertainty of a quantitative NMR result is dominated by contributions that are easy to enumerate and, with the exception of the relaxation term discussed above, easy to control. Table 4 sets out the budget for the present method with indicative magnitudes; the entries flagged as author-supplied must be replaced by values from the laboratory validation record before the table is used for an accredited report.

Table 4. Indicative uncertainty budget for the beer qNMR method. Entries marked as author-supplied are placeholders to be replaced by measured values.

Contribution	Typical relative magnitude	Control measure
Mass of internal standard	0.1–0.3 %	Analytical balance calibrated and verified; gravimetric preparation of stock
Purity of internal standard	0.1–0.5 %	Certificate of analysis for the lot in use; content assigned by qNMR with stated uncertainty
Volume of beer aliquot	0.5–1.0 %	Positive-displacement pipette, calibrated; gravimetric verification recommended for the 175 µL step
Volume of standard aliquot	0.5–1.0 %	As above; alternatively weigh the standard directly into the tube
Incomplete relaxation (analyte vs standard)	2–14 % (see Table 3)	Inversion-recovery T_1 survey and per-signal correction factors; or extended recycle period
Signal-to-noise of reporter signal	0.1 % (ethanol) to >20 % (trace analytes)	Transient count matched to the analyte of interest; report a limit of quantitation per signal
Integration limits and baseline	0.5–3 %	Fixed integral windows in a locked template; consistent baseline algorithm; lineshape fitting in congested regions

Contribution	Typical relative magnitude	Control measure
Phase error	0.2–2 %	Automated zeroth- and first-order phasing with manual review; first-order term bounded
Signal overlap in the reporter window	0–20 % depending on region	Deconvolution; selection of alternative reporter signals; two-dimensional confirmation
Loss of volatiles during degassing	Author-supplied	Compare vortex agitation against brief sonication and against a sealed undegassed control
Loss of volatiles during lyophilization	Author-supplied	Quantify residual ethanol in the reconstituted aliquot in every run as a process control
Repeatability (within-day, single analyst)	Author-supplied	n ≥ 6 replicate preparations of a control beer
Intermediate precision (between-day, between-analyst)	Author-supplied	Control chart on a retained reference beer or a synthetic control mixture

Two entries deserve a further word. Degassing by vigorous vortex agitation is effective against carbon dioxide but is not selective, and the compounds most vulnerable to it are precisely those of greatest interest to a brewer: acetaldehyde, the acetate esters, and dimethyl sulfide all have appreciable vapor pressures and will be stripped to some degree. The magnitude of that loss has not, to the author's knowledge, been measured in this laboratory, and it is straightforward to measure — a sealed, undegassed sample analyzed at a field homogeneity sufficient for the volatile region only, compared against the routine preparation, settles the question in a single afternoon. Similarly, quantifying the residual ethanol in every lyophilized aliquot costs nothing, since the signal is present in the spectrum in any case, and converts an unknown into a recorded process control that will reveal a drifting freeze-dryer long before it corrupts a client result.

> *Author data placeholder — degassing and lyophilization recovery study. Results of the volatile-recovery comparison and the residual-ethanol control chart are to be inserted here.*

4. Reading the Spectrum: Region by Region

4.1 The Global View

Before individual assignments are considered it is worth looking at the whole spectrum at once, and at many spectra at once. Figure 1 superimposes the full ^{1}H spectra of thirty commercial beers acquired under the conditions of Section 3.5. The display is instructive in two opposite ways. It shows, first, how much of the spectrum is common to every beer: the maleic acid singlet at δ 6.40 normalized to 100, the ethanol methylene quartet near δ 3.65, the ethanol methyl triplet near δ 1.18, and the broad carbohydrate massif are present in every trace and in similar proportion. It shows, second, that essentially every region outside those landmarks fans out into a spread of traces whose vertical dispersion is the chemical variability of the product class. That dispersion is the analytical signal. It is what a chemometric model will eventually be asked to organize, and it is worth appreciating that it is visible by eye before any statistics are applied.

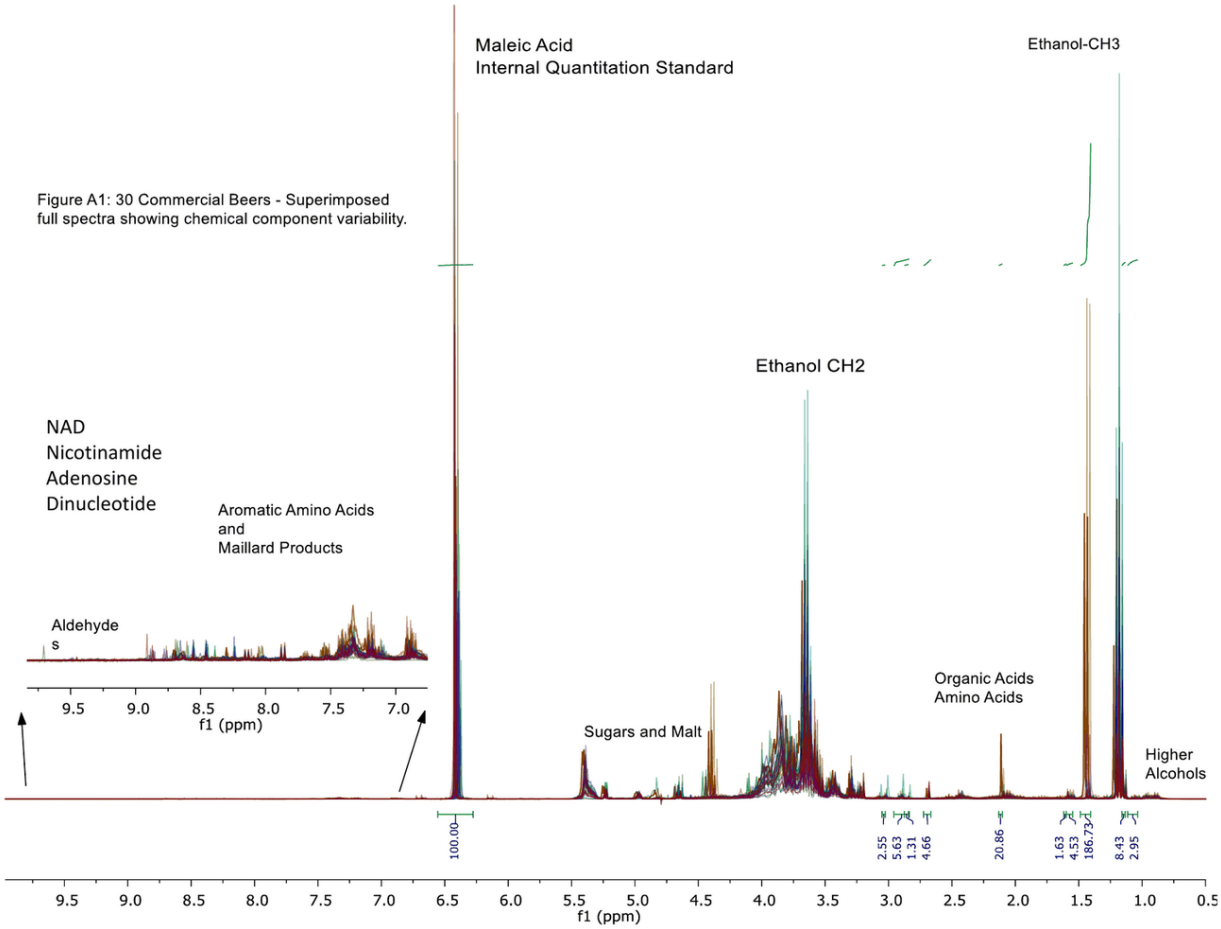


Figure 1. Superimposed 300 MHz ^{1}H NMR spectra of thirty commercial beers, prepared as described in Section 3, showing the full chemical-shift range and the principal compositional windows. The maleic acid internal quantitation standard at δ 6.40 is normalized to an integral of 100 in every trace. Regions are labeled from high to low frequency, that is from left to right as displayed: aldehydes above δ 9.4; the nicotinamide and adenine ring protons of the dinucleotide cofactors between δ 8.7 and 9.0; the aromatic amino acid, polyphenol, and Maillard product manifold between δ 6.8 and 8.6; the carbohydrate anomeric and ring-proton regions between δ 3.2 and 5.5; the organic acid and amino acid region between δ 1.4 and 3.2; and the higher alcohols below δ 1.1. Process NMR Associates data.

The layout of Figure 1 also makes the dynamic-range problem concrete. The ethanol methyl integral on this normalization approaches 190 in the trace whose integrals are displayed, while the aldehyde region above δ 9.4 and the nucleotide region near δ 8.8 carry integrals of a few hundredths. Four orders of magnitude separate the largest and smallest quantifiable features in a single acquisition, and the receiver, the digitizer, and the water suppression must all accommodate that span without distortion. This is the practical reason the technique matured only after the pulsed-field-gradient and oversampling era, and it is the reason the lyophilized aliquot, which removes the two largest contributors, is so valuable for the minor components.

Table 5 summarizes the constituent classes, their typical levels, and the windows in which they are observed, and functions as an index to the sections that follow.

Table 5. Constituent classes of beer, typical levels, and their ^{1}H NMR observability under the Process NMR Associates protocol.

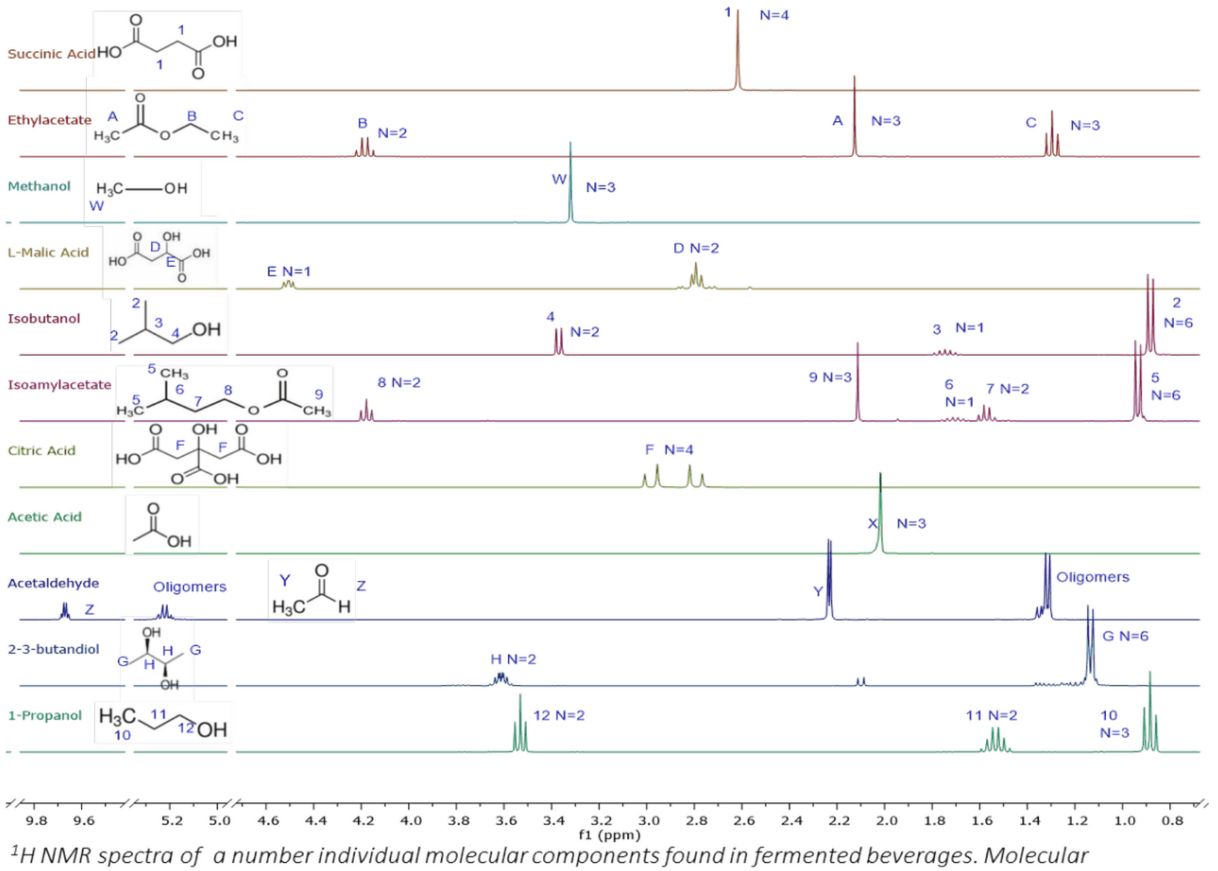
Class	Representative constituents	Typical level	Principal window (δ, ppm)	Aliquot and remarks
Water	H_2O / HDO	900–950 g/L	4.7–4.9	Presaturated; residual line sets local dynamic range. Largely removed by lyophilization
Ethanol	ethanol	30–50 g/L	1.18; 3.65	Native aliquot. ^{13}C satellites at δ 0.97 and 1.39 interfere with lactate and branched-chain amino acids
Higher alcohols	1-propanol, isobutanol, isopentanol, methanol	40–250 mg/L	0.85–1.0; 3.3–3.6	Native aliquot; sharp resolved methyl multiplets
Esters	ethyl acetate, isoamyl acetate, ethyl lactate	10–60 mg/L	1.28; 2.07; 4.12	Native aliquot; near or below quantitation limit in many lagers
Aldehydes	acetaldehyde and its hydrate	2–20 mg/L	2.22; 9.66	Native aliquot; vulnerable to loss during degassing
Organic acids	lactic, acetic, succinic, citric, malic, pyruvic	0.3–1.5 g/L total; to >10 g/L in sour styles	1.3–3.1	Lyophilized aliquot; observed in their fully protonated forms (Section 3.4.1)
Volatile acids	acetic, formic	50–1000 mg/L	2.08; 8.44	Native aliquot; both are more volatile than water and are not reliably retained through lyophilization
Polyols and diols	glycerol, 2,3-butanediol, 1,3-propanediol	1.0–2.5 g/L glycerol	1.14; 1.76; 3.5–3.8	Lyophilized aliquot; 1,3-propanediol diagnostic of wild fermentation
Free amino acids	proline, alanine, GABA, valine, leucine, isoleucine, aromatics	0.3–1.5 g/L total	0.9–4.2; 6.8–8.7	Lyophilized aliquot; proline dominant in finished beer
Free sugars	glucose, maltose, maltotriose, lactose, trehalose	0.5–15 g/L	4.4–5.5 (anomeric)	Lyophilized aliquot; resolved anomeric doublets
Residual dextrins	branched and linear α-limit dextrins	1–45 g/L	4.95–5.43 (anomeric)	Lyophilized aliquot; the structural core of Section 6
Cereal polysaccharides	(1→3),(1→4)-β-glucan, arabinoxylan	0.1–4 g/L	4.5–4.8; 5.2–5.4	Broad; diffusion- and linkage-distinct from α-glucans
Nucleosides and cofactors	uridine, adenosine, inosine, NAD^+	5–60 mg/L	5.9–6.2; 7.8–9.0	Lyophilized aliquot; clean low-field markers, hopping-regime sensitive
Aromatics and polyphenols	tyrosol, 2-phenylethanol, gallic acid, ferulic derivatives	10–150 mg/L	6.8–7.5	Lyophilized aliquot; congested but information-rich
Hop bitter acids	cis- and trans-iso-α-acids	10–100 mg/L	1.0–1.1; 2.4–3.1; 5.0–6.1	Below one-dimensional quantitation in finished beer; see Section 7.6

Levels are indicative for conventional all-malt and adjunct products; sour, wheat, high-gravity, and non-alcoholic beers depart from several entries. Windows are quoted against sodium 3-(trimethylsilyl)propionate-d_4 at δ 0.00 and refer to the low-pH condition established by the internal standard (Section 3.4.1).

4.2 Pure-Component Spectra as the Basis of Assignment

The interpretive strategy that underlies the entire method is simple and is worth stating explicitly, because it is what distinguishes a quantitative fingerprint from a pattern-recognition exercise. The spectrum of a beer is the linear superposition of the spectra of its constituents, each scaled by its molar concentration and

by the number of protons contributing to each multiplet. No constituent perturbs the spectrum of another except through overlap and through the shared solvent environment. It follows that a library of pure-component spectra, acquired under matched conditions, is sufficient to identify and to quantify any component whose signals include at least one region where it does not overlap with anything else. Figure 2 reproduces such a library for a selection of fermented-beverage constituents, annotated with the proton count that each multiplet represents, and Figure 3 extends it to a set of pure amino acids measured alongside a commercial yeast nutrient preparation.



^{1}H NMR spectra of a number individual molecular components found in fermented beverages. Molecular assignments of the various NMR peaks that represent proton chemistries present in each molecule are show along with the molar number of protons that each peak represents. These pure component spectra of individual molecules found in beer are superimposed on each other in the final NMR spectrum. However, a knowledge of these component spectra allows the identification of unique NMR signals for most molecular components allowing the identification and quantification of the components present in the complex mixture that is the beer.

Figure 2. Pure-component 300 MHz ^{1}H spectra of individual constituents found in fermented beverages, with structures and per-multiplet proton counts annotated: succinic acid, ethyl acetate, methanol, L-malic acid, isobutanol, isoamyl acetate, citric acid, acetic acid, acetaldehyde and its oligomers, 2,3-butanediol, and 1-propanol. The spectrum of a beer is the sum of such component spectra, and the existence for each component of at least one non-overlapped multiplet is what makes targeted quantitation possible in the mixture. Process NMR Associates data.

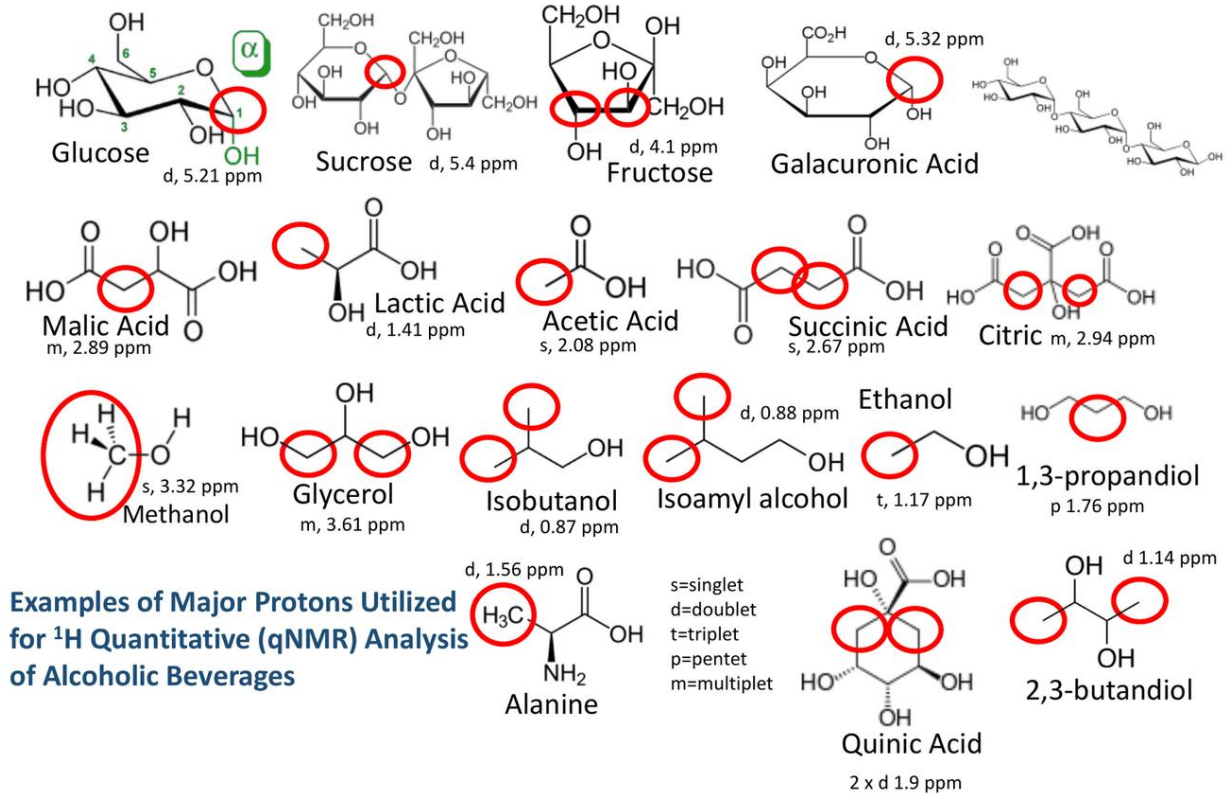


Figure 3. Structures and reporter chemical shifts for the principal species quantified by ^{1}H qNMR in fermented beverages, with multiplicity indicated. Reporter signals identified on this map include glucose (d, δ 5.23), sucrose (d, δ 5.40), fructose (d, δ 4.10), malic acid (m, δ 2.89), lactic acid (d, δ 1.41), succinic acid (s, δ 2.67), citric acid (m, δ 2.94), acetic acid (s, δ 2.08), methanol (s), glycerol (m, δ 3.61), ethanol (t), the fusel alcohols (d, δ 0.87–0.88), 1,3-propanediol (quintet, δ 1.76), 2,3-butanediol (d, δ 1.14), alanine (d) and quinic acid. Chemical shifts are reproduced as annotated on the original figure; where they differ from the tabulated values of Tables 6 to 8 the tabulated values, which refer to the low-pH condition of Section 3.4.1, should be preferred. Process NMR Associates data.

One qualification is required, and it is the subject of Section 3.4.1. The chemical shift of a carboxylic acid in fast exchange is a population-weighted average of its protonated and deprotonated forms, so it moves continuously with pH; the lactate methyl doublet, for example, lies at δ 1.33 for the fully dissociated anion and at δ 1.42 for the free acid, and the corresponding excursions for acetate, succinate, citrate, and malate are of comparable size. In most published beer work that dependence is a nuisance, because beer sits at pH 3.9 to 4.6 for conventional styles and at 3.2 to 3.6 for sour styles, squarely among the dissociation constants of lactic acid (pK_a 3.86), acetic acid (4.76), succinic acid (pK_{a1} 4.21), citric acid (3.13, 4.76, 6.40), and malic acid (3.40, 5.20), so that peak positions differ from product to product. Under the present protocol it is not a nuisance, because 133 mmol L^{-1} of maleic acid overwhelms the buffering of the sample and fixes every preparation near pH 1.5 to 2.5. The acids are therefore observed at their fully protonated limits — lactate at δ 1.41, acetate at δ 2.08, succinate at δ 2.67 — and at the same positions in every beer regardless of style.

Two practical consequences follow. Fixed integral windows are safe here in a way they are not in buffered or native-pH work, and the spectral alignment by interval correlation-optimized shifting that is the standard preprocessing step in most beer NMR studies is correspondingly less critical,[37] although it remains prudent as a guard against referencing drift. Against that, the chemical-shift-based quantification approach demonstrated for beer, in which concentration is inferred from peak position rather than from area, cannot

be applied to these spectra, since the position no longer responds to the analyte.[8] It must also be remembered that the spectrum is not a spectrum of the beer: the acids have been protonated, the carbon dioxide removed, the solvent exchanged for deuterium oxide, and, in the lyophilized preparation, the concentrations raised by a third. Assignment tables imported from the buffered literature will not match, and the tables that follow are stated for the present conditions.

4.3 The High-Field Region: δ 0.8 to 1.8

The region opens with the overlapped methyl doublets and triplets of the fusel alcohols and the branched-chain amino acids between δ 0.85 and 1.05. At 300 MHz these are not individually baseline-resolved, and the practical approach adopted in this laboratory has been to integrate the composite envelope for a total higher-alcohol figure and to deconvolute for the individual species where the concentrations warrant it. Moving downfield, the 2,3-butanediol doublet at δ 1.14 is usually clean, the ethanol methyl triplet at δ 1.18 dominates everything, the ethyl triplet of ethyl acetate falls at δ 1.28 beneath the acetaldehyde hydrate doublet, the lactate methyl appears between δ 1.33 and 1.42 according to pH, the alanine doublet sits at δ 1.48, the pyruvate hydrate singlet at δ 1.49, and the central methylene quintet of 1,3-propanediol closes the region at δ 1.76.

Two integration hazards are present in this region and both have been discussed already: the ethanol ^{13}C satellite at δ 1.39 sits on top of the lactate doublet and the satellite at δ 0.97 sits among the branched-chain amino acid methyls. Neither can be ignored in a native-beer spectrum. In the lyophilized aliquot both are attenuated in proportion to the residual ethanol, and it is in that preparation that lactate, alanine, and the amino acid methyls should be quantified.

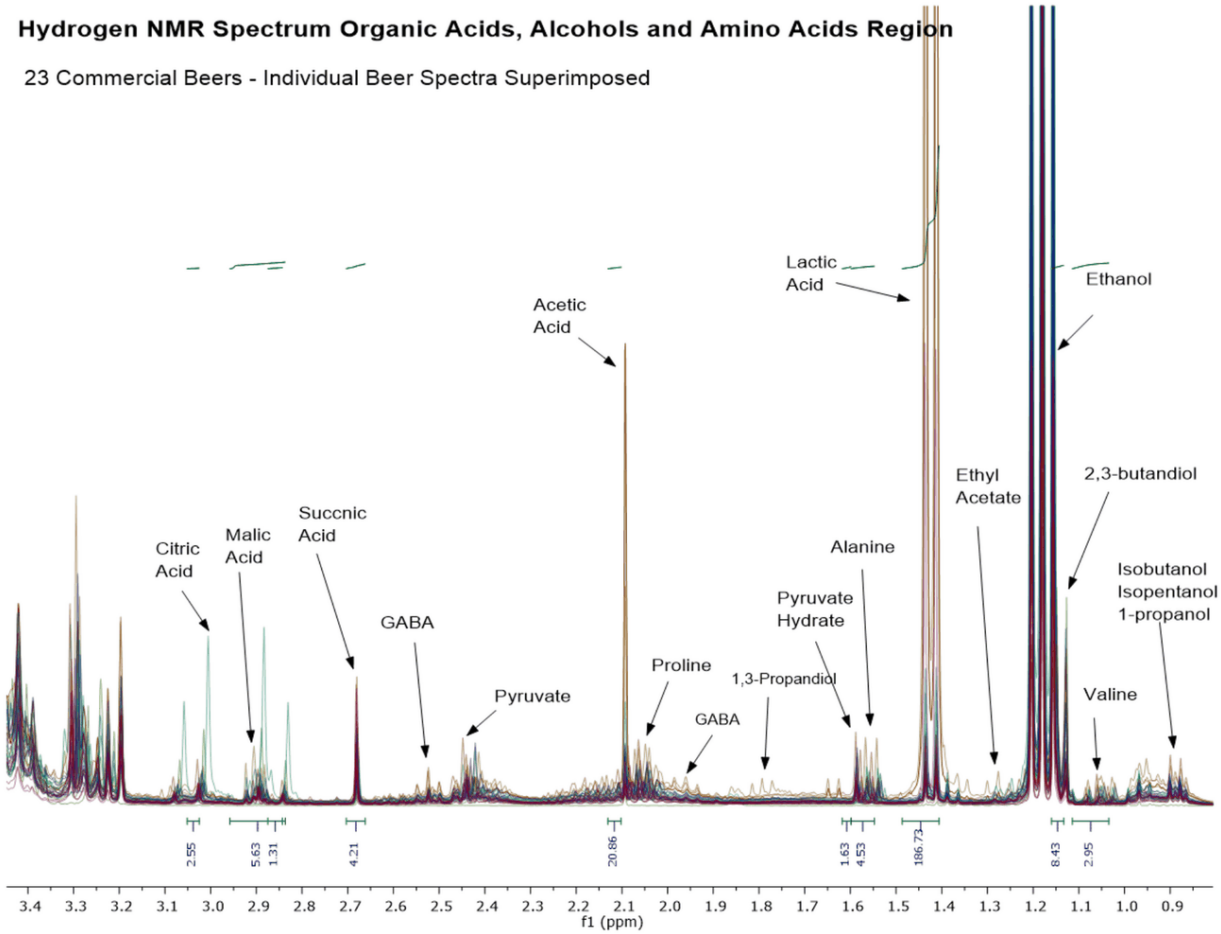


Figure 4. Superimposed 300 MHz ^{1}H spectra of twenty-three commercial beers over the organic acid, alcohol, and amino acid region, δ 0.85 to 3.45. Labeled features, from high to low frequency: citric acid, malic acid, succinic acid, γ-aminobutyric acid, pyruvate, acetic acid, proline, 1,3-propanediol, pyruvate hydrate, alanine, lactic acid, ethyl acetate, ethanol, 2,3-butanediol, valine, and the composite isobutanol / isopentanol / 1-propanol envelope. The green integral traces beneath the spectrum indicate the fixed windows used for quantitation. The integral values displayed belong to a single trace, one of the deliberately soured products in the set: the acetic acid integral of 20.9 corresponds through Table 9 to 4.1 g/L of acetic acid, and the ethanol methyl integral of 186.7 to 3.6 % v/v. Process NMR Associates data.

Table 6. ^{1}H assignments and reporter signals in the high-field region, δ 0.8 to 1.8, as observed in the Process NMR Associates preparations.

Compound	Reporter	δ (ppm)	Mult. (J, Hz)	N	Remarks
Isobutanol	$(CH_3)_2$	0.87	d (6.7)	6	Overlaps isopentanol and 1-propanol at 300 MHz
Isopentanol (isoamyl alcohol)	$(CH_3)_2$	0.88	d (6.6)	6	Principal fusel alcohol in most ales
1-Propanol	CH_3	0.89	t (7.4)	3	CH_2 sextet at 1.55; CH_2OH triplet at 3.56
Isoleucine	δ-CH_3	0.93	t (7.4)	3	γ-CH_3 doublet at 1.01
Leucine	(δ-CH_3)$_2$	0.95, 0.96	d (6.3)	6	Two inequivalent methyls
Ethanol ^{13}C satellite (low)	CH_3	0.97	t	—	Artifact: 0.55 % of parent, −62.5 Hz

Compound	Reporter	δ (ppm)	Mult. (J, Hz)	N	Remarks
Valine	(γ-CH_3)$_2$	0.99, 1.04	d (7.0)	3 + 3	Well resolved in lyophilized aliquot
2,3-Butanediol	(CH_3)$_2$	1.14	d (6.3)	6	meso and D/L forms differ slightly
Ethanol	CH_3	1.18	t (7.1)	3	Primary ethanol reporter; native aliquot
Ethyl acetate	CH_3 of ethyl	1.28	t (7.1)	3	Acetyl singlet at 2.07 is the alternative reporter
Acetaldehyde hydrate	CH_3	1.31	d (5.3)	3	Free aldehyde CH_3 doublet at 2.22
Threonine	γ-CH_3	1.32	d (6.6)	3	Coincident with ethanol ^{13}C satellite region
Lactic acid / lactate	CH_3	1.33–1.42	d (6.9)	3	Strongly pH-dependent; δ 1.41 observed in these samples
Ethanol ^{13}C satellite (high)	CH_3	1.39	t	—	Artifact: 0.55 % of parent, +62.5 Hz; interferes with lactate
Ethyl lactate	CH_3 (lactyl)	1.42	d (7.0)	3	Observed in wild and barrel-aged products
Alanine	CH_3	1.48	d (7.2)	3	Most reliable single amino acid reporter
Pyruvate hydrate	CH_3	1.49	s	3	2,2-dihydroxypropanoate; equilibrium partner of pyruvate
1-Propanol	CH_2	1.55	sext (7.3)	2	Secondary reporter
Isopentanol	CH_2	1.48	q	2	CH multiplet at 1.66
1,3-Propanediol	central CH_2	1.76	quint (6.4)	2	Diagnostic of anaerobic glycerol catabolism (Section 7.3)
Isobutanol	CH	1.79	non (6.7)	1	Weak; methyl doublet preferred

4.4 The Mid-Field Region: δ 1.8 to 3.2

Between δ 1.8 and 3.2 lie the methylene manifolds of proline and γ-aminobutyric acid, the acetate and pyruvate singlets, the succinate singlet, the AB and ABX systems of citrate and malate, the acetyl singlet of ethyl acetate, and the benzylic triplets of tyrosol and 2-phenylethanol. In buffered or native-pH work this is where pH sensitivity is most acute; under the present protocol the acids are held at their protonated limits and the positions are stable, but the region remains the most congested part of the aliphatic spectrum. It is also the most information-dense part of the aliphatic spectrum from a process standpoint, since every one of the organic acids reports on a distinct metabolic route: lactate on lactic acid bacteria, acetate on acetic acid bacteria and on oxidative spoilage, succinate on the reductive branch of the yeast tricarboxylic acid cycle, malate and citrate on wort composition and on malolactic activity, pyruvate on the glycolytic node and on incomplete fermentation, and formate on pyruvate–formate lyase activity in contaminating bacteria.

Proline deserves separate comment because it dominates the free amino acid pool of finished beer. It is the one proteinogenic amino acid that Saccharomyces cannot assimilate under the anaerobic conditions of a normal fermentation, since proline oxidase requires molecular oxygen, so wort proline passes essentially

unchanged into the finished product. Its concentration therefore reports on malt protein and on mashing rather than on fermentation, and its ratio to the assimilable amino acids, all of which are drawn down during the growth phase, provides a direct measure of nitrogen utilization.[59] The proline δ-methylene resonances at δ 3.34 and 3.41 and the β and γ multiplets between δ 2.00 and 2.35 are the reporters, with the caveat that the latter overlap the glutamate and glutamine manifolds.

Table 7. ^{1}H assignments and reporter signals in the mid-field region, δ 1.8 to 3.2.

Compound	Reporter	δ (ppm)	Mult. (J, Hz)	N	Remarks
γ-Aminobutyric acid (GABA)	β-CH_2	1.90	quint (7.5)	2	α-CH_2 triplet at 2.30; γ-CH_2 triplet at 3.01
Proline	β/γ-CH_2	2.00–2.35	m	4	Overlaps glutamate; δ-CH_2 at 3.34/3.41 preferred
Ethyl acetate	acetyl CH_3	2.07	s	3	Clean when ethyl triplet is obscured
Acetic acid	CH_3	2.08	s	3	Fully protonated at the working pH; native aliquot
Glutamic acid	γ-CH_2	2.35	m	2	β-CH_2 at 2.05–2.15
Pyruvic acid / pyruvate	CH_3	2.38	s	3	Hydrate partner at δ 1.49; sum is total pyruvate
Citric acid	CH_2 (AB)	2.90, 3.05	2 × d (15.5)	4	Fully protonated form; the dianion values of δ 2.55/2.66 do not apply here
Succinic acid	CH_2CH_2	2.67	s	4	Fully protonated form; the dianion resonates at δ 2.41
Malic acid / malate	CH_2 (ABX)	2.68, 2.85	dd (15.6, 3.1 / 15.6, 10.1)	2	CH at 4.30; reports wine must, fruit adjunct, malolactic activity
Tyrosol	benzylic CH_2	2.83	t (6.9)	2	CH_2OH triplet at 3.78; aromatics at 6.86/7.20
2-Phenylethanol	benzylic CH_2	2.90	t (6.8)	2	CH_2OH triplet at 3.85; aromatics at 7.30–7.45
Asparagine / aspartate	β-CH_2	2.70, 2.85	dd	2	Overlaps malate
γ-Aminobutyric acid	γ-CH_2	3.01	t (7.5)	2	Cleaner than the α-CH_2 in most beers

4.5 The Carbohydrate Bulk Region: δ 3.2 to 4.4

The massif between δ 3.2 and 4.4 contains the H2 through H6 ring protons of every glucose residue in the sample — free, oligomeric, and polymeric — together with glycerol, the ethanol methylene quartet, the methanol singlet at δ 3.36, the trimethylammonium singlets of choline and betaine, the α-protons of the amino acids, and the hydroxymethylene resonances of the higher alcohols. With two exceptions, little compound-specific quantitation is attempted here in one dimension and none should be attempted without deconvolution. The region serves two other purposes. It is the mass-balance anchor for total carbohydrate, since the integrated ring-proton envelope divided by the appropriate proton count per glucose residue gives a total independent of the anomeric determination and can be used to check it. And it is the region in which

the two-dimensional correlation experiments are most productive, since the through-bond connectivities that establish linkage and sequence are found here.

The exceptions are methanol, whose singlet at δ 3.36 stands clear in the native aliquot, and glycerol, quantified from the five-proton multiplet between δ 3.55 and 3.80. The glycerol window must be integrated in the lyophilized preparation, since in the native aliquot it lies beneath the ethanol methylene quartet at δ 3.65; the proline δ-methylene pair at δ 3.34 and 3.41 sits at its edge and requires deconvolution in beers of high residual proline. Its concentration in a normally fermented beer, of the order of one to two and a half grams per liter, is a stable function of yeast osmotic response and redox balance, and departures from it are informative: elevated glycerol accompanies high-gravity fermentation and osmotic stress, while its disappearance in the presence of 1,3-propanediol identifies anaerobic glycerol catabolism by contaminating lactic acid bacteria (Section 7.3).

4.6 The Anomeric Region: δ 4.4 to 5.5

The anomeric window is the most information-rich part of the beer spectrum and is treated in full in Section 6, since its content is dominated by the residual dextrin fraction. In outline it contains, moving from low to high frequency: the galactose anomeric doublet of lactose near δ 4.45; the β-anomeric doublets of free glucose near δ 4.63 and of the maltooligosaccharide reducing end near δ 4.65; the β-glucan anomeric signals between δ 4.5 and 4.8; the suppressed water resonance near δ 4.79; the α-(1→6) branch-point anomeric envelope between δ 4.95 and 5.00; a series of minor disaccharide and trisaccharide anomeric signals between δ 5.05 and 5.25; the α-anomeric doublets of free glucose and of the maltooligosaccharide reducing end near δ 5.23; and the internal α-(1→4) envelope between δ 5.29 and 5.43 which carries the bulk of the dextrin signal, with kojibiose, kestose, and sucrose contributing above and within its high-frequency edge.

4.7 The Aromatic, Nucleoside, and Maillard Region: δ 5.5 to 9.8

Downfield of the anomeric envelope the spectrum thins dramatically and correspondingly minor species become tractable. Figure 5 shows this region for thirty commercial beers, and the dispersion among the traces is far greater in relative terms than anywhere else in the spectrum — a consequence of the fact that these signals report on malt kilning intensity, hop variety and timing, yeast strain and health, and oxidative history, all of which differ far more between products than does the fermentable extract.

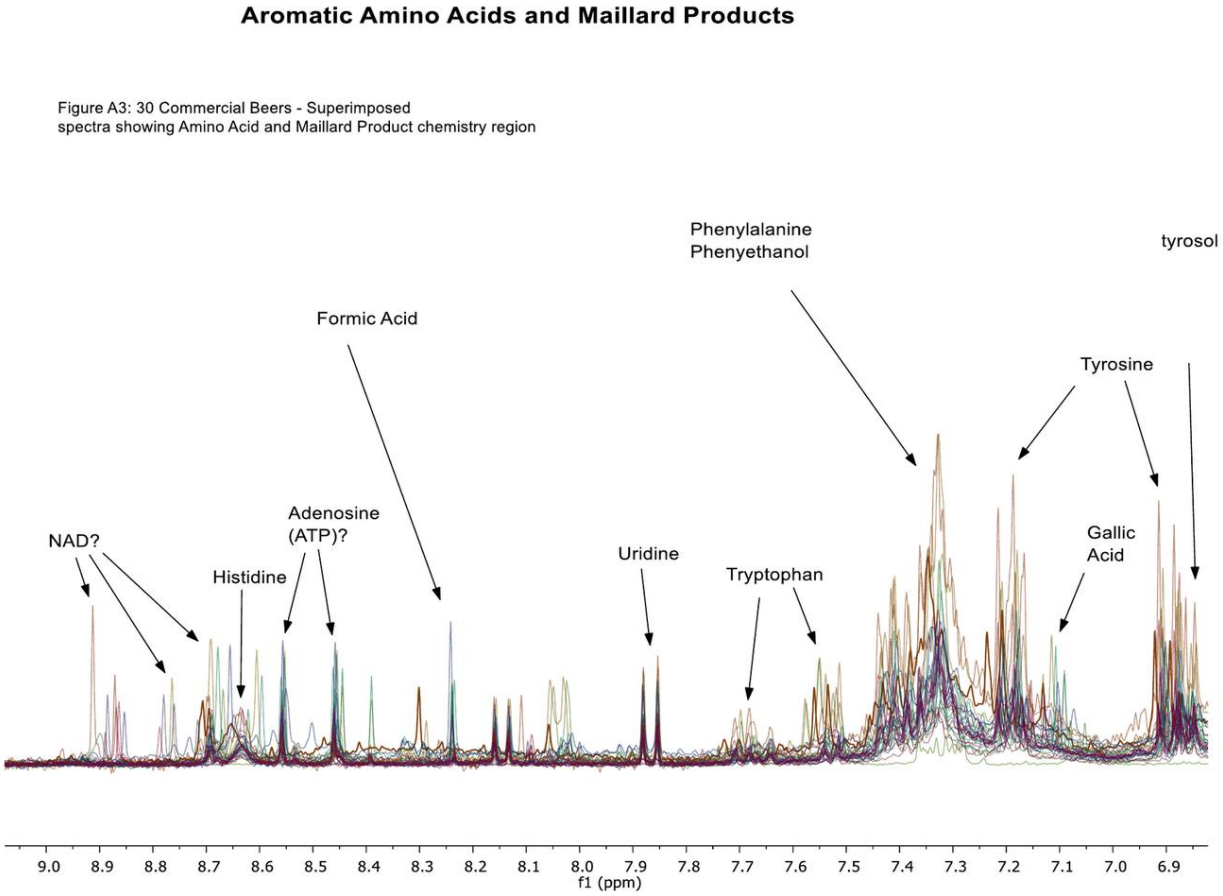


Figure 5. Superimposed 300 MHz ^{1}H spectra of thirty commercial beers over the aromatic amino acid, nucleotide, and Maillard product region, δ 6.85 to 9.05. Labeled features include the nicotinamide and adenine ring resonances attributed to the dinucleotide cofactors near δ 8.8 to 8.9, histidine at δ 8.65, purine nucleosides and nucleotides tentatively assigned at δ 8.47 and 8.55, formic acid at δ 8.30, uridine H6 at δ 7.87, tryptophan at δ 7.55 to 7.70, the phenylalanine and 2-phenylethanol manifold at δ 7.30 to 7.42, tyrosine at δ 7.19, gallic acid at δ 7.10, and tyrosol at δ 6.86. The vertical dispersion in this region substantially exceeds that of the aliphatic regions and is the principal source of style discrimination in multivariate models. Process NMR Associates data.

The purine and pyrimidine signals deserve particular attention because they carry process information available from no other routine measurement. Yeast purine metabolism responds to hopping regime, and a controlled study has shown that late and dry hopping produce a differential effect on the nucleoside and nucleotide pool of the finished beer, with adenosine and inosine levels distinguishing hopping schedules that are otherwise chemically similar.[10] The nicotinamide adenine dinucleotide resonances near δ 8.8 to 9.0 are, so far as the author is aware, not routinely quantified in any brewery, yet they are visible in these spectra and report directly on cellular redox state at the point of separation.

The Maillard products of kilning and boiling occupy the same window. 5-Hydroxymethylfurfural and 2-furaldehyde appear as heat-load markers, hydroxymethylfurfural through its ring protons near δ 6.68 and 7.53 and its aldehyde at δ 9.46, and they track kilning intensity and thermal abuse in the package; the systematic NMR study of beer aging chemistry by Rodrigues and co-workers established which of these markers move reproducibly with storage and which do not.[11] The polyphenolic fraction — gallic acid, catechin and epicatechin, and the ferulic acid derivatives — is congested and largely unresolved at 300 MHz but is not featureless, and in wheat beers the yeast decarboxylation product 4-vinylguaiacol

contributes an identifiable vinyl doublet-of-doublets near δ 6.67 with terminal methylene doublets at δ 5.63 and 5.10.[16]

Table 8. ^{1}H assignments in the olefinic, aromatic, nucleoside, and aldehyde regions, δ 5.5 to 9.8.

Compound	Reporter	δ (ppm)	Mult. (J, Hz)	N	Process significance
4-Vinylguaiacol	CH= / =CH_2	6.67 / 5.63, 5.10	dd / d	1 / 2	Ferulic acid decarboxylation; wheat and Belgian styles
Uridine	H5	5.90	d (8.1)	1	Nucleoside pool; yeast autolysis
Maleic acid (standard)	CH=CH	6.40	s	2	Internal quantitation reference, normalized to 100
5-Hydroxymethylfurfural	H3 / H4	7.53 / 6.68	d (3.5)	1 / 1	H3 lies adjacent to the carbaldehyde; kilning and thermal load; CHO at 9.46
Tyrosol	H ortho / meta to OH	6.86 / 7.20	d (8.5)	2 / 2	Yeast Ehrlich pathway product from tyrosine
Tyrosine	H ortho / meta to OH	6.90 / 7.19	d (8.5)	2 / 2	Residual assimilable nitrogen; overlaps tyrosol
Gallic acid	H2,6	7.10	s	2	Malt and, where used, oak polyphenols
Catechin / epicatechin	ring H	6.8–7.0	m	—	Haze-active polyphenol fraction
Phenylalanine	H2,6 / H3,4,5	7.33 / 7.38–7.43	m	2 / 3	Residual assimilable nitrogen
2-Phenylethanol	ring H	7.30–7.45	m	5	Rose-like fermentation aroma; Ehrlich product
Tryptophan	H2 / H4 / H7	7.32 / 7.73 / 7.55	s / d / d	1 / 1 / 1	Assimilable nitrogen; indole precursor
Uridine	H6	7.87	d (8.1)	1	Clean, isolated marker
Formic acid / formate	CHO	8.30–8.46	s	1	Bacterial pyruvate–formate lyase; long T_1 (Section 3.8)
Purine nucleosides and nucleotides	H2 / H8	8.2–8.6	s	1 each	Adenosine, inosine and the adenine nucleotides; assignment within the group is tentative at 300 MHz; hopping-regime sensitive
Histidine	H2 (imidazolium)	8.60–8.65	s	1	Strongly pH-dependent; H4 near δ 7.30
NAD^+ (nicotinamide)	H2 / H6	8.80–9.00	m	1	Cellular redox state; rarely measured elsewhere
5-Hydroxymethylfurfural	CHO	9.46	s	1	Aldehyde window essentially background-free
Acetaldehyde	CHO	9.66	q (2.9)	1	Green-apple flavor defect; vulnerable to degassing loss

4.8 Two-Dimensional Support

One-dimensional assignment in a mixture as congested as beer is only as good as its confirmation, and two-dimensional experiments provide that confirmation without recourse to spiking. Figure 6 shows a two-

dimensional J-resolved spectrum of a lyophilized Scottish ale, in which the chemical-shift and scalar-coupling information that are convolved in the one-dimensional trace are separated onto orthogonal axes. Projection onto the chemical-shift axis yields a proton-decoupled one-dimensional spectrum in which every multiplet collapses to a singlet, dramatically reducing overlap in the crowded aliphatic region; the coupling axis simultaneously reports the multiplet structure that establishes identity. The approach was applied to beer differentiation early in the development of the field and its simplified projections proved particularly well suited to multivariate treatment.[9]

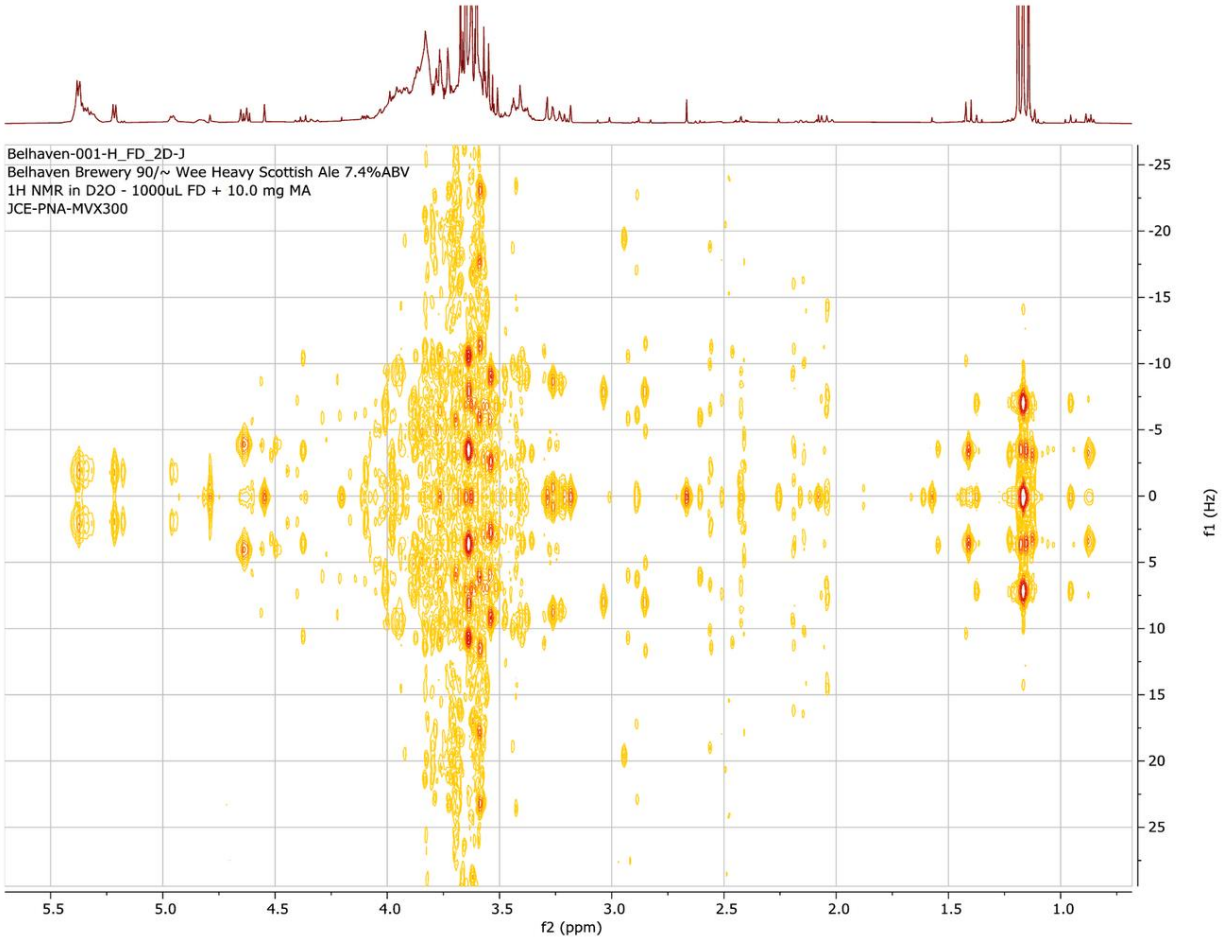


Figure 6. Two-dimensional J-resolved 300 MHz ^{1}H NMR spectrum of a lyophilized and reconstituted Belhaven 90/– Wee Heavy Scottish ale of 7.4 % v/v declared strength, prepared from 1000 µL of beer with 10.0 mg of maleic acid. The direct dimension carries chemical shift and the indirect dimension scalar coupling over ±25 Hz. The one-dimensional trace above the contour plot is the conventional spectrum of the same sample. Projection of the two-dimensional data onto the chemical-shift axis yields a proton-decoupled spectrum in which each spin system contributes a single line. Process NMR Associates data.

Beyond J-resolved spectroscopy the standard repertoire applies. Correlation and total correlation spectroscopy establish the through-bond networks that identify individual sugars and amino acids within the massif; heteronuclear single-quantum correlation spectroscopy exploits the roughly twentyfold greater chemical-shift dispersion of carbon-13 to resolve anomeric signals that are hopelessly overlapped in the proton dimension, and is discussed further in Section 6.13; and diffusion-ordered spectroscopy adds a molecular-size dimension that separates monosaccharide, oligosaccharide, and polymeric contributions without physical fractionation.[49,50] The coupling of liquid chromatography to NMR detection, applied to

beer by the Aveiro group, resolved the oligosaccharide series directly and remains the firmest experimental basis for the carbohydrate assignments used in Section 6.[4]

4.9 The Working Response-Factor Table

All of the foregoing reduces, for routine work, to a single table. Once the reporter signal, its proton count, and the molar mass of the component are fixed, equations (5) and (6) supply a scalar that converts the normalized integral directly into milligrams per liter. Table 9 gives those scalars for the principal analytical panel. The table is the operational heart of the method: it should be embedded in the integration template, checked against the certificate of the standard lot whenever that lot changes, and — once the relaxation survey recommended in Section 3.8 has been performed — multiplied through by the corresponding relaxation correction factors.

Table 9. Response factors k for the Process NMR Associates beer panel. Concentration in mg/L is the product of k and the reporter integral on the scale that sets the maleic acid singlet to 100. Native-aliquot factors are 9.797 M/N; lyophilized-aliquot factors are 1.714 M/N. The final column flags reporter signals that are not baseline-resolved at 300 MHz and that require lineshape fitting rather than fixed-window integration.

Component	δ (ppm)	N	M (g/mol)	Aliquot	k (mg/L per unit)	Resolved at 300 MHz?
Ethanol	1.18	3	46.07	Native	150.4 (0.01906 % v/v)	Yes
Methanol	3.36	3	32.04	Native	104.6	Yes
1-Propanol	0.89	3	60.10	Native	196.3	No — fusel envelope
Isobutanol	0.87	6	74.12	Native	121.0	No — fusel envelope
Isopentanol	0.88	6	88.15	Native	143.9	No — fusel envelope
Acetic acid	2.08	3	60.05	Native	196.1	Yes
Formic acid	8.44	1	46.03	Native	451.0	Yes
Ethyl acetate	1.28	3	88.11	Native	287.7	No — acetaldehyde hydrate
Acetaldehyde, free	2.22	3	44.05	Native	143.8	Yes; add hydrate for total
Acetaldehyde hydrate	1.31	3	62.07	Native	202.7	No — threonine, ethanol satellite
Lactic acid	1.41	3	90.08	Lyophilized	51.5	Yes in the lyophilizate
Succinic acid	2.67	4	118.09	Lyophilized	50.6	Yes
Malic acid	2.68 / 2.85	2	134.09	Lyophilized	114.9	No — aspartate
Citric acid	2.90 / 3.05	4	192.12	Lyophilized	82.3	Yes
Pyruvic acid	2.38	3	88.06	Lyophilized	50.3	Yes
Pyruvate hydrate	1.49	3	106.08	Lyophilized	60.6	No — alanine at δ 1.48
Glycerol	3.55–3.80	5	92.09	Lyophilized	31.6	No — proline, sugars
2,3-Butanediol	1.14	6	90.12	Lyophilized	25.7	Yes
1,3-Propanediol	1.76	2	76.09	Lyophilized	65.2	Yes
Alanine	1.48	3	89.09	Lyophilized	50.9	No — pyruvate hydrate
Valine	0.99 + 1.04	6	117.15	Lyophilized	33.5	No — fusel envelope

Component	δ (ppm)	N	M (g/mol)	Aliquot	k (mg/L per unit)	Resolved at 300 MHz?
Leucine	0.95, 0.96	6	131.17	Lyophilized	37.5	No — fusel envelope
Isoleucine	0.93	3	131.17	Lyophilized	75.0	No — fusel envelope
γ-Aminobutyric acid	3.01	2	103.12	Lyophilized	88.4	Yes
Proline	3.34 / 3.41	2	115.13	Lyophilized	98.7	No — sugar region
Tyrosine	6.90	2	181.19	Lyophilized	155.3	No — tyrosol, catechins
Phenylalanine	7.33	2	165.19	Lyophilized	141.6	No — 2-phenylethanol
Tryptophan	7.73 (H4)	1	204.23	Lyophilized	350.2	Partial
Histidine	8.62	1	155.15	Lyophilized	265.9	Yes
Uridine	7.87	1	244.20	Lyophilized	418.7	Yes
D-Glucose, total	5.23 (α)	1	180.16	Lyophilized	308.9 ÷ fα	No — malt α-reducing end
Lactose	4.45 (Gal-1H)	1	342.30	Lyophilized	586.9	Yes
α-Glucan, as anhydroglucose	4.95–5.43	1	162.14	Lyophilized	278.0	Envelope; see Section 6.3
Residual ethanol, control	1.18	3	46.07	Lyophilized	26.3	Yes

Factors computed for a maleic acid mass of 10.0 mg at 99.5 % purity and molar mass 116.07 g mol⁻¹, and not corrected for incomplete relaxation (Section 3.8). Glucose is quantified from the α-anomeric doublet and divided by the α-anomer mole fraction fα, for which see Section 6.5. Acetaldehyde is roughly half hydrated in aqueous solution, so the free-aldehyde and hydrate signals must be summed; the value obtained from δ 2.22 alone under-reports the total by approximately a factor of two. Formic acid has been assigned to the native aliquot because it is more volatile than acetic acid and its recovery through lyophilization has not been established; the lyophilized factor, should recovery be demonstrated, is 78.9. The α-glucan factor expresses concentration as anhydroglucose residues, which is the correct basis for a carbohydrate mass balance but is not the mass of carbohydrate present, for which see the note to Table 10. Entries flagged as unresolved cannot be integrated by fixed windows at 300 MHz and require global spectral deconvolution.

5. What the Numbers Say: A Survey of Commercial Beers

The commercial-beer set on which much of this document rests comprises twenty-three products analyzed in the original 2016 study, extended subsequently to thirty. The set was chosen for breadth rather than for statistical design and spans mass-market American lagers, light lagers, an imported lager, stouts including a milk stout and an imperial stout, an India pale ale, a Berliner Weisse, a spruce porter, Belgian-style abbey and fruit ales, a gose, an oak-aged sour, a coffee stout, and an apple ale. That breadth is a strength for demonstrating the reach of the technique and a weakness for any inference about population statistics, a point returned to in Section 8.4.

The routine analytical panel returned for each of these products comprises the alcohols ethanol, methanol, 1-propanol, isobutanol and isopentanol; the organic acids lactic, acetic, malic, succinic, pyruvic, pyruvic hydrate, tartaric and formic; the carbohydrates maltose, glucose, fructose, sucrose, lactose, isomaltose and kojibiose together with the malto-oligosaccharide series resolved by degree of polymerization and the limit dextrins; the amino acids alanine, valine, proline, γ-aminobutyric acid, tyrosine, tryptophan, histidine, glutamate, asparagine and phenylalanine; the nucleosides and nucleotides uridine and adenosine; and the further metabolites glycerol, acetoin, 2,3-butanediol, ethyl acetate and 1,3-propanediol. Where adjuncts are present, theobromine from cocoa, caffeine from coffee or tea, sorbate and benzoate preservatives, and tartaric acid from grape must are added to the report. The stated working limitation is that components

below approximately five to ten milligrams per liter are difficult to observe and quantify, which excludes the hop-derived bitter compounds and most low-concentration flavor defects from direct measurement in finished beer.

5.1 Ethanol

Ethanol is the least interesting analyte scientifically and the most consequential commercially, and it is the natural place to begin because it provides the method's cleanest accuracy check against an external truth. Figure 7 compares the NMR-determined alcoholic strength against the declared value for each product in the survey. The agreement is close across the range from light lagers below 4 % to imperial stouts approaching 10 %, and the residual scatter is the sum of three contributions that should not be conflated: the accuracy of the NMR determination, the accuracy of the brewer's own measurement, and the legal tolerance within which a declaration may lawfully differ from the contents. In the United States that tolerance is 0.3 percentage points for beers above 0.5 % alcohol by volume, which alone accounts for most of the observed spread. A disagreement between NMR and label of less than a third of a percentage point is therefore not evidence of an NMR error, and any attempt to use label values as reference data for method validation is methodologically unsound.

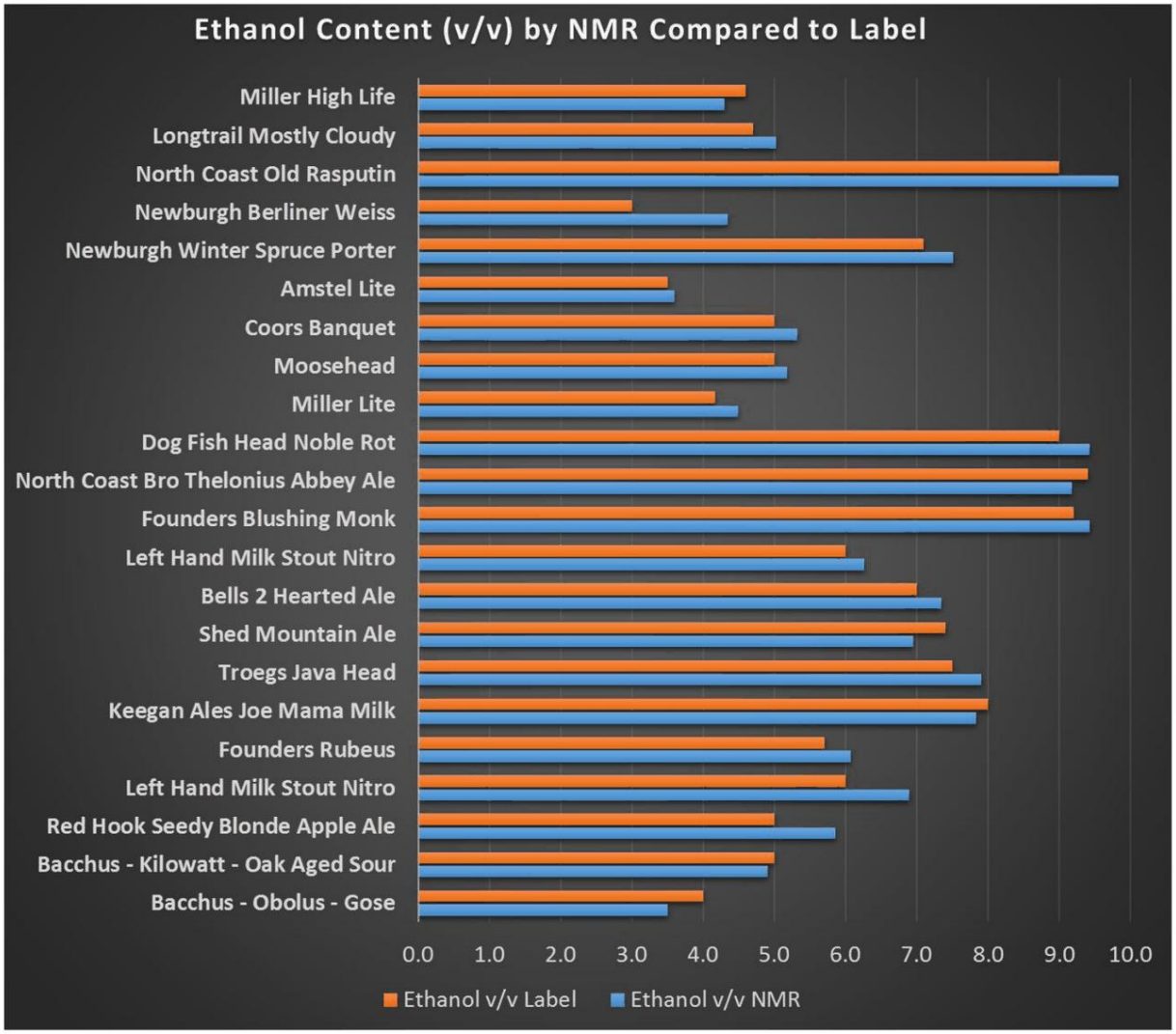


Figure 7. Alcoholic strength of twenty-three commercial beers determined by ^{1}H qNMR (orange) compared with the value declared on the package or at the tap (blue). NMR values were obtained from the ethanol methyl triplet of the native-beer aliquot using equations (5) and (7). Process NMR Associates data.

The determination has been shown elsewhere to correlate closely with headspace gas chromatography, refractometric and densitometric methods, and the distillation procedures of the American Society of Brewing Chemists, and the linearity of the NMR response across the full range from non-alcoholic products to distillates has been confirmed repeatedly.[63,64] Two properties distinguish the NMR determination in practice. It is unaffected by dissolved extract, so no correction is required for high-gravity or heavily dextrinous products where density methods require the real-extract correction; and it can be performed on a turbid or particulate sample without filtration.

5.2 Organic Acids

The organic acid profile is the single most diagnostic panel that the analysis produces, because each acid maps onto a distinct organism or metabolic route. Figure 8 shows the distribution across the survey set as stacked contributions of lactic, succinic, acetic, malic, pyruvic, pyruvate hydrate, citric, and formic acids.

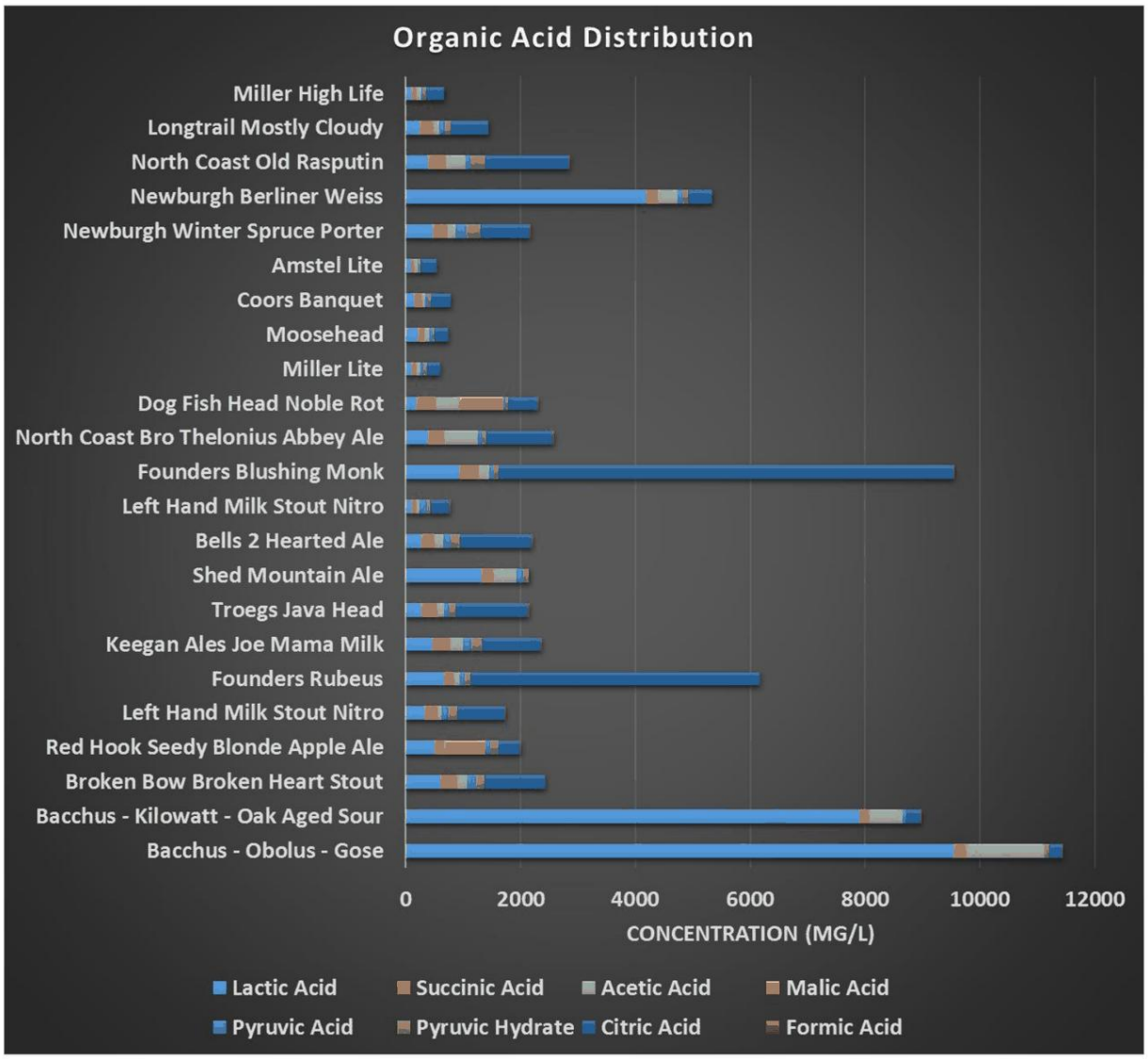


Figure 8. Organic acid distribution across twenty-three commercial beers, determined by ^{1}H qNMR on the lyophilized aliquot. Stacked contributions are lactic, succinic, acetic, malic, pyruvic, pyruvate hydrate, citric, and formic acids, in mg/L. The sour and mixed-fermentation products at the foot of the chart carry lactic acid burdens an order of magnitude above the conventionally fermented products above them. Process NMR Associates data.

Several patterns are immediately legible. Conventionally fermented lagers and ales carry total organic acid burdens of a few hundred to somewhat over a thousand milligrams per liter, dominated by succinate and acetate with lactate present at low level. The deliberately soured products — the Berliner Weisse, the gose, and the oak-aged sour — separate from the rest by an order of magnitude in lactate, and in the oak-aged product acetate rises with it in the ratio characteristic of a mixed lactic and acetic fermentation. The presence of malate identifies fruit or must additions, since malic acid is not a significant product of a normal barley fermentation; the apple ale and the wine-must-containing products in the set are identified by malate alone. Citrate arises from wort and from any citrus or fruit addition and is drawn down by lactic acid bacteria possessing citrate lyase.

The forensic application follows directly. Unexpected lactate in a product that was not intended to be soured identifies lactic acid bacterial activity, and its ratio to acetate discriminates homofermentative from

heterofermentative organisms. Formate, which arises from pyruvate–formate lyase and is essentially absent from a clean Saccharomyces fermentation, is a specific marker of enterobacterial or clostridial contamination; because formic acid is more volatile than acetic acid it is quantified in the native aliquot, where its formyl singlet at δ 8.44 stands alone in an otherwise empty region, and its relaxation time is long enough that the correction of Section 3.8 applies to it more strongly than to any other analyte in the panel. Elevated pyruvate together with residual fermentable sugar identifies a stalled or nitrogen-limited fermentation rather than a microbiological one. None of these inferences requires a separate assay; all are read from the same spectrum that supplied the alcohol result.

Two further readings of the acid panel deserve to be made explicit because they are easily missed. Pyruvate is observed as two species in equilibrium — the free ketone through its methyl singlet at δ 2.38 and the geminal diol hydrate through its singlet at δ 1.49 — and the two must be summed for a total; the partition between them is reproducible under the fixed conditions of Section 3.4.1, so a departure from the usual ratio flags an integration or assignment problem rather than chemistry. Succinate carries a diagnostic value complementary to that of lactate: it is produced by yeast through the reductive branch of the tricarboxylic acid cycle and through nitrogen metabolism under anaerobiosis, typically at fifty to one hundred and fifty milligrams per liter in a clean fermentation, so elevated succinate in the absence of elevated lactate points to yeast stress — osmotic, nitrogen, or temperature — rather than to bacterial activity, a distinction that determines whether the corrective action belongs in the cellar or in the sanitation program.

> *Author data placeholder — organic acid concentration table. The tabulated per-product concentrations underlying Figure 8, with replicate statistics, are to be inserted here. A table of mean, range, and coefficient of variation by beer style would materially strengthen the argument and would supply the reference distribution against which a suspect sample is later judged.*

5.3 Amino Acids and Yeast-Assimilable Nitrogen

Figure 9 shows the free amino acid and nucleoside distribution across the survey, and Figure 10 the pure-component spectra against which those assignments were made. Proline dominates, for the reason set out in Section 4.4, and is followed by alanine, γ-aminobutyric acid, valine, and the aromatic amino acids. The analytically useful quantity is not the total but the partition: proline, which the yeast cannot use anaerobically, against the assimilable remainder, which it can. A high residual assimilable fraction in a finished beer indicates that nitrogen was not limiting and that the fermentation ended for another reason; a fully depleted assimilable pool alongside residual fermentable sugar indicates nitrogen limitation directly. Neither inference is available from a ninhydrin free amino nitrogen number, which sums the two categories into a single figure and cannot distinguish them.[59] In the products surveyed here, proline spans roughly one hundred and fifty to seven hundred milligrams per liter and scales with all-malt character and original gravity, while the assimilable pool of a well-attenuated beer is drawn down to a few tens of milligrams per liter per amino acid.

γ-Aminobutyric acid warrants separate mention. It arises from glutamate decarboxylation, is present in malt, is produced and consumed differentially by yeast and by lactic acid bacteria, and rises markedly in sour and mixed-culture fermentations. In the sour mash study of Section 7.1 it was tracked explicitly as a contaminant marker.

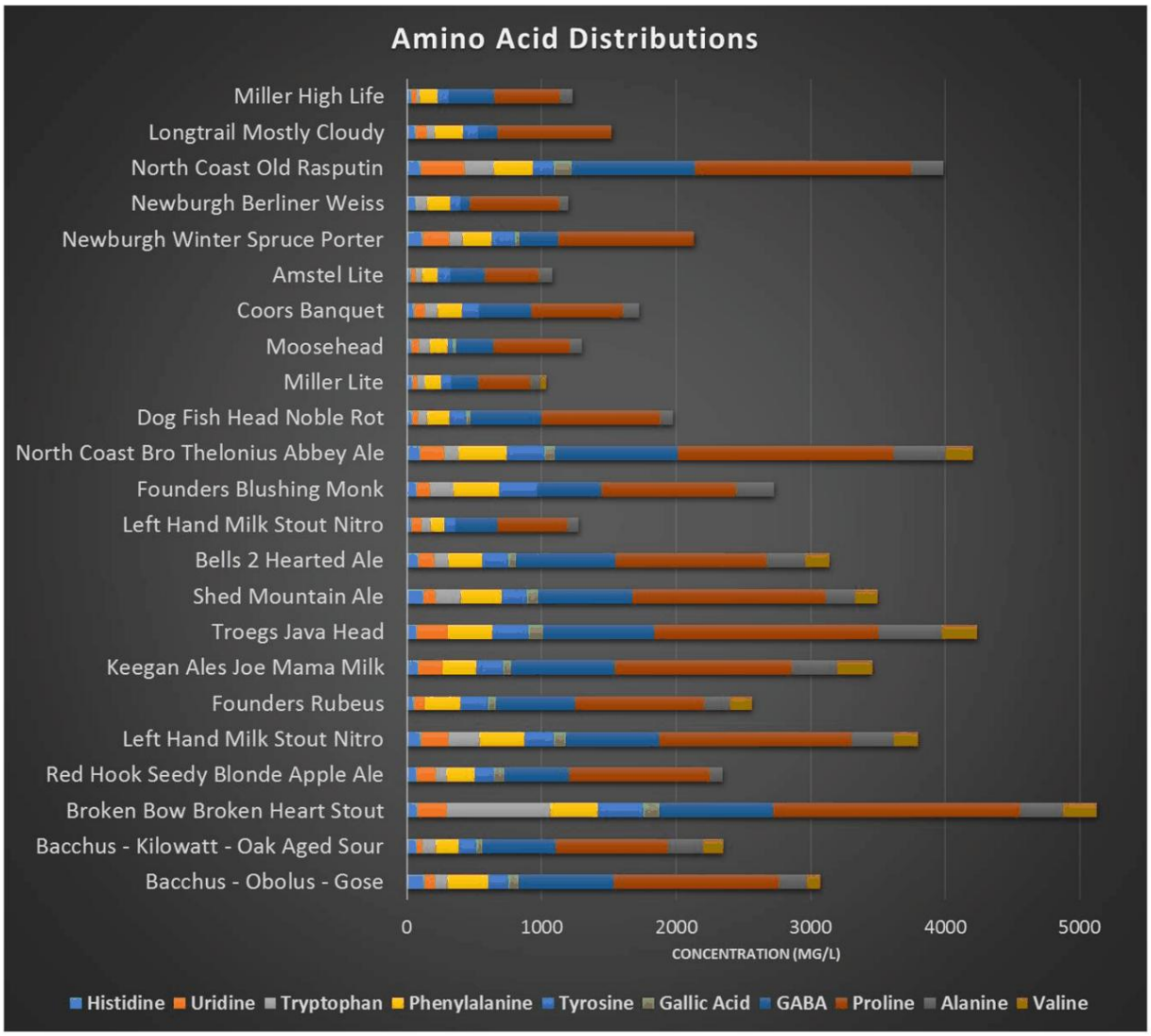


Figure 9. Free amino acid and nucleoside distribution across twenty-three commercial beers by ^{1}H qNMR. Stacked contributions are histidine, uridine, tryptophan, phenylalanine, tyrosine, gallic acid, γ-aminobutyric acid, proline, alanine, and valine, in mg/L. Proline is the largest single contributor in nearly every product, reflecting its non-assimilability under anaerobic fermentation conditions. Process NMR Associates data.

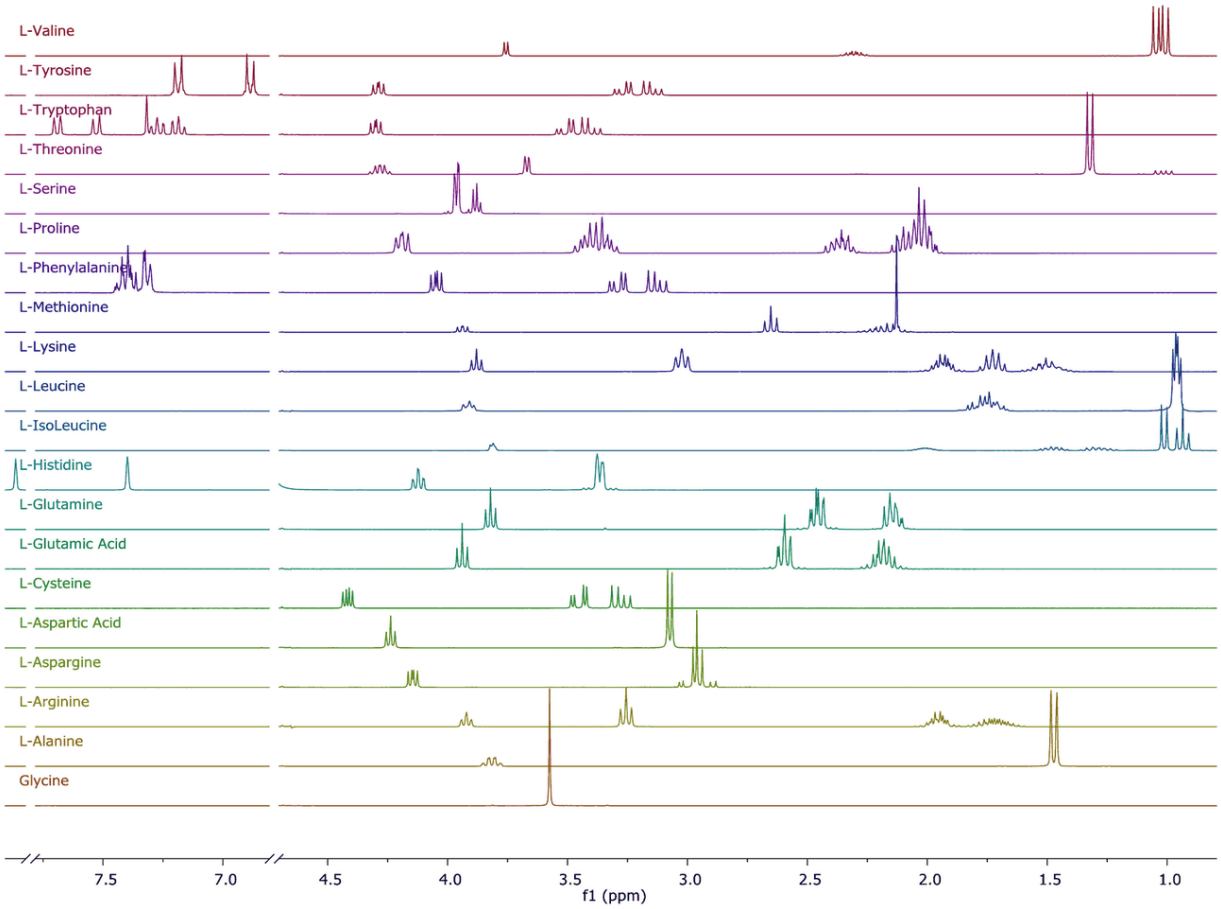


Figure 10. Pure-component 300 MHz ^{1}H spectra of the amino acids used to establish the assignments of Figure 9, acquired in acidified D_2O under matched conditions. The library approach shown here is what permits confident assignment within the congested mixture spectrum. Process NMR Associates data.

5.4 Higher Alcohols, Esters, and Diols

The fusel alcohols — 1-propanol, isobutanol, and isopentanol — arise from the Ehrlich degradation of the corresponding branched-chain and aliphatic amino acids and from de novo synthesis, and their aggregate concentration tracks fermentation temperature, pitching rate, wort nitrogen, and yeast strain. They are quantified in the native aliquot from their methyl multiplets between δ 0.85 and 1.0, with the caveat regarding the ethanol carbon-13 satellite noted in Section 3.9. 2,3-Butanediol, the reduction product of acetoin and hence the terminal member of the vicinal diketone pathway, is quantified from its clean methyl doublet at δ 1.14; its presence at appreciable concentration alongside a low diacetyl result indicates that the diketone rest was effective, and it is one of the few handles NMR offers on a pathway whose immediate intermediates lie below the detection limit.

The acetate esters are at the margin of one-dimensional quantitation in most beers. Ethyl acetate at thirty to sixty milligrams per liter yields an ethyl triplet integral of roughly 0.1 to 0.2 on the maleic acid scale in the native aliquot, which is measurable but carries a large relative uncertainty and sits beneath the acetaldehyde hydrate doublet. Isoamyl acetate, typically below five milligrams per liter, is not reliably quantified by this method and should be referred to headspace gas chromatography. The limitation is real and should be stated to clients rather than passed over.

5.5 Nutritional Bookkeeping

Because the analysis returns a complete quantitative inventory rather than a set of disconnected results, the nutritional declaration follows arithmetically without further measurement. The energy content of a serving is

$$E\ (\text{kcal}) = V \cdot [\ 7.0 \cdot c_EtOH + 4.0 \cdot c_carb + 4.0 \cdot c_AA + 3.0 \cdot c_acid\ ] \quad (10)$$

in which V is the serving volume in liters, the concentrations c are in grams per liter, the coefficients are the conventional energy factors in kilocalories per gram for ethanol, available carbohydrate, protein and amino acids, and organic acids respectively, and the product V·c is therefore a mass in grams. For a twelve United States fluid ounce serving, V = 0.3549 L. The carbohydrate term is the sum of the free sugars and the residual dextrins expressed as anhydroglucose, which is precisely what the anomeric integration of Section 6 provides, and it is worth emphasizing that no other routine method delivers that term directly — density-based real extract requires an assumed composition, and chromatographic sugar panels stop short of the dextrins.

The bookkeeping can be checked against a declaration. A non-alcoholic malt beverage analyzed in this laboratory returned 7.6 g of carbohydrate per twelve-ounce serving and an alcoholic strength of 0.47 % v/v. The ethanol mass in the serving is $0.0047 \times 354.9\ \text{mL} \times 0.789\ \text{g mL}^{-1} = 1.316$ g, contributing 9.2 kcal; the carbohydrate contributes 30.4 kcal; the amino acids and organic acids together contribute approximately 0.5 kcal. The total, 40.1 kcal, was returned against a declared 41 kcal and a declared 8 g of carbohydrate. The agreement should not be read as two independent confirmations, since three-quarters of the calculated energy is the carbohydrate term and the calorie result is therefore largely a restatement of the carbohydrate result. Nor are the two carbohydrate figures the same measurand: a declared total carbohydrate is conventionally obtained by difference from protein, fat, moisture, and ash, whereas the NMR figure is a direct sum of the sugars and dextrins actually observed. Figure 11 presents the same calculation as a component breakdown across the survey set, and the partition it displays — the proportion of a beer's energy that comes from alcohol against the proportion that comes from carbohydrate — is a genuinely useful product-development variable that is not otherwise easy to obtain.

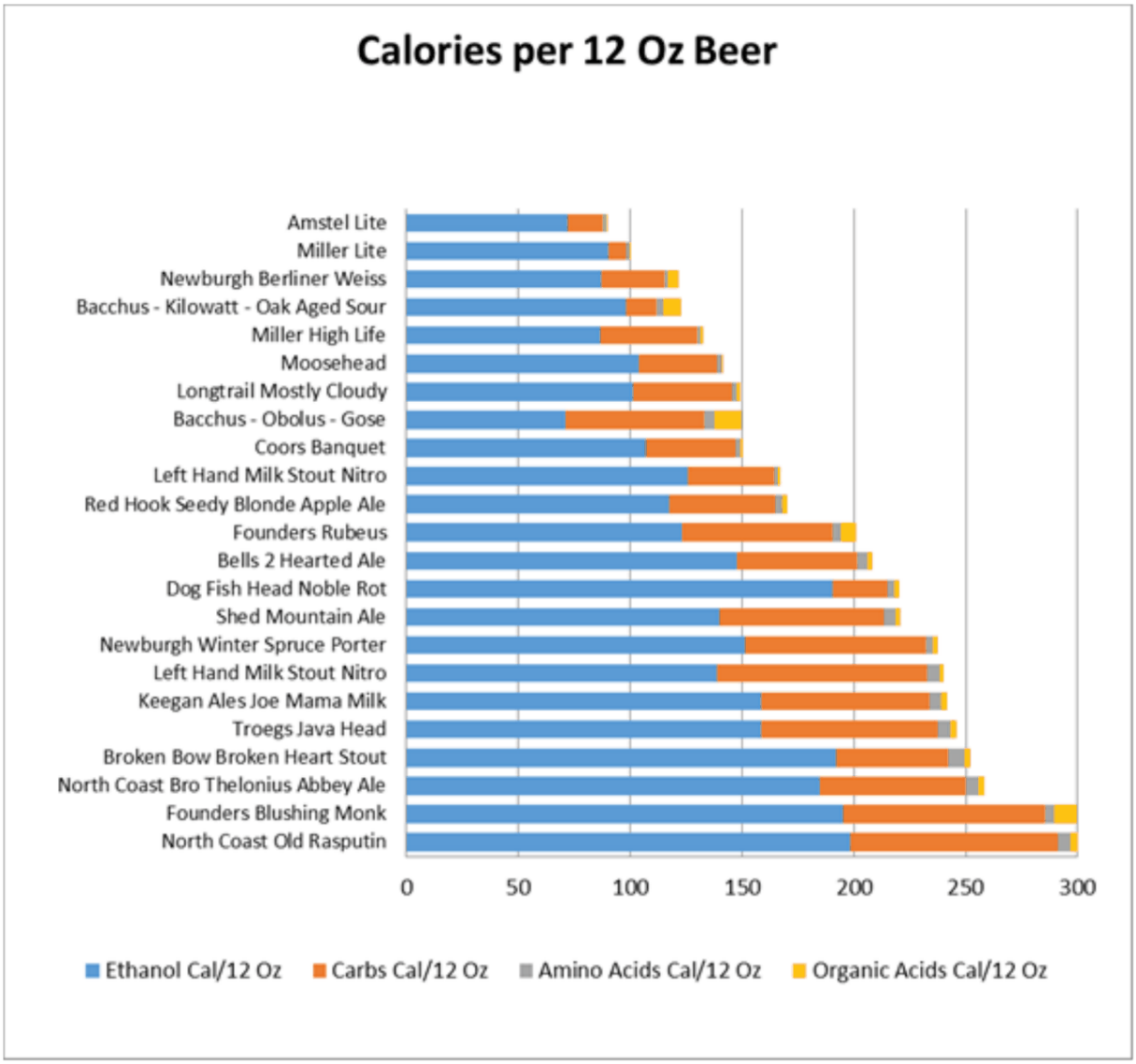


Figure 11. Energy content per twelve fluid ounce serving for the commercial beer survey, resolved into contributions from ethanol, carbohydrate, amino acids, and organic acids, computed from the qNMR composition by equation (10). The ordering makes clear that products of similar total energy can differ greatly in the origin of that energy. Process NMR Associates data.

Table 10. Energy factors and the derivation of nutritional declaration values from the qNMR composition.

Declared quantity	Derived from	Factor	Notes
Alcohol by volume	Ethanol methyl triplet, native aliquot	k = 150.4; ÷ 7890	Density 0.789 g/mL at 20 °C
Total carbohydrate	Anomeric envelope as anhydroglucose plus free sugars	k = 277.9 per residue	Includes non-fermentable dextrins; the term no other routine method supplies directly
Energy from alcohol	Ethanol mass in the serving	7.0 kcal/g	Universal factor
Energy from carbohydrate	Total carbohydrate mass in the serving	4.0 kcal/g	Available carbohydrate basis

Declared quantity	Derived from	Factor	Notes
Energy from protein	Sum of free amino acids	4.0 kcal/g	Underestimates where peptide nitrogen is significant
Energy from organic acids	Sum of quantified organic acids	3.0 kcal/g	Significant only in sour styles
Total energy	Sum of the above	—	Reproduced a declared 41 kcal as 40.1 kcal in the worked case
Sugars	Free glucose, fructose, maltose, lactose anomeric signals	compound-specific k	Lactose in milk stouts is resolved and quantified separately

Two refinements should be applied before a declaration is issued. The anomeric integral counts anhydroglucose residues of mass 162.14 g mol⁻¹, whereas the carbohydrate actually present has mass 162.14 × residues + 18.02 × chains, the second term being the water taken up on hydrolysis; at a number-average degree of polymerization near 2.4 this raises the carbohydrate figure by some 4.6 percent, and at a degree of polymerization near 6 by about 1.9 percent. The protein term is a lower bound, since qNMR quantifies free amino acids and not peptide-bound nitrogen; where a regulatory protein declaration is required a Kjeldahl or Dumas determination remains necessary.

5.6 Other Nuclei

Proton is not the only accessible nucleus and the opportunity should be noted even though it has not yet been developed in this laboratory. Sodium-23 is a spin-3/2 quadrupolar nucleus of one hundred percent natural abundance and high receptivity, and sodium in beer, which must be declared nutritionally and which matters in gose and in water-treatment control, is quantifiable at the milligram-per-liter level in a short acquisition with essentially no sample preparation beyond that already performed. Phosphorus-31 offers access to the phosphate and organophosphate pool, including inositol phosphates from malt and the residual nucleotide phosphates, in a spectrum that is uncluttered by comparison with the proton spectrum. Carbon-13, at natural abundance and in the two-dimensional heteronuclear correlation format discussed in Section 6.13, is where the dextrin structural work has its greatest remaining headroom.

> *Author data placeholder — sodium-23 feasibility. A short ²³Na acquisition on a representative gose and a representative lager, with a sodium chloride external standard, would establish the detection limit and the achievable precision and would extend the nutritional declaration package to sodium without a separate technique.*

5.7 Traditional Brewing Parameters from the NMR Composition

A brewer does not think in milligrams per liter of maltotriose. The working vocabulary of the brewhouse is original extract in degrees Plato, apparent and real extract, alcohol by volume, and the apparent and real degrees of fermentation, and a compositional method that cannot speak that vocabulary will not displace the hydrometer however superior its chemistry. Every one of those parameters is, however, derivable from the qNMR composition, because each is definitionally a function of two quantities the analysis measures directly — the ethanol content and the dissolved solids — connected through the fermentation mass balance formulated by Balling in the 1840s and re-examined against modern pilot-plant and commercial data by Cutaia and co-workers.[66]

The mass balance states that 2.0665 g of fermented extract yields 1.0000 g of ethanol together with 0.9565 g of carbon dioxide, which leaves the beer, and 0.1100 g of new yeast mass, which is removed with the crop. Because the carbon dioxide departs, the original wort cannot be reconstructed by simple addition of what remains; the Balling relation performs the bookkeeping,

$$OE = 100 \times (2.0665 \cdot A + E_r) / (100 + 1.0665 \cdot A) \quad (11)$$

in which OE is the original extract in g per 100 g of wort (degrees Plato), E_r the real extract in g per 100 g of beer, and A the ethanol content in g per 100 g of beer. Both inputs come from the spectrum. A follows from the volumetric ethanol determination of Section 5.1 as $A = 0.789 \cdot ABV/\rho$, in which ρ is the density of the beer in g mL^{-1}; the density enters only as a scale factor, and adopting $\rho = 1.010$ for a conventional beer introduces less than 0.2 percent relative error in A, though nothing prevents a measured density from being used where one is available. The real extract is the sum of the observed dissolved solids — the carbohydrate total with the chain-water correction of the note to Table 10, glycerol, the organic acids, and the free amino acids — plus an explicit allowance of 0.3 to 0.5 g per 100 mL for the soluble protein, polyphenol, and mineral matter that the proton spectrum does not observe. The NMR real extract without that allowance is a defined lower bound and should be reported as such.

The apparent extract, which is what a hydrometer reads in the presence of ethanol, is connected to the real extract through the empirical relation of Balling,

$$E_r = 0.1808 \cdot OE + 0.8192 \cdot AE \quad (12)$$

which is rearranged for AE once OE is in hand, and the two attenuation figures follow by definition,

$$ADF\ (\%) = 100 \times (OE - AE) / OE \quad (13)$$

$$RDF\ (\%) = 100 \times (OE - E_r) / OE \quad (14)$$

with the small corrections for dissolved carbon dioxide and for the nonlinearity of the Plato scale discussed by Cutaia and co-workers applied where certificate-grade values are required.[66] Specific gravities for the brewing record follow from the Plato values through the usual conversion, for which the approximation $SG \approx 1 + 0.004 \cdot °P$ suffices at the precision of a brewhouse log.

Carried through for the worked lager of Section 3.7, with an illustrative observed-solute total of 41.5 g L^{-1} standing in for the per-product value: the ethanol of 4.98 % v/v gives A = 3.89 g/100 g; the observed solutes give 4.11 g/100 g, and with a 0.3 g allowance the real extract is 4.4 g/100 g; equation (11) returns an original extract of 11.94 °P, corresponding to an original gravity near 1.048; equation (12) returns an apparent extract of 2.74 °P, a final gravity near 1.011; and the attenuations follow as ADF = 77.1 % and RDF = 63.2 %. These are the numbers of a conventional twelve-degree lager, recovered from a single spectrum without a hydrometer, a distillation, or a density meter, and they are the numbers a brewmaster will actually read.

On the wort side of the fermenter the same quantities are measured rather than reconstructed. The mash and wort carbohydrate totals of Section 6.10, at 128 to 147 g L^{-1}, place the carbohydrate contribution to extract at twelve to fourteen degrees Plato; wort extract exceeds its carbohydrate by roughly a tenth of protein, mineral, and phenolic matter, so the same explicit allowance applied on the beer side belongs here before an original-extract figure is claimed. On that basis, and the fermentable-to-non-fermentable partition of Section 6.6 converts a wort measurement into a predicted apparent extract and attenuation before the yeast is pitched — which is the information content of the forced-fermentation attenuation-limit test, obtained in sixteen minutes instead of two days. A free-amino-nitrogen analogue is likewise available: the molar sum of the quantified amino acids converts to α-amino nitrogen as $N\ (mg/L) = 14.007 \times \Sigma\, c_i/M_i$, with the caveat that the ninhydrin method against which the result will be compared responds to proline only weakly, so the NMR figure is best reported both with and without the proline contribution.

What the spectrum cannot supply should be stated with equal clarity. Bitterness units are not accessible, because the iso-α-acids lie below the one-dimensional detection limit in finished beer (Sections 7.6 and 9). Color is a visible-wavelength property with no proton signature. And pH is not recoverable from a preparation whose pH has been fixed near 1.5 by the internal standard, as Section 3.4.1 establishes — the one brewhouse number for which the electrode remains irreplaceable. Table 11 collects the parameter set.

Table 11. Traditional brewing parameters and their derivation from the qNMR composition. Worked values refer to the illustrative lager of Section 3.7 and are flagged as illustrative pending per-product data.

Parameter	Conventional determination	NMR route	Relation	Worked value
Alcohol by volume	Distillation + pycnometry; GC; densitometry	Ethanol CH_3 integral, native aliquot	Eqs (5), (7)	4.98 % v/v
Alcohol by weight	Calculated from ABV and density	$A = 0.789 \cdot ABV/\rho$, $\rho \approx 1.010$	—	3.89 g/100 g
Real extract	Distillation residue + pycnometry	Σ observed solutes + 0.3–0.5 g/100 mL allowance	Table 10 note	4.4 g/100 g
Original extract	Brewhouse record; Balling back-calculation	Reconstructed from A and E_r	Eq (11)	11.94 °P
Original gravity	Hydrometer on wort	From OE	SG ≈ 1 + 0.004·°P	≈ 1.048
Apparent extract	Hydrometer on beer	From OE and E_r	Eq (12)	2.74 °P
Final gravity	Hydrometer on beer	From AE	SG ≈ 1 + 0.004·°P	≈ 1.011
Apparent degree of fermentation	Hydrometer pair	From OE and AE	Eq (13)	77.1 %
Real degree of fermentation	Distillation pair	From OE and E_r	Eq (14)	63.2 %
Calories per serving	Calculation from composition	Direct from the quantified inventory	Eq (10)	Section 5.5
Wort fermentability / attenuation limit	Forced fermentation, two days	Fermentable partition of the anomeric integrals	Section 6.6	—
Free amino nitrogen	Ninhydrin colorimetry	$N = 14.007 \times \Sigma\, c_i/M_i$ over the amino acid panel	Section 5.3	—
Bitterness (IBU)	Iso-octane extraction, A_{275}	Not accessible at the 1D detection limit	Sections 7.6, 9	—
Color	Absorbance at 430 nm	Not accessible	—	—
pH	Electrode	Not accessible; tube pH fixed by the standard	Section 3.4.1	—

The Balling coefficient of 2.0665 g extract per g ethanol and the relation of equation (12) are as re-examined by Cutaia and co-workers, whose small corrections for dissolved CO_2 and Plato-scale nonlinearity should be applied where certificate-grade attenuation values are required.[66]

> *Author data placeholder — brewing-parameter table for the survey. Applying equations (11) to (14) to each product of the twenty-three-beer survey, once the per-product solute totals are tabulated, yields OE, ADF, and RDF columns that can be checked directly against brewers' declarations and that translate the entire chemometric data set into the vocabulary its commercial audience uses.*

6. Residual Dextrin Chemistry

The material treated in this section is, in the author's judgment, where quantitative NMR of beer has least competition and most remaining headroom. Everything else the method measures can in principle be measured another way, at greater cost and in more separate operations. The structural distribution of the residual α-glucan dextrins cannot: the chromatographic sugar panels used in most breweries resolve glucose, maltose, maltotriose, and maltotetraose and then report everything larger as a single undifferentiated peak, while the density-based real-extract determination that carries most of the commercial weight infers a carbohydrate mass from a physical property without any structural content whatever. The anomeric region of the ^{1}H spectrum contains, directly and quantitatively, the linkage type, the branch density, the approximate chain-length distribution, and the number of reducing termini. The purpose of this section is to set out what can be extracted from it, how, and with what confidence.

6.1 Where Limit Dextrins Come From

Barley starch is a mixture of amylose, an essentially linear α-(1→4)-linked glucan, and amylopectin, a very large branched glucan in which α-(1→6) branch points occur at roughly one residue in twenty. Gelatinization during mashing renders both accessible to the amylolytic enzymes of the malt, and the composition of the resulting wort is determined by the relative activity of three enzyme classes acting under a common set of temperature and pH conditions.

α-Amylase is an endo-acting enzyme that hydrolyzes internal α-(1→4) bonds at random and reduces the substrate rapidly to a broad distribution of dextrins, but it cannot cleave α-(1→6) linkages and is sterically hindered in their vicinity. β-Amylase is an exo-acting enzyme that removes maltose units successively from non-reducing chain ends; it too cannot pass a branch point and halts two or three residues short of one. Limit dextrinase, the malt debranching enzyme, is the only activity capable of hydrolyzing α-(1→6) bonds, and it is present at low levels, is largely bound to an endogenous inhibitor, and is thermally fragile at conventional mashing temperatures. The practical consequence is that the branch points survive.

What remains at the end of mashing is therefore not a uniform low-molecular-weight sugar mixture but a bimodal one: a fermentable fraction consisting of glucose, maltose, and maltotriose, which yeast will convert to ethanol and carbon dioxide, and a non-fermentable fraction consisting of branched α-limit dextrins in which every remaining α-(1→6) linkage is flanked by the α-(1→4) residues that the amylases could not reach. Figure 12 illustrates the process schematically. The classical structural characterization of this material was performed in the late 1960s and early 1970s by Enevoldsen and co-workers, who used β-amylase digestion in combination with the debranching enzyme pullulanase to establish that wort dextrins comprise singly-branched and multiply-branched species with characteristic chain-length distributions,[47,48] and that account remains the reference description of what the anomeric region of a beer spectrum is looking at.

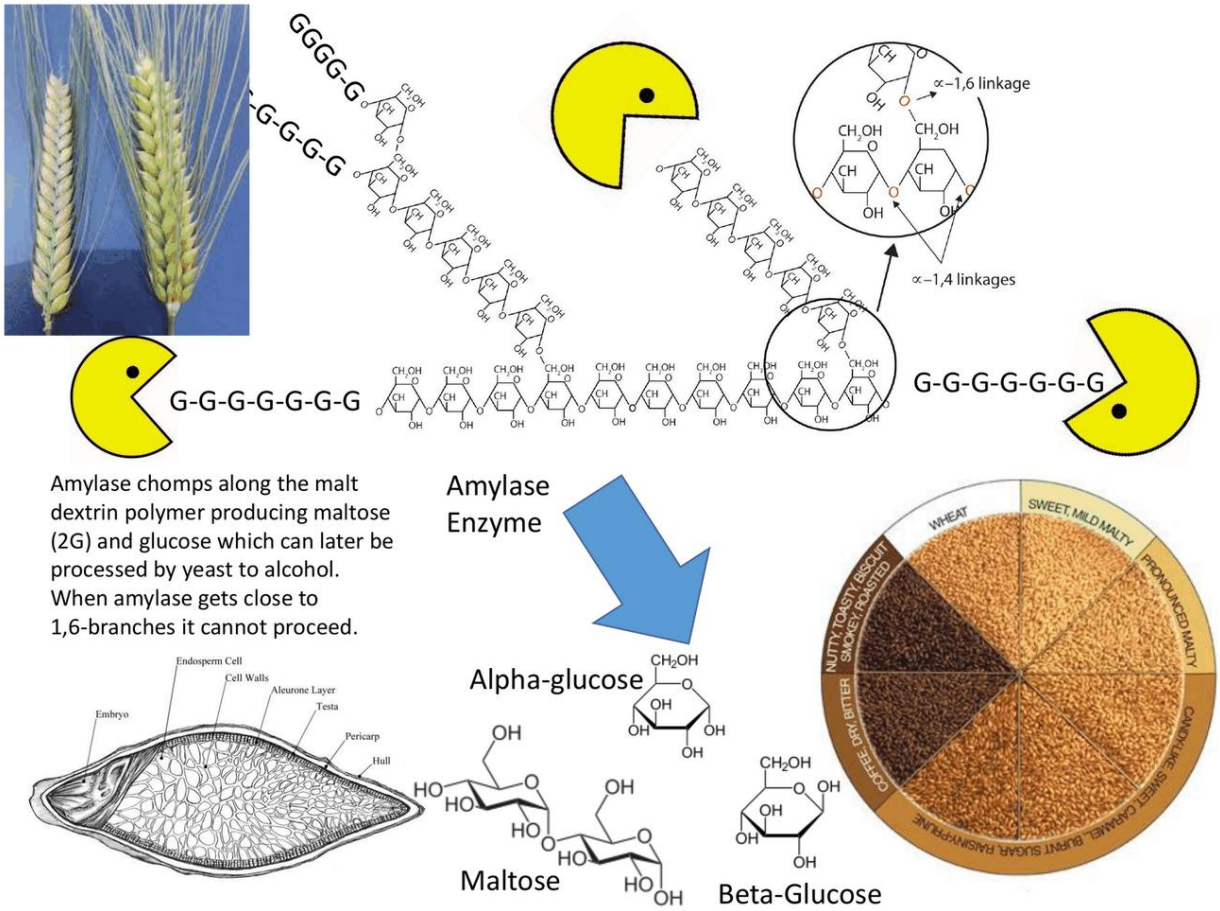


Figure 12. Schematic representation of amylolysis during mashing. Amylase acts processively along the α-(1→4)-linked glucan chain, liberating maltose and glucose which the yeast subsequently ferments, but is unable to proceed past an α-(1→6) branch point. The residue is a branched α-limit dextrin whose branch-proximal α-(1→4) linkages and α-(1→6) linkage survive into the finished beer. Anomeric configurations of the liberated α- and β-glucose and of maltose are indicated. Process NMR Associates presentation material.

6.2 The Anomeric Fingerprint of Finished Beer

Figure 13 is the central experimental result of this document. It superimposes the anomeric region, δ 4.42 to 5.57, of the lyophilized preparations of twenty-three commercial finished beers, with the water resonance suppressed and a break inserted across the suppression zone. The assignments annotated on it were established at Process NMR Associates over several years of work on beers, worts, mashes, malt extracts, and reference sugars, and they agree in every essential respect with the independent assignments published by the Carlsberg and Technical University of Denmark groups on the basis of liquid chromatography with NMR detection, chemically synthesized limit dextrin model compounds, and heteronuclear correlation spectroscopy.[4,38,40,41]

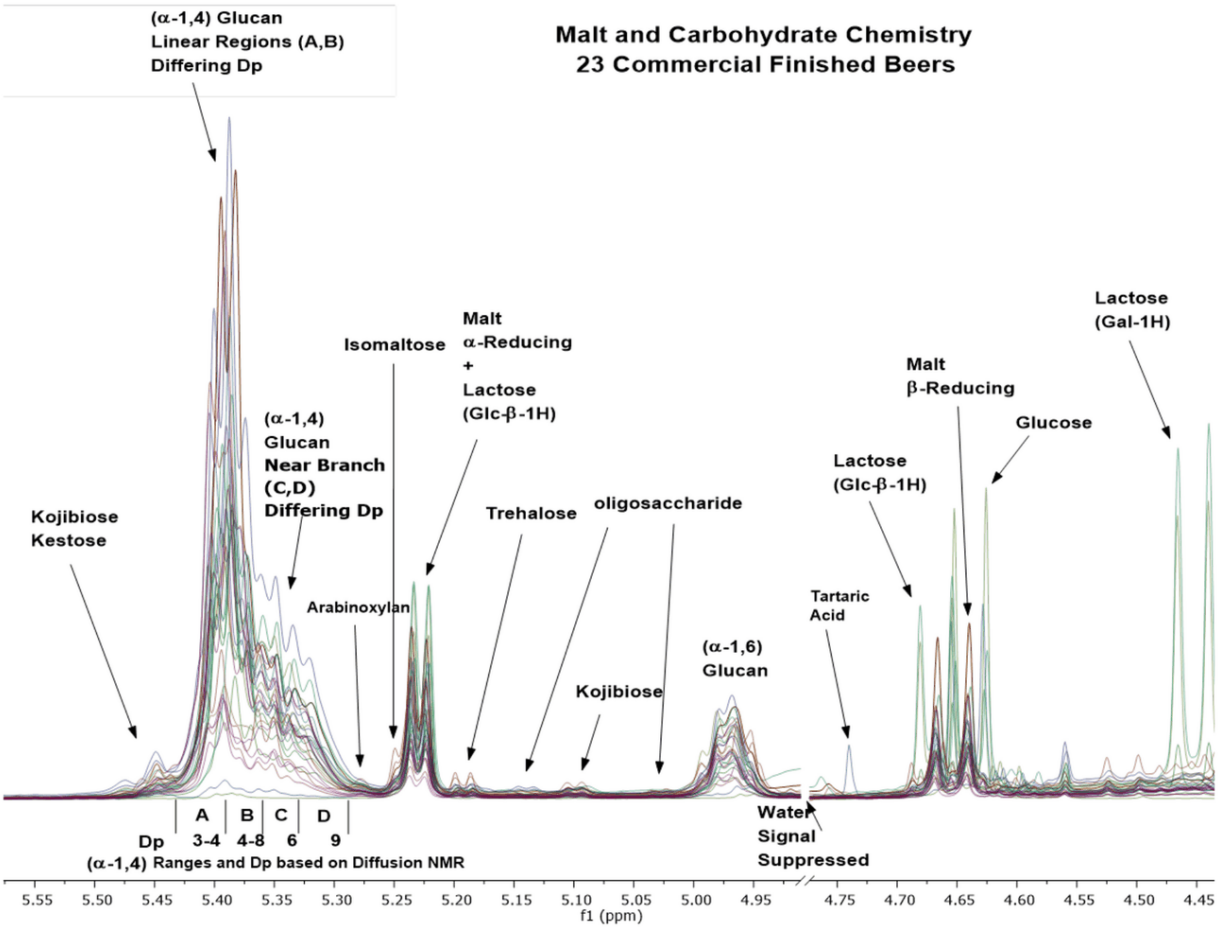


Figure 13. Superimposed 300 MHz ^{1}H NMR spectra of twenty-three commercial finished beers over the anomeric region, δ 4.42 to 5.57, acquired on lyophilized and reconstituted preparations. The water resonance is suppressed and the spectrum is broken across the suppression zone. Annotated assignments, from low to high frequency: lactose galactose anomeric proton at δ 4.45; free glucose β-anomeric doublet at δ 4.63; the malt β-reducing-end doublet at δ 4.65; the lactose glucose β-anomeric doublet at δ 4.67; tartaric acid near δ 4.74; the α-(1→6) glucan branch-point envelope at δ 4.95 to 5.00; minor oligosaccharide and kojibiose signals between δ 5.03 and 5.15; trehalose at δ 5.19; the composite malt α-reducing end and lactose glucose α-anomeric doublet at δ 5.22; isomaltose at δ 5.25; arabinoxylan at δ 5.28; and the α-(1→4) glucan envelope from δ 5.29 to 5.43, subdivided into windows A and B for the linear regions and C and D for the branch-proximal regions, with the degrees of polymerization indicated beneath having been assigned on the basis of diffusion NMR. Kojibiose and kestose appear at δ 5.44 to 5.46. Process NMR Associates data.

Three families of signal carry the structural argument and it is worth separating them clearly. The α-(1→4) envelope between δ 5.29 and 5.45 arises from the anomeric protons of internal glucose residues joined by α-(1→4) linkages, and it therefore counts the α-(1→4) bonds in the sample. The α-(1→6) envelope between δ 4.95 and 5.00 arises from the anomeric protons of residues joined through the 6-position, and it therefore counts the branch points; its separation from the nearest α-(1→4) resonance by some 0.3 ppm, remarked upon in the model-compound work, is what makes branch quantitation straightforward.[40] The envelope is free of α-(1→4) overlap; it is not free of every interference, and the isomaltose contribution discussed in Section 6.11 lies within it. The reducing-end pair — the α doublet near δ 5.22 and the β doublet near δ 4.65 — counts the chains, since every oligosaccharide molecule possesses exactly one reducing terminus regardless of its size or branching.

One annotation carried on the figure itself requires correction, and has been corrected in the caption above. The figure labels the signal at δ 5.22 as the malt α-reducing end together with the glucose β-anomeric proton of lactose. That cannot be right on chemical grounds: the β-anomeric proton of the reducing glucose of lactose resonates near δ 4.67, where the figure correctly labels a second lactose feature, while the resonance at δ 5.22 is the corresponding α-anomeric proton. The galactose anomeric proton, which is fixed in the β configuration by the glycosidic bond, gives the doublet at δ 4.45. The three lactose signals are therefore Glc-α-1H at δ 5.22, Glc-β-1H at δ 4.67, and Gal-1H at δ 4.45, and the annotation should be amended accordingly. The correction matters practically, because lactose in a milk stout adds to the malt α-reducing signal at δ 5.22 in proportion to its α-anomer fraction and must be subtracted before the reducing-end count is used to compute a degree of polymerization; the galactose doublet at δ 4.45, which is free of interference, is the correct handle for that subtraction.

Table 12. Assignments in the anomeric region of lyophilized beer, δ 4.4 to 5.5, with structural significance. Chemical shifts are those observed in the Process NMR Associates preparations; literature values for reference sugars are drawn from the carbohydrate reference library of Petersen and co-workers.[39]

δ (ppm)	Assignment	Mult. (J, Hz)	Counts	Remarks
4.45	Lactose, Gal-1H	d (7.8)	lactose molecules	Anomerically fixed; the correct reporter for lactose
4.55–4.60	β-glucan anomeric (minor)	d (7.9)	(1→3),(1→4)-β-glucan	Cereal polysaccharide; broad, diffusion-distinct
4.63	D-Glucose, β-anomer	d (7.9)	free glucose (β fraction)	Partner of the δ 5.23 α-doublet
4.65	Malt oligosaccharide reducing end, β	d (7.9)	chains (β fraction)	Principal β reducing-end reporter
4.67	Lactose, Glc-β-1H	d (7.9)	lactose (β fraction)	Overlaps the malt β-reducing signal
4.6–4.75	Tartaric acid	s	grape must addition	Position depends strongly on protonation; at the working pH the fully protonated form is observed near δ 4.74, at the edge of the suppression zone. Confirm against a spiked standard before forensic use
4.79	HDO	—	—	Suppressed; spectrum broken across this zone
4.95–5.00	α-(1→6) glucan, branch point	d (3.8)	α-(1→6) branch points	Isolated from all other signals; the branch reporter
4.96	Isomaltose, α-(1→6) anomeric	d (3.8)	isomaltose	Coincides with the branch envelope
5.03–5.15	Minor oligosaccharides; kojibiose	d	α-(1→2)-linked species	Low level; malt- and process-dependent
5.19	α,α-Trehalose	d (3.8)	trehalose	Yeast stress metabolite released on autolysis
5.22	Malt oligosaccharide reducing end, α	d (3.8)	chains (α fraction)	Composite with lactose Glc-α-1H where lactose is present
5.23	D-Glucose, α-anomer	d (3.8)	free glucose (α fraction)	Partially resolved from the malt α-reducing signal
5.25	Isomaltose, reducing end α	d (3.8)	isomaltose	—

δ (ppm)	Assignment	Mult. (J, Hz)	Counts	Remarks
5.28	Arabinoxylan, α-L-arabinofuranosyl	d	arabinoxylan substitution	Cereal pentosan; broad
5.29–5.335 (D)	α-(1→4) glucan, branch-proximal	d (3.8)	α-(1→4) bonds near branches	Assigned Dp ≈ 9 by diffusion NMR
5.335–5.36 (C)	α-(1→4) glucan, branch-proximal	d (3.8)	α-(1→4) bonds near branches	Assigned Dp ≈ 6 by diffusion NMR
5.36–5.385 (B)	α-(1→4) glucan, linear	d (3.8)	internal α-(1→4) bonds	Assigned Dp ≈ 5–8 by diffusion NMR
5.385–5.43 (A)	α-(1→4) glucan, linear	d (3.8)	internal α-(1→4) bonds	Assigned Dp ≈ 3–4 by diffusion NMR; largest single feature
5.41	Sucrose, Glc-1H	d (3.8)	sucrose	Where sugar adjunct or priming sugar is present
5.44–5.46	Kojibiose; kestose	d	α-(1→2) and fructo-oligosaccharides	Minor; adjunct- and malt-dependent

6.3 The Four-Window Integral Scheme

The practical scheme in use at Process NMR Associates divides the α-(1→4) envelope into four contiguous integration windows, designated A through D from high to low frequency, and treats their integrals as the primary structural variables. The windows and their nominal degree-of-polymerization assignments are those annotated on Figure 13 and are collected in Table 13. Windows A and B are described as linear and windows C and D as branch-proximal, and the physical basis of that distinction is the well-established upfield displacement of an α-(1→4) anomeric proton whose residue lies adjacent to an α-(1→6) branch point relative to one embedded in an unbranched run.

Two points about what these windows count must be stated before any structural parameter is computed from them, because both are easy to get wrong. The windows count linkages, not molecules: a maltooligosaccharide of degree of polymerization n contributes one reducing-end anomeric proton and n − 1 internally linked anomeric protons, so the α-(1→4) integral is a bond count while only the reducing-end integral is a molecule count. And the degree-of-polymerization labels are diffusion-weighted averages over the species that populate each window, not exclusive assignments: maltose itself contributes its single α-(1→4) anomeric proton to window A, which is why the published diffusion measurement centered on that window returns an average of three to four for a population understood to comprise maltose, maltotriose, and maltotetraose. A window labeled Dp 3–4 therefore contains maltose, and the absence of a separate maltose window is not an omission.

A useful closure follows directly. If the anomeric assignments are correct and the integrals are honest, then for the oligomeric fraction the residue count must equal the chain count plus the linkage count,

$$I(\text{residues}) = I(\text{red}) + I(\text{A}\rightarrow\text{D}) + I(1\rightarrow6) \tag{15}$$

and this identity can be tested on every sample without additional data. Applied to the standard mash of Section 6.10, the oligomeric residue concentration is 724.1 mmol L^{-1} and the reducing-end count 301.0 mmol L^{-1}, so the linkages must amount to 423.1 mmol L^{-1}; the four measured α-(1→4) windows sum to 58.6 g L^{-1}, or 361.4 mmol L^{-1}, leaving 61.7 mmol L^{-1} to be carried by the α-(1→6) branch points together

with any unassigned intensity. That places an upper bound of about fifteen percent on the fraction of glycosidic linkages that are branch points, which is high for a finished wort but not implausible for a mash sampled before conversion is complete, and the closure is therefore satisfied to within the precision of the input data. A sample that fails equation (15) badly carries an integration error somewhere in the anomeric window, and the identity is worth computing routinely for that reason alone.

Table 13. The four-window α-(1→4) integration scheme, with nominal degree-of-polymerization assignments and derived variables.

Window	δ range (ppm)	Character	Nominal Dp	Role in the derived variables
A	5.385–5.43	α-(1→4) linear	3–4	Maltose through maltotetraose predominating; largest contributor; tracks amylolytic completeness. Sucrose at δ 5.41 falls within this window and must be subtracted where priming or adjunct sugar is present
B	5.36–5.385	α-(1→4) linear	5–8	Intermediate linear dextrin; rises with restricted β-amylolysis
C	5.335–5.36	α-(1→4) branch-proximal	6	Branch-adjacent linkage; enters the branch-proximal fraction
D	5.29–5.335	α-(1→4) branch-proximal	9	Branch-adjacent linkage in longer dextrins; enters the branch-proximal fraction
α-(1→6)	4.95–5.00	Branch point	—	Numerator of the branch fraction
Red-α	5.22	Reducing end, α	—	With Red-β, counts chains; denominator of DP_n
Red-β	4.65	Reducing end, β	—	With Red-α, counts chains; denominator of DP_n

Window boundaries are those in routine use and should be re-examined whenever the field strength, the reconstitution pH, or the water-suppression profile changes. The α-(1→4) envelope is bounded above at δ 5.43; the region from δ 5.43 to 5.46, which carries kojibiose and kestose, lies outside window A and is integrated separately.

Figure 14 shows why the scheme is useful. It overlays the anomeric region of a wort taken after cooling against the same brew after fermentation. The transformation is dramatic and entirely interpretable: the maltose and glucose signals that dominate the wort collapse, the reducing-end pair falls with them, and what remains in the finished beer is the branch-proximal envelope and the α-(1→6) branch signal, together with the longer linear dextrins that the yeast could not touch. The figure is, in effect, a direct visualization of attenuation, resolved by chain length and by linkage rather than reported as a single degree-of-fermentation number.

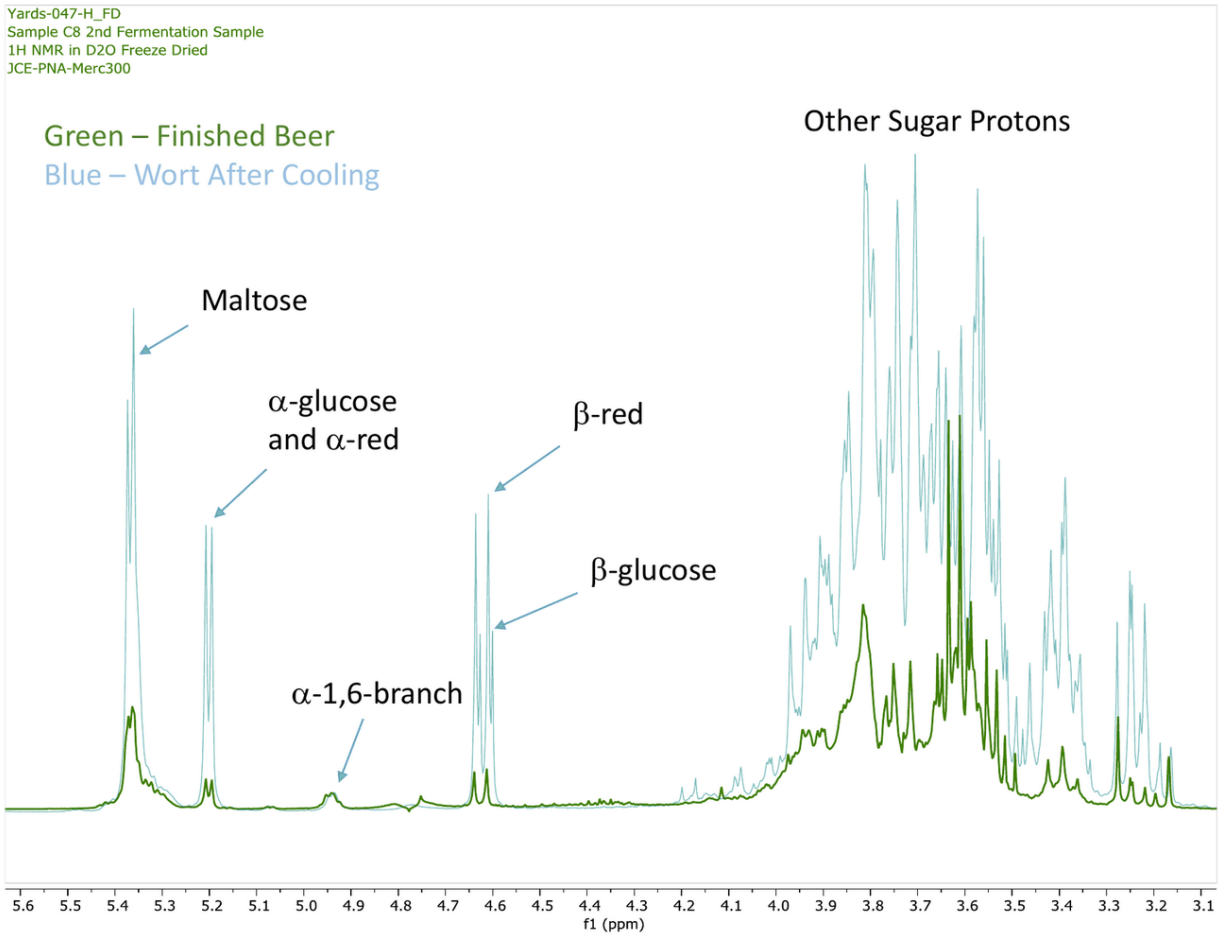


Figure 14. Anomeric region of the ^{1}H NMR spectrum of wort after cooling (blue) overlaid with the same brew after fermentation (green), δ 3.1 to 5.6. Labeled features are maltose, the composite α-glucose and α-reducing-end signal, the β-reducing-end signal, β-glucose, and the α-(1→6) branch-point resonance, together with the bulk ring-proton region. The disappearance of the fermentable maltose and glucose signals and the persistence of the α-(1→6) and branch-proximal envelopes constitute a direct, linkage-resolved measurement of attenuation. Process NMR Associates data.

6.4 Independent Corroboration of the Chain-Length Assignments

A degree-of-polymerization label attached to a chemical-shift window is a strong claim and requires external support, since chemical shift responds to local environment rather than to molecular size directly. That support exists and it is quantitative. Petersen and co-workers applied high-resolution diffusion-ordered spectroscopy with biexponential fitting to the anomeric signals of non-fractionated lager beer and reported translational self-diffusion coefficients of the order of 4×10^{-10} m^2 s^{-1} for the maltooligosaccharide signals at approximately δ 5.39, corresponding to a weighted-average degree of polymerization of three to four, consistent with predominating maltose, maltotriose, and maltotetraose. The α-(1→4) anomeric signals in the vicinity of branches, at approximately δ 5.35, gave an average degree of polymerization of around eight.[38]

Those published values bear directly on the scheme of Table 13, and the comparison should be stated precisely rather than favorably. Window A is centered near δ 5.40, where the published diffusion measurement returns an average of three to four, and the window is labeled Dp 3–4; that is a direct correspondence. The published near-branch measurement is centered at δ 5.35, which falls within window

C, and window C is labeled Dp 6; the published value at that position is eight. Window D, immediately below, is labeled Dp 9. The honest summary is therefore that the high-frequency label is confirmed, that the branch-proximal labels bracket the single published value but that the window in which that value was measured carries the lower of the two labels, and that the scheme should be described as literature-consistent in its ordering and in its high-frequency anchor rather than as calibrated throughout. A further caveat attaches to any diffusion-based degree-of-polymerization assignment: the diffusion coefficient scales with solution viscosity, and a reconstituted lyophilizate at 1.3 times the original beer concentration is measurably more viscous than the lager on which the published measurement was made, which displaces the inferred degree of polymerization by one to two units unless a viscosity correction is applied. The general relationship between diffusion coefficient and molar mass for neutral glucans on which such assignments rest was established for polysaccharides by Viel and co-workers.[49]

The corroboration extends further. The Carlsberg group synthesized a series of branched α-dextrin model compounds of degree of polymerization two to ten and assigned every ^{1}H and ^{13}C resonance, establishing that the chemical shift at a branch point depends primarily on the residues extending toward the non-reducing end of the backbone, with smaller contributions from branch and backbone extension toward the reducing end.[40] That structure–shift relationship is precisely what allows a shift window to encode a chain-length range. Independent work using optimized heteronuclear spectroscopy quantified glucans in complex mixtures to high accuracy,[41] and a survey of forty-five commercial beers by ^{1}H–^{13}C correlation showed that lager and ale samples differ systematically in the chain length of their branched starch fragments, with fragments of Dp 2 to 5 abundant in lager and fragments above Dp 5 predominating in ale.[42] A style difference of exactly that kind should be recoverable from the A-to-D window ratios of Figure 13, and testing whether it is provides an immediate and inexpensive validation of the present scheme against an independent published result.

> *Recommended validation experiment. The forty-five-beer ^{1}H–^{13}C study of Sundekilde and Meier reports that ale and lager separate on the branched-fragment chain-length distribution.[42] The twenty-three-beer Process NMR Associates data set contains both classes. Testing whether the A:B:C:D window ratios reproduce that separation, by simple discriminant analysis, would confirm the four-window scheme against an independent method and an independent laboratory at no experimental cost.*

6.5 Reducing-End Bookkeeping and the Anomeric-Ratio Internal Check

A reducing terminus in aqueous solution is not a single species. It equilibrates between the α- and β-pyranose forms through the open-chain aldehyde, and at equilibrium the two forms are present in a fixed ratio that is a property of the sugar and, weakly, of the temperature and the solvent. For D-glucose in water the equilibrium proportions are close to 36 % α and 64 % β, a value established by direct NMR measurement and refined subsequently.[51,52] For the reducing terminus of a maltooligosaccharide, where the 4-position carries a glycosidic substituent, the α fraction is somewhat higher, and values in the region of 0.40 are commonly quoted for maltose. The precise expectation for the malt oligosaccharide population of a wort is not established in the literature and should be measured in this laboratory on maltose and maltotriose standards prepared and acquired exactly as samples are; until that is done the expected value carries an uncertainty of several hundredths and the test below must be applied with that in mind.

This fixed relationship supplies something valuable that appears not to have been exploited in this laboratory: a sample-by-sample internal audit of integration accuracy across the anomeric window,

requiring no standard, no reference method, and no additional experiment. The α and β signals of a given reducing species lie at opposite ends of the anomeric region, at δ 5.22 and δ 4.65 respectively, separated by the water suppression zone and subject to entirely different local overlap. If the two integrals, converted to concentration, do not reproduce the known mutarotation ratio, then at least one of them is wrong, and the magnitude of the discrepancy bounds the error.

Applying the test to the mash series reported in Section 6.10 is instructive. For free glucose, the α and β concentrations reported for the four samples give α fractions of 0.326, 0.319, 0.323, and 0.321 — remarkably consistent across the set, but consistently below the expected value of approximately 0.36 by roughly ten percent in relative terms. A discrepancy reproducible across four independent samples is not random error but a systematic bias in the integration of one or both signals. Two mechanisms are available and they act in opposite directions, which is why the diagnosis cannot be settled from these data alone. Presaturation at δ 4.79 bleaches signals in proportion to their proximity to the irradiation frequency, and the β-anomeric doublet at δ 4.63 lies some forty-eight hertz from it against the one hundred and thirty hertz that separates the α doublet at δ 5.23; partial saturation of the β signal would raise the apparent α fraction, not lower it. Overlap acts the other way: the α doublet sits on the shoulder of the malt α-reducing envelope and the β doublet abuts the malt β-reducing resonance at δ 4.65, so a deconvolution that apportions intensity imperfectly can bias either signal in either direction. The observation that the free-glucose α fraction is consistently low therefore points to overlap rather than to saturation. Measuring the presaturation bleaching profile directly, by acquiring a standard of known composition with and without the suppression element, would separate the two mechanisms in a single afternoon and should be done before the size of the bias is quoted to a client.

The same test applied to the malt oligosaccharide reducing ends gives α fractions of 0.306, 0.307, and 0.330 for the three conventional mashes and 0.510 for the turbid mash. The first three are low against any reasonable expectation and, if the maltose value near 0.40 is the right comparator, they are further from it in relative terms than the free-glucose values are from 0.36; the same integration bias is therefore likely to affect the chain count as well as the glucose determination, and both should be regarded as provisional until the standards described above have been run. The turbid-mash value is a different matter, since it is not plausible on any chemical grounds. A reducing terminus cannot be predominantly α at equilibrium, and a value near 0.5 indicates that the α and β integrals for that sample are not measuring the same population: either the β signal has been under-integrated, most likely through interaction with the water suppression profile, or the α signal has absorbed intensity from a neighboring species. The practical consequence is direct, since the sum of the two integrals is the chain count that appears in the denominator of every degree-of-polymerization calculation, and an error there propagates into every structural parameter derived for that sample.

> ***Recommended practice.*** *The α-anomer fraction should be computed and reported for every sample, both for free glucose and for the malt reducing end, as a routine quality-control statistic. The acceptance window should be set empirically at the measured equilibrium value plus or minus three hundredths, determined once on glucose, maltose, and maltotriose standards prepared and acquired exactly as samples are; on the published equilibria that implies approximately 0.33 to 0.39 for free glucose and approximately 0.37 to 0.43 for the malt reducing end. Applied to the four mash samples reported here, all four free-glucose values and all four reducing-end values would fall outside those windows, which is the finding. A result outside the window should trigger re-integration before the structural parameters are released. The check costs*

> *nothing, requires no additional data, and is sensitive to precisely the failure mode — overlap-driven integration error in a congested region — that is otherwise hardest to detect.*

6.6 Structural Parameters

With the integrals defined, four structural parameters follow. Throughout, I denotes an integral converted to molar concentration of the responsible moiety, so that I(A→D) is the molar concentration of internal α-(1→4)-linked residues, I(1→6) that of branch-point residues, and I(red) = I(red,α) + I(red,β) that of reducing termini.

The number-average degree of polymerization is the ratio of total glucose residues to total chains,

$$DP_n = [\ I(A\rightarrow D) + I(1\rightarrow 6) + I(red)\ ] / I(red) \tag{16}$$

in which the numerator counts every anhydroglucose residue in the α-glucan population and the denominator counts the molecules. Where free glucose is to be included in the chain population, as a degree-of-polymerization-one member, its α and β integrals are added to I(red); where the interest is in the oligomeric fraction alone, they are not. The two conventions differ materially and must be stated whenever a number is reported.

The α-(1→6) branch fraction, expressed as the percentage of glycosidic linkages that are branch points, is

$$\text{Branch}\ (\%) = 100 \times I(1\rightarrow 6) / [\ I(A\rightarrow D) + I(1\rightarrow 6)\ ] \tag{17}$$

which is the ^{1}H NMR branching determination in the form established by Gidley for starch polysaccharides and applied subsequently to potato starch.[45,46] Native amylopectin gives values near 5 %; a β-limit dextrin, from which the linear outer chains have been removed, gives substantially higher values because the denominator has shrunk while the numerator has not, and the branch fraction of a beer dextrin population is therefore a direct readout of how far amylolysis proceeded.

The branch-proximal fraction, a variable proposed here as a compact descriptor of amylolytic completeness, is

$$\varphi_NB = [\ I(C) + I(D)\ ] / [\ I(A) + I(B) + I(C) + I(D)\ ] \tag{18}$$

and expresses the proportion of surviving α-(1→4) linkages that lie in the immediate neighborhood of a branch. Its physical meaning is straightforward: as amylolysis approaches its limit, the linear runs are consumed preferentially and the surviving material is increasingly branch-adjacent, so φ_NB rises toward an asymptote set by the branch density of the original amylopectin. Read from the twenty-three-beer survey of Figure 15, φ_NB ranges from approximately 0.29 to approximately 0.46 across the commercial set, a spread that is far too large to be experimental scatter and that ought to correlate with mash regime, with apparent attenuation limit, and — if the mouthfeel claims commonly made for dextrins have any substance — with sensory body.

The dextrose equivalent, the reducing-power measure by which starch hydrolysates are conventionally graded, follows from the number-average degree of polymerization as

$$DE \approx 100 \times 180.16 / (162.14 \cdot DP_n + 18.02) \tag{19}$$

in which 180.16 and 162.14 g mol^{-1} are the molar masses of glucose and of an anhydroglucose residue and 18.02 g mol^{-1} accounts for the terminal water of hydrolysis. Equation (19) provides a bridge between the

NMR result and the vocabulary of the starch and syrup industries, and it is worth noting that it is derived rather than measured, so that any bias in DP_n propagates into it directly.

Finally, the fermentable-to-non-fermentable ratio, which is what a brewer actually wants from a wort analysis, is obtained by partitioning the anomeric integrals at the boundary of yeast assimilability. Glucose, maltose, and maltotriose are fermentable by conventional brewing strains; maltotetraose and above are not, save by diastatic strains possessing an extracellular glucoamylase. In the four-window scheme the fermentable fraction is carried predominantly by window A together with the free-glucose signals, and the non-fermentable fraction by windows B, C, and D together with the α-(1→6) envelope. The partition is approximate, since window A spans Dp 3 to 4 and therefore straddles the assimilability boundary, and improving it is one of the clearest targets for the additional data to be added to this study.

6.7 A Worked Example

The arithmetic is carried through here for the standard mash of the New England India pale ale trial described in Section 6.10, using the reported concentrations directly. Total carbohydrate was 146 800 mg L^{-1}; the α-glucan reducing-end concentrations were 16 100 mg L^{-1} in the α form and 32 700 mg L^{-1} in the β form; free glucose was present at 9500 mg L^{-1} as the α-anomer and 19 900 mg L^{-1} as the β-anomer. All concentrations are expressed on an anhydroglucose basis of 162.14 g mol^{-1}.

Converting to molar terms, the total residue concentration is 146 800 / 162.14 = 905.4 mmol L^{-1}. The oligosaccharide chain count is (16 100 + 32 700) / 162.14 = 301.0 mmol L^{-1} and the free-glucose count is (9500 + 19 900) / 162.14 = 181.3 mmol L^{-1}. Including free glucose as a chain of unit length, the total chain count is 482.3 mmol L^{-1} and

$$DP_n = 905.4 / 482.3 = 1.88 \tag{20}$$

while excluding free glucose from both numerator and denominator gives a chain count of 301.0 mmol L^{-1} against an oligomeric residue concentration of 905.4 − 181.3 = 724.1 mmol L^{-1}, hence DP_n = 2.41 for the oligomeric fraction alone. Both figures are appropriate to a fully converted single-infusion mash dominated by maltose. From equation (19), evaluated with the unrounded value DP_n = 1.877, the dextrose equivalent is 100 × 180.16 / (162.14 × 1.877 + 18.02) = 55.9, again consistent with a well-converted mash.

Repeating the calculation for the turbid mash of the same trial, in which total carbohydrate was 128 000 mg L^{-1}, the α-glucan reducing ends 10 300 and 9900 mg L^{-1}, and free glucose 7900 and 16 700 mg L^{-1}, gives a total residue concentration of 789.4 mmol L^{-1}, a chain count of 276.3 mmol L^{-1} including free glucose, and DP_n = 2.86 — an increase of roughly fifty percent in average chain length relative to the standard mash, with a corresponding fall in dextrose equivalent to 37.4. On the oligomeric fraction alone the effect is larger still, DP_n rising from 2.41 to 5.12. That is a large and brewing-relevant difference, and it is exactly the outcome a turbid mash is intended to produce.

The caveat established in Section 6.5 must however be attached to the turbid-mash figure. Its reducing-end α fraction of 0.51 fails the mutarotation check, which means the chain count in the denominator of equation (16) is suspect and the DP_n of 2.86 should be treated as provisional pending re-integration. Had the check not been applied, the fifty-percent increase would have been reported without qualification. This is the practical value of the internal audit and the reason it is recommended as routine.

Table 14. Structural parameters derived from the anomeric integrals for the four mash samples of Section 6.10. Concentrations as reported; molar quantities on an anhydroglucose basis.

Sample	Total carbohydrate (mg/L)	Chains incl. glucose (mmol/L)	DP_n (incl. glucose)	DP_n (oligomer only)	DE	Reducing-end α fraction
Lab Mash #2	139 000	407.7	2.10	2.37	50.2	0.306
Lab Mash #3	147 000	434.8	2.09	2.36	50.6	0.307
Standard Mash	146 800	482.3	1.88	2.41	55.9	0.330
Turbid Mash	128 000	276.3	2.86	5.12	37.4	0.510 — fails check

The turbid-mash reducing-end α fraction falls outside the acceptance window of 0.30 to 0.42 established in Section 6.5, and the derived parameters for that sample are provisional. The oligomer-only column excludes free glucose from both the residue count and the chain count and is systematically higher, which is why the convention must be stated whenever a degree of polymerization is quoted. Dextrose equivalents are computed from the unrounded degree of polymerization rather than from the rounded value printed in the adjacent column. Input concentrations were transcribed from the charts of Figure 18 and should be replaced by the primary integration values before publication.

6.8 The Commercial Survey

Figure 15 applies the four-window scheme to the twenty-three-beer commercial survey. Total α-(1→4) glucan varies by a factor of roughly thirty-five across the set, from little more than one gram per liter in the light lagers and in a heavily attenuated wild-fermented ale to some forty-seven grams per liter in an imperial stout. That span is unsurprising and largely reflects original gravity and attenuation. What is more interesting, and what the stacked presentation makes visible, is that the internal distribution among the four windows is not conserved. The branch-proximal fraction φ_NB of equation (18) varies from roughly 0.29 in the mass-market lagers to roughly 0.46 in a Berliner Weisse, and the products with the highest total dextrin content are not those with the highest branch-proximal fraction. Total dextrin and dextrin architecture are therefore independent variables, and a compositional description that reports only the former is discarding information.

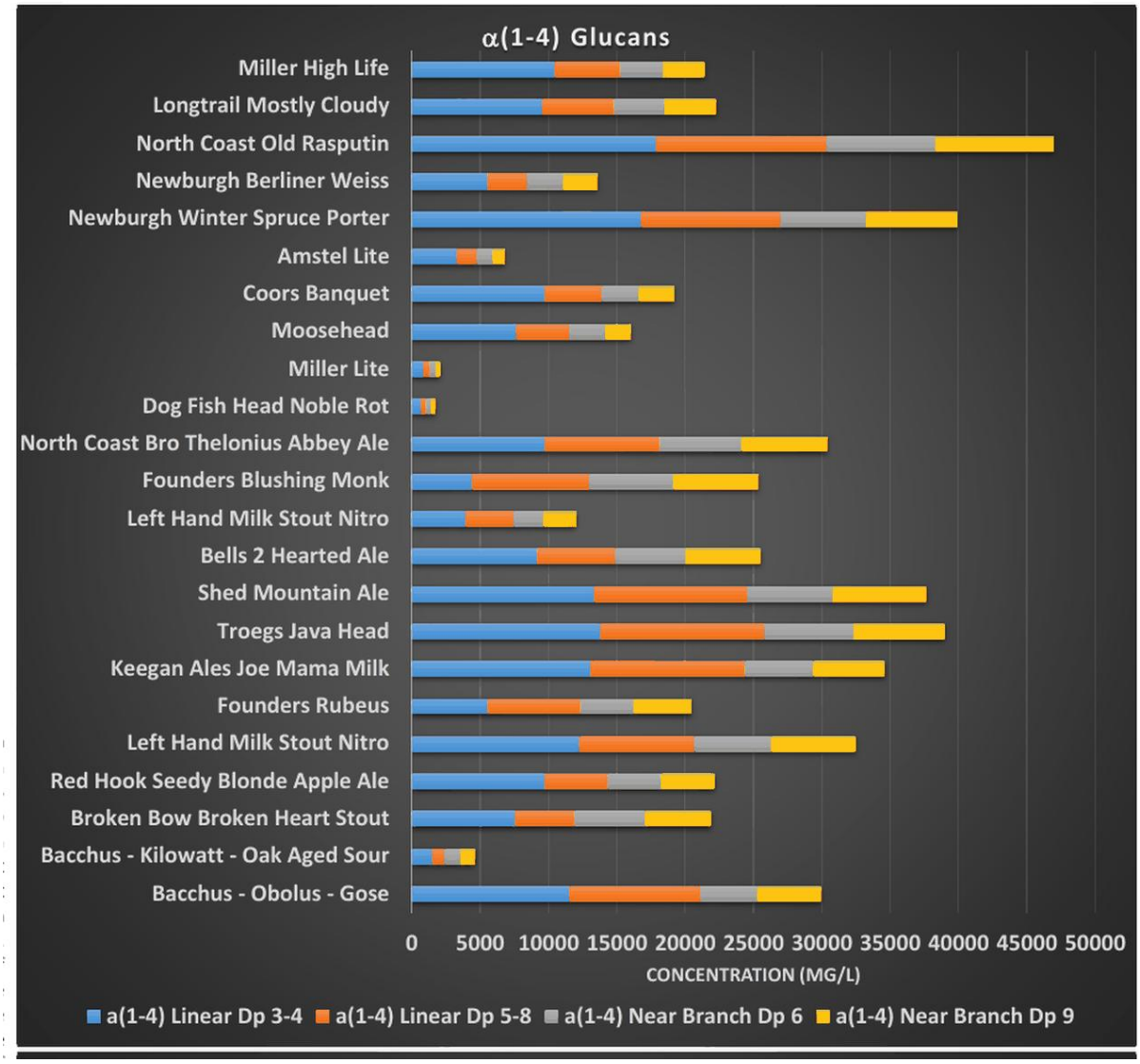


Figure 15. α-(1→4) glucan distribution across twenty-three commercial beers by ^{1}H qNMR, resolved into the four windows of Table 13: linear Dp 3–4 (blue), linear Dp 5–8 (orange), branch-proximal Dp 6 (gray), and branch-proximal Dp 9 (yellow), in mg/L. Total α-(1→4) glucan spans roughly 1.3 to 47 g/L across the set, while the branch-proximal fraction φ_NB spans approximately 0.29 to 0.46 independently of the total. Process NMR Associates data, World Brewing Congress 2016.

> *Author data placeholder — the four-window integrals. The tabulated A, B, C, D, α-(1→6), and reducing-end integrals underlying Figure 15, together with the derived DP_n, branch percentage, φ_NB, and dextrose equivalent for each of the twenty-three products, are to be inserted here. Those columns are the input matrix for the chemometric treatment described in Section 8 and are the single most valuable data addition that can be made to this document.*

6.9 Malt and Hot-Water Extract Survey

The same measurement applied upstream of the brewhouse addresses a different question. Figure 16 shows the anomeric and carbohydrate regions of hot-water extracts prepared from a substantial series of malts spanning base malts, Munich and Vienna types, crystal and caramel malts at several color grades, chocolate

and roasted malts, roasted barley, and specialty wheat and rye products. The extracts were prepared under a common protocol so that differences among the traces reflect the malt rather than the extraction.

Two kinds of information are available. The first is the carbohydrate that the malt brings to the mash independently of enzymatic conversion, which for crystal and caramel malts is considerable, since the sugars in those malts were produced during a stewing step within the husk rather than by mash amylolysis. The second, and analytically more interesting, is the chain-length signature of that pre-formed carbohydrate: the crystal malts contribute a distribution weighted toward the windows corresponding to intermediate degrees of polymerization, whereas base malt extract contributes primarily free sugars and short oligosaccharides together with the intact substrate that mash enzymes will later attack. A brewer wishing to understand why two grists of nominally identical color and extract behave differently in the mash tun will find the answer here rather than in a Congress mash number.

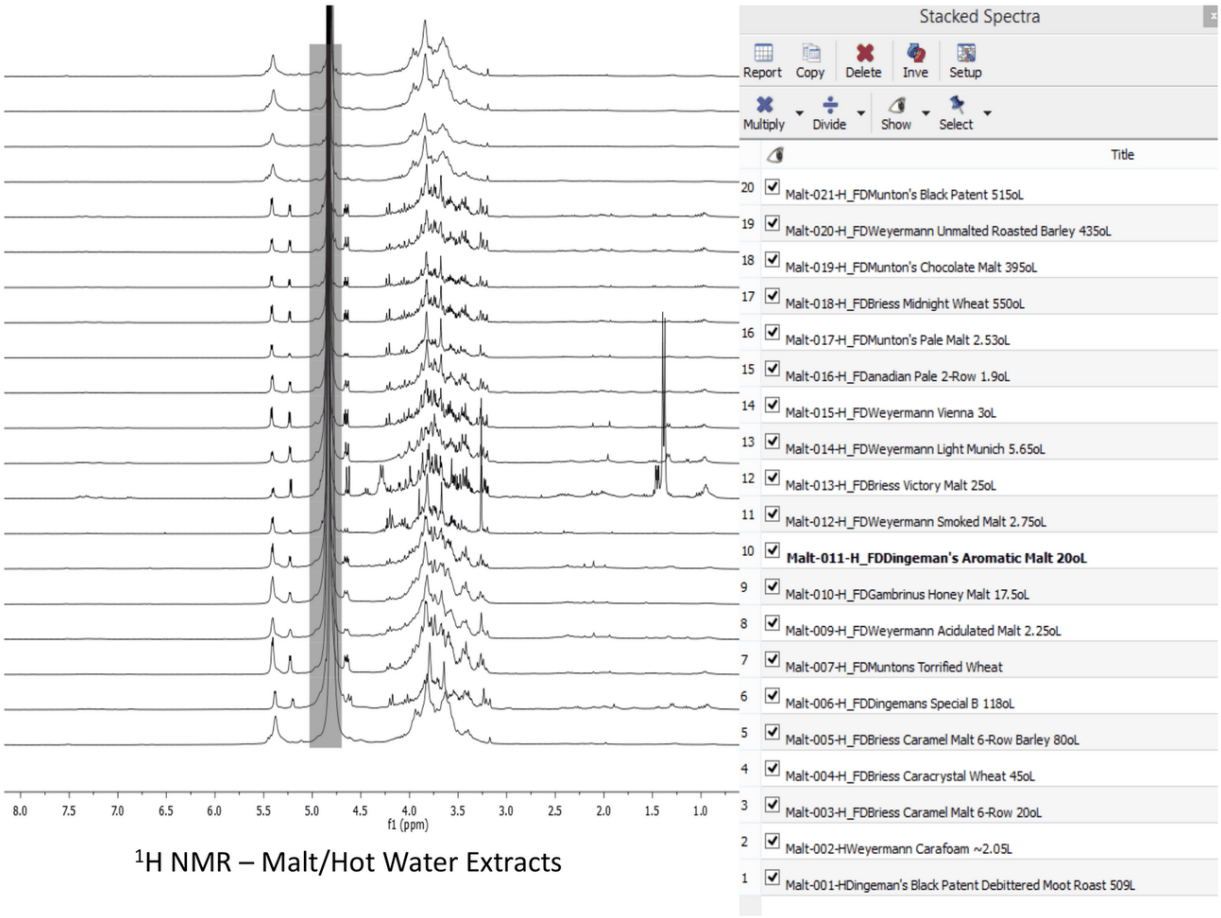


Figure 16. Stacked 300 MHz ^{1}H NMR spectra of hot-water extracts of a malt series, including base malts, Munich and Vienna malts, crystal and caramel malts at several color grades, chocolate and roasted malts, roasted barley, and specialty wheat and rye malts, prepared under a common extraction protocol. The carbohydrate region carries the pre-formed sugar and dextrin distribution that each malt contributes to the mash independently of enzymatic conversion. Process NMR Associates data.

6.10 Turbid Mashing: a New England India Pale Ale Case Study

The turbid mash, in which a portion of the mash liquor is drawn off before conversion is complete, boiled, and returned, is a traditional lambic technique that has been adopted in modern American brewing for the

hazy India pale ale style, where the intention is to leave a higher residual dextrin load and a fuller mouthfeel. Whether it does so, and by how much, is a question the anomeric region answers directly.

Figure 17 overlays the anomeric region of a standard mash against a turbid mash performed at the same brewery, and Figure 18 presents the derived carbohydrate quantities for four mashes: two laboratory-scale mashes, a production standard mash, and the production turbid mash. The results are unambiguous. Total carbohydrate is somewhat lower in the turbid mash, at 128 g L^{-1} against 147 g L^{-1} for the standard, which is consistent with the partial denaturation of enzymes in the boiled portion. But the distribution shifts sharply: the linear Dp 5–8 window rises from 8.6 to 27.3 g L^{-1}, more than a threefold increase, while the Dp 3–4 window falls from 42.1 to 32.5 g L^{-1}, and the reducing-end population falls by more than half. The number-average degree of polymerization rises correspondingly, as computed in Section 6.7.

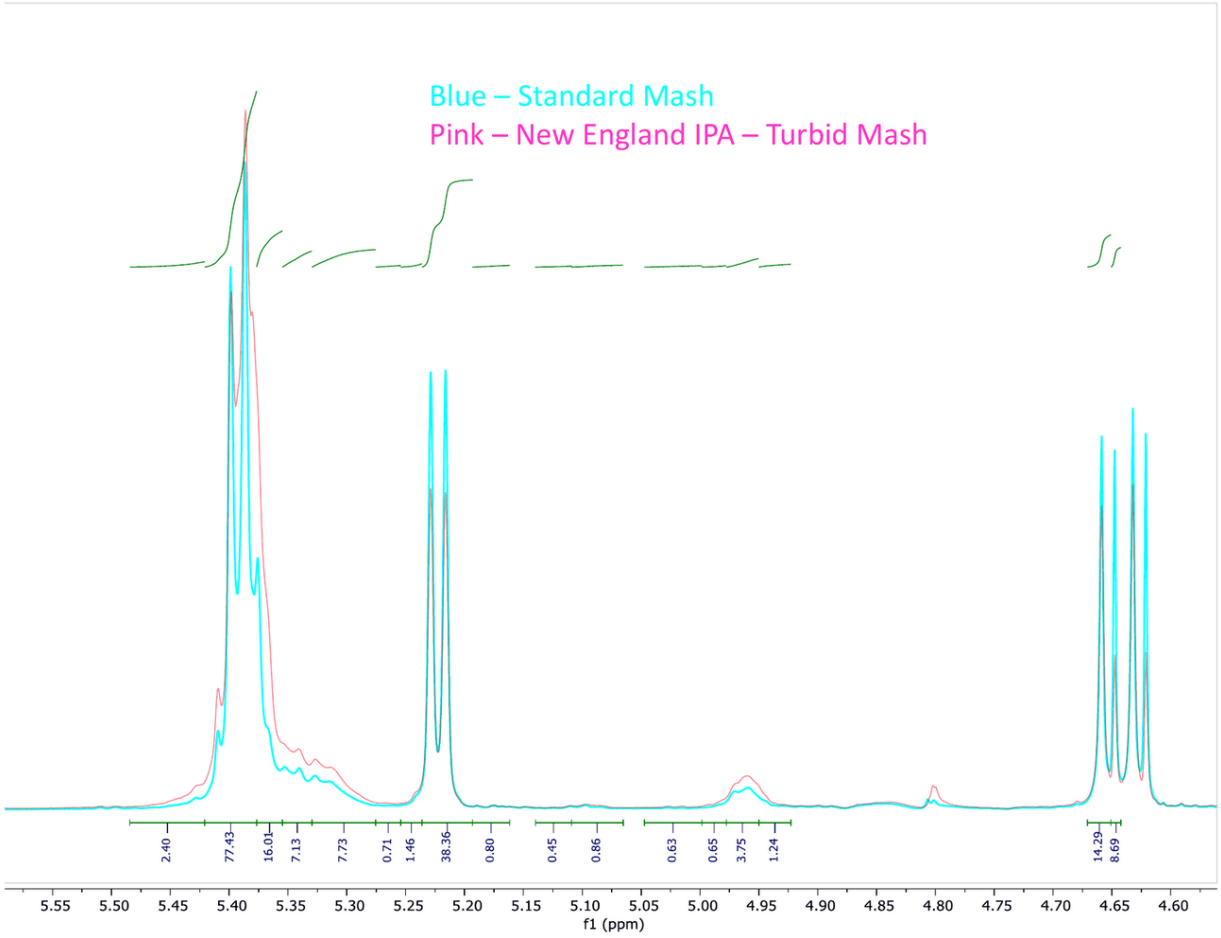


Figure 17. Anomeric region of the ^{1}H NMR spectrum of a standard mash (blue) overlaid with a turbid mash for a New England India pale ale (pink), acquired at the same brewery under matched preparation. The redistribution of intensity from the short-chain windows toward the intermediate linear windows is visible directly. Process NMR Associates data.

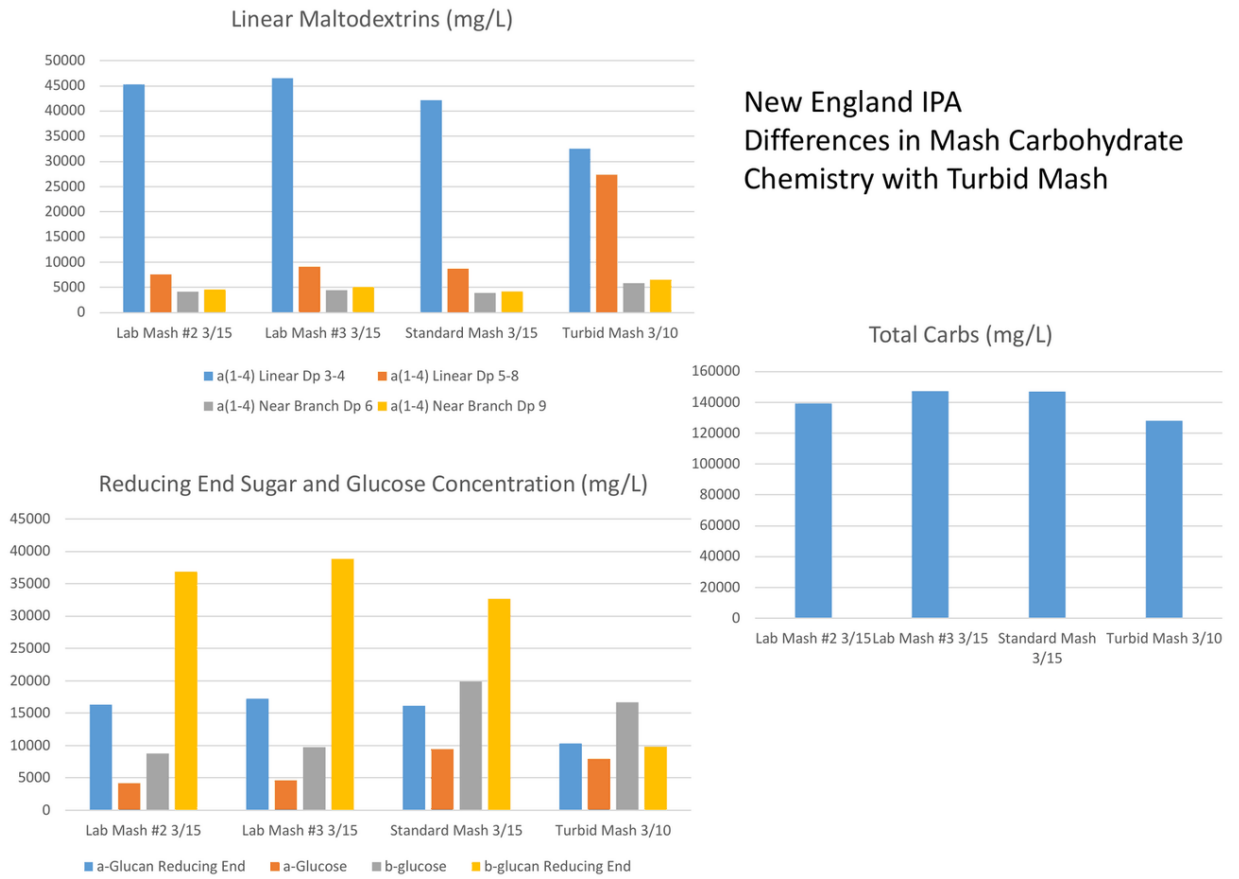


Figure 18. Carbohydrate quantities derived from the anomeric integrals for four mashes of the New England India pale ale trial. Upper left: linear and branch-proximal maltodextrin windows, mg/L. Right: total carbohydrate, mg/L. Lower left: α-glucan reducing end, α-glucose, β-glucose, and β-reducing-end concentrations, mg/L. The turbid mash carries roughly three times the intermediate linear dextrin of the standard mash and less than half its reducing-end population. Process NMR Associates data.

It is worth being precise about what has and has not been demonstrated. The measurement establishes that turbid mashing produces a carbohydrate distribution of higher average chain length, and the effect size is large and reproducible across the mash pairs examined. It does not establish that the resulting beer has more body, because no sensory measurement accompanied the chemistry. The proposition that residual dextrin content governs perceived mouthfeel is widely repeated in brewing texts and is not as securely founded as its ubiquity suggests; controlled dosing studies have given mixed results, and viscosity, β-glucan, protein, and carbon dioxide all contribute. The honest statement is that the analysis quantifies a compositional difference of the kind that is believed to affect body, and that linking it to sensory outcome requires a sensory panel rather than a spectrometer.

One further caution attaches to the lower panel of Figure 18, where the fourth series is labeled as a β-glucan reducing end. On the assignment established in Section 6.2 that signal at δ 4.65 is the β-anomeric form of the malt oligosaccharide reducing terminus, not a cereal β-glucan, and the label is a shorthand that should be corrected in any external presentation of the data. The distinction is not pedantic: a genuine (1→3),(1→4)-β-glucan determination is a different measurement with different implications for filtration and haze, and is discussed in Section 6.11.

6.11 Interferents and Look-Alikes

Four classes of material occupy the anomeric region alongside the α-glucan dextrins and must be accounted for before an integral is converted into a structural parameter. Table 15 collects them.

The cereal β-glucans, mixed-linkage (1→3),(1→4)-β-D-glucans derived from the barley endosperm cell wall, contribute broad anomeric intensity between δ 4.5 and 4.8 and are of independent interest because they govern lauter runoff and filtration behavior. They are distinguishable from the α-glucans on three grounds: their anomeric protons are β and therefore appear in a different window with a large vicinal coupling of about 7.9 Hz against the 3.8 Hz of the α anomers; their much larger molecular size gives a diffusion coefficient an order of magnitude smaller, so diffusion-ordered spectroscopy separates them cleanly; and their transverse relaxation is faster, so a spin-echo filter attenuates them preferentially. Their quantitation by optimized heteronuclear methods has been demonstrated to good accuracy in complex mixtures.[41,44]

The arabinoxylans, the other major cereal pentosan, contribute α-L-arabinofuranosyl anomeric intensity near δ 5.28, at the low-frequency edge of window D, where they inflate the branch-proximal integral if not accounted for. Their contribution is usually small in a well-lautered wort but rises with malt modification and with wheat content.

Added sugars constitute the third class. Lactose, added to milk stouts and increasingly to hazy pale ales, contributes the three signals discussed in Section 6.2; it is not fermentable by conventional brewing yeast and therefore persists intact into the package, where it must be excluded from the dextrin bookkeeping and reported separately. Sucrose from priming or from adjunct contributes an anomeric doublet at δ 5.41 within window A. Trehalose at δ 5.19, released from yeast during autolysis, and isomaltose at δ 4.96 and 5.25, arising from acid or transglucosidase reversion, both sit within or adjacent to structurally significant windows.

The fourth class is the residual free sugars themselves, whose α-anomeric doublet at δ 5.23 is only partially resolved from the malt α-reducing envelope at δ 5.22 at 300 MHz. At 600 MHz the separation is comfortable; at 300 MHz it requires deconvolution, and the mutarotation check of Section 6.5 is the most reliable way to confirm that the deconvolution succeeded.

Table 15. Species that interfere with the α-glucan anomeric integration, and the means of resolving them.

Interferent	δ (ppm)	Window affected	Discrimination
(1→3),(1→4)-β-glucan	4.5–4.8	Reducing end β	β coupling ≈ 7.9 Hz; low diffusion coefficient; short T_2 — use DOSY or a spin-echo filter
Arabinoxylan	5.28	D (branch-proximal)	Distinct multiplet structure; rises with wheat and with high modification
Lactose	4.45, 4.67, 5.22	Reducing end α and β	Quantify from the interference-free Gal-1H doublet at δ 4.45 and subtract
Sucrose	5.41	A (linear Dp 3–4)	Sharp doublet on a broad envelope; priming and adjunct sugar
Trehalose	5.19	Adjacent to reducing end α	Yeast autolysis marker; report separately
Isomaltose	4.96, 5.25	α-(1→6) branch envelope	Inflates the apparent branch count; distinguish by its reducing-end pair

Interferent	δ (ppm)	Window affected	Discrimination
Kojibiose, kestose	5.44–5.46	Above window A	Minor; adjunct- and malt-dependent. Kojibiose contributes at both of its anomeric centers, near δ 5.10 and near δ 5.44
Free glucose	4.63, 5.23	Reducing end α and β	Deconvolution; confirm with the mutarotation check of Section 6.5
Residual water	4.79	Between the reducing-end signals	Suppression profile must be symmetric and stable between samples

6.12 What the Present Data Cannot Yet Support

Three claims that could reasonably be made from Figure 13 should not be made from it without further work, and it is better to say so here than to have an expert reviewer say it later.

The first concerns the degree-of-polymerization labels themselves. They are consistent with the published diffusion measurements, as Section 6.4 establishes, but consistency is not calibration. Chemical shift in this region responds to the local environment of the anomeric proton — how many residues extend toward the non-reducing end, whether a branch is adjacent, whether the residue is second or third from a terminus — and these local factors are correlated with, but not determined by, overall chain length. A window centered at δ 5.40 is therefore populated preferentially, not exclusively, by short chains. The correct statement is that windows A through D are reproducible integral bins with a monotonic and literature-supported relationship to chain length, and that they are excellent chemometric variables; the assertion that window A is Dp 3–4 and window D is Dp 9 should be treated as a working label until the scheme has been calibrated against high-performance anion-exchange chromatography with pulsed amperometric detection or against matrix-assisted laser desorption mass spectrometry on the same samples.

The second concerns the resolving power of diffusion measurements in a polydisperse mixture. The diffusion coefficient of a neutral oligosaccharide scales approximately as the inverse square root of molar mass, so the difference between Dp 6 and Dp 9 amounts to a change in diffusion coefficient of roughly twenty percent. That is measurable on a pure compound and marginal in a continuous distribution where every signal is a superposition of contributions from many species. Diffusion-ordered spectroscopy on beer therefore returns weighted averages, as its authors are careful to state, and the assignment of a single degree of polymerization to a window inherits that averaging.

The third concerns the branch fraction of equation (17). The α-(1→6) envelope at δ 4.95 to 5.00 is clean in the sense of being free from α-(1→4) overlap, but it is not free from isomaltose, and it contains contributions from branch points in environments that the model-compound work shows to be chemically distinct. Broadband homonuclear decoupling has been shown to resolve that envelope into separately quantifiable signals corresponding to different limit-dextrin branch types, at a modest sensitivity cost, and applying it would convert a single branch number into a branch-type distribution.[38] That is the natural next experiment for this line of work.

6.13 Extensions: Heteronuclear, Homodecoupled, and Diffusion Methods

Three developments would materially extend what the present protocol delivers, and all three are established in the literature on precisely this material.

The first is heteronuclear correlation with narrow spectral width in the carbon dimension. Carbon-13 offers roughly twenty times the chemical-shift dispersion of proton, and the anomeric carbon region of an α-glucan spans some four parts per million between δ 97.7 and 101.7. Sampling that window with extensive aliasing in a $^{1}H–^{13}C$ correlation experiment yields anomeric signals with linewidths below three hertz against chemical-shift differences of two hundred hertz, and projections onto the carbon axis resolve structural motifs that are hopelessly overlapped in the proton spectrum even at 800 MHz. A forty-five-beer survey conducted in this way separated ale from lager by orthogonal partial least-squares discriminant analysis on the branch-point projection alone, and regressed alcoholic strength against the same data.[42] The experiment takes about three-quarters of an hour, comparable to a chromatographic run, and does not require the data to be absolutely quantitative, since the multivariate treatment operates on normalized spectra.

The second is broadband homonuclear decoupling, which collapses the anomeric multiplets to singlets and thereby recovers resolution that scalar coupling has consumed. Applied directly to beer without pre-concentration, it resolved the α-(1→6) region into non-overlapping signals from different limit-dextrin branch types with a sensitivity penalty that proved acceptable.[38] For a laboratory whose highest-value question concerns branch architecture, this is a high-return modification. The same laboratory has demonstrated that enzymatic starch degradation can be followed in situ and in real time by NMR without quenching or fractionation, which points toward a mash-monitoring experiment in which the dextrin distribution is watched as it forms rather than inferred after the fact.[43]

The third is diffusion-ordered spectroscopy, which adds a molecular-size axis and permits the polymeric, oligomeric, and monomeric contributions to a congested region to be separated without physical fractionation. Its application to the closely analogous oligosaccharide ladder of Port wine demonstrated the principle,[50] and it is the technique that underwrites the chain-length assignments of Section 6.4. In routine use it is better regarded as a periodic assignment-confirmation experiment than as a per-sample measurement, since the acquisition and fitting burden is substantial.

> *Author data placeholder — the residual dextrin extension. The additional dextrin data foreshadowed for this study should be inserted here: the anion-exchange or mass-spectrometric calibration of the A-to-D windows, the homodecoupled α-(1→6) branch-type distribution, and the heteronuclear anomeric projections. Together these would convert the four-window scheme from a well-supported working model into a validated structural method.*

7. Process and Product Case Studies

7.1 Biological Acidification of the Mash

Sour mashing, the deliberate encouragement of the native lactic acid bacteria carried on barley malt to acidify a portion of the mash, is a traditional German brewhouse practice whose importance derives from the Reinheitsgebot: a biologically produced acid is a permissible means of adjusting mash pH where a mineral or food-grade organic acid addition is not. The practice carries an accumulated body of received wisdom, the most durable element of which is that the souring vessel should be held near 49 °C. Whether that number has a chemical basis, or is merely the temperature at which a mash tun happens to sit overnight, is a question that quantitative NMR is unusually well placed to answer, because it measures all of the

relevant metabolites simultaneously in a single experiment and requires no assumption about which of them matters.

The study reported here held acidified mashes prepared from Canadian two-row malt at a series of temperatures from approximately 32 °C to 60 °C and quantified lactic acid, acetic acid, succinic acid, ethanol, and γ-aminobutyric acid by ^{1}H qNMR with maleic acid as internal standard, using manual integration supported by global spectral deconvolution and simple mixture analysis. Figure 19 shows the stacked spectra across the temperature series and Figure 20 the resulting metabolite trends. The work was published in the Journal of the Institute of Brewing.[28]

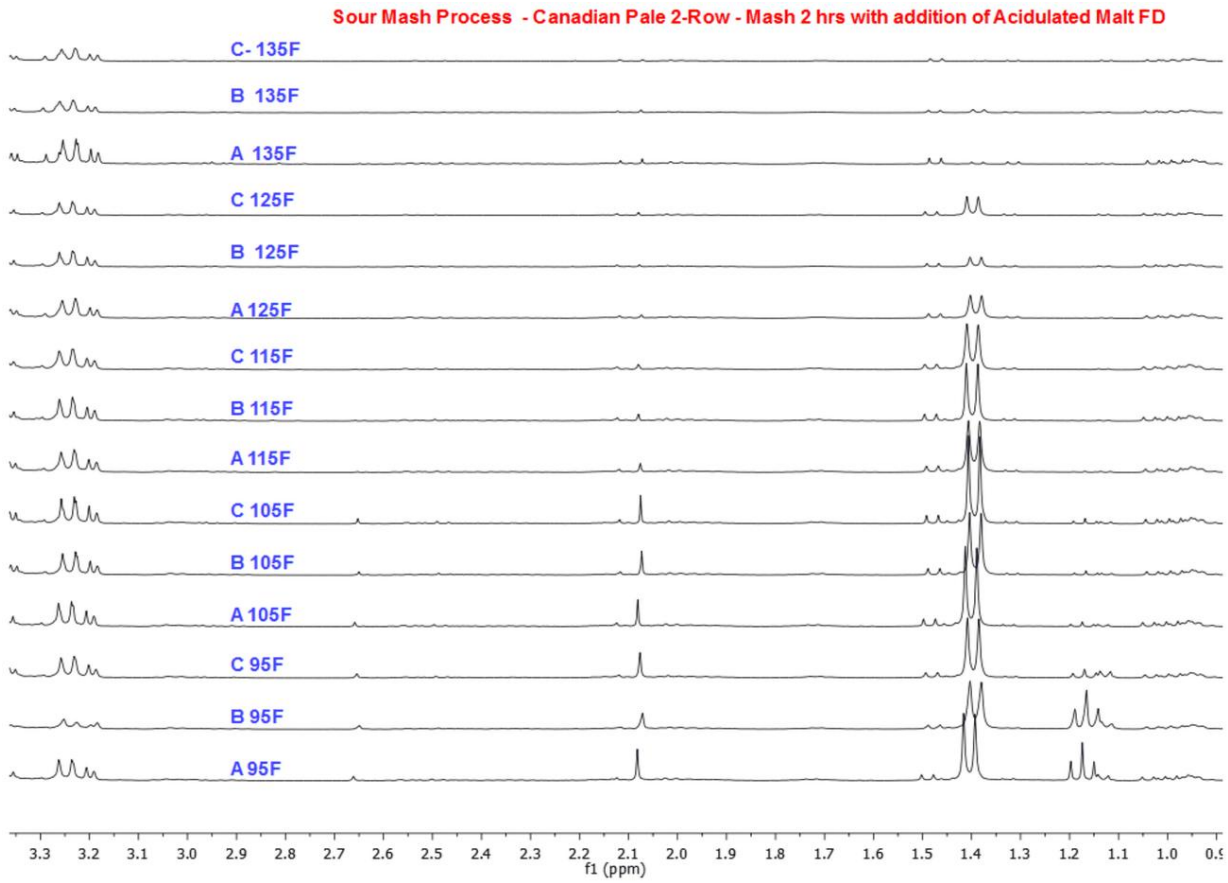


Figure 19. Stacked 300 MHz ^{1}H NMR spectra of freeze-dried sour mash samples from a Canadian pale two-row malt held for two hours at temperatures from approximately 32 °C to 60 °C after addition of acidulated malt. The growth and decline of the lactate methyl doublet across the series is visible directly. Process NMR Associates data.

Absolute Metabolite Proportions

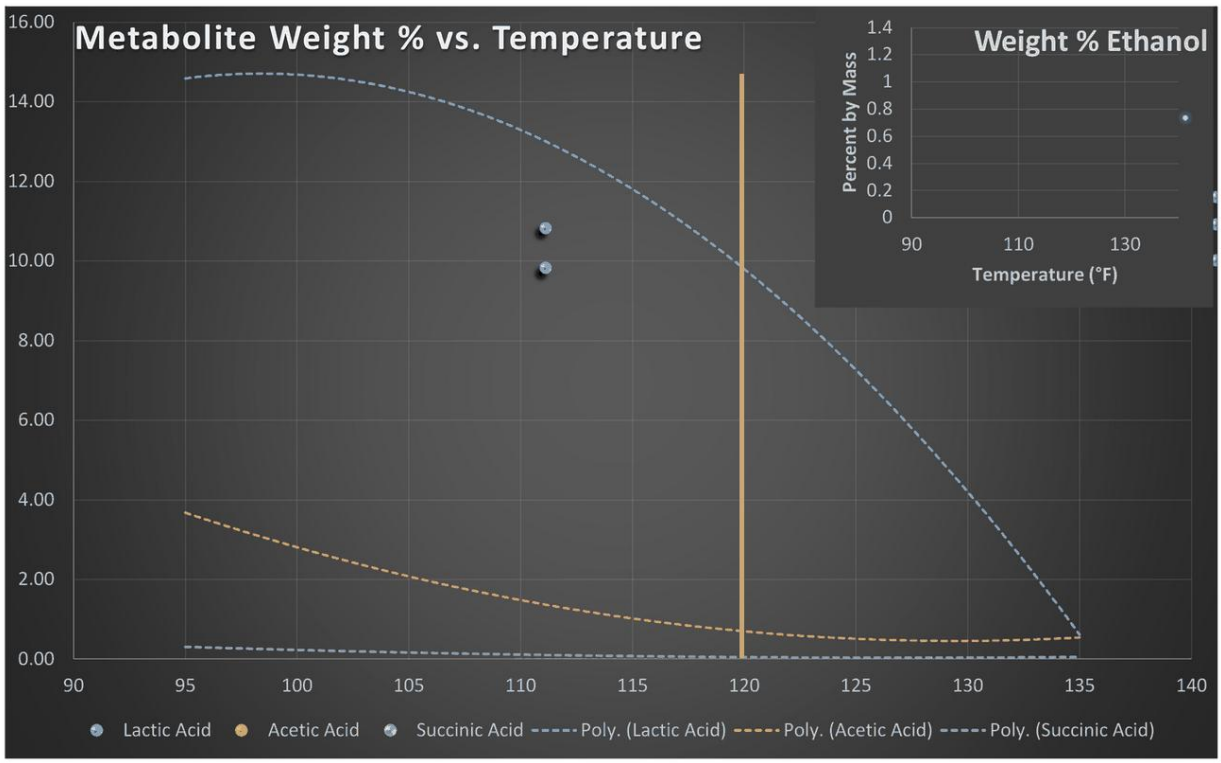


Figure 20. Metabolite mass fraction against souring temperature for the sour mash series, showing lactic acid (blue), acetic acid (orange), and succinic acid (gray) with second-order polynomial trends, and, inset, ethanol. The vertical gold line marks the traditional 49 °C (120 °F) hold. Process NMR Associates data.

The absolute picture is unambiguous and, on first inspection, unhelpful to tradition: lactic acid production is greatest at the low end of the range, passing through a broad maximum near 36 to 38 °C at approximately fifteen percent on the mass basis used in the original study, and falls away steadily thereafter to near zero at 57 °C. If maximum acidification were the objective, the mash should be held cooler than tradition dictates. Acetic acid, the marker of heterofermentative and acetic-acid-bacterial activity and an off-flavor in this context, falls more steeply than lactic acid over the lower part of the range, from roughly 3.7 percent at 35 °C to below one percent by 50 °C, and then plateaus rather than continuing to fall. Ethanol, the marker of wild yeast activity, follows the same downward trend. Succinic acid is negligible throughout.

The informative quantity is not either acid alone but their ratio, since it is the balance between clean lactic acidity and acetic sharpness that determines whether a soured mash is usable. Computed from the fitted trends of Figure 20, the lactic-to-acetic mass ratio rises from approximately four at 35 °C through eight at 43 °C to a maximum in the region of twelve between 47 and 52 °C, and then collapses above 55 °C because lactic acid production ceases while the acetic residue does not. The ratio quoted here is read from two second-order polynomial fits at a temperature where the denominator is small, so its numerical value is soft and no uncertainty can be attached to it; the ordering of the trends is robust, the position of the maximum is robust to within a few degrees, and the magnitude should be recomputed from the measured points with replicate uncertainties before it is quoted outside this document. The traditional hold therefore sits at the temperature that maximizes acid quality rather than acid quantity, and it does so while simultaneously

suppressing the wild yeast that would otherwise contribute ethanol and its associated flavors to a vessel that is not intended to ferment. That is the conclusion reported in the published account, which states that the customary temperature is optimal not for absolute lactic acid concentration but for the acid balance that shapes the flavor profile of the finished beer.[28]

The result illustrates what the untargeted character of the measurement provides. A targeted lactic acid assay would have found the maximum at 36 °C and would have recommended changing a practice that has survived for a century. It is the simultaneous, calibration-free measurement of the contaminant metabolites alongside the target that recovers the reason the practice exists.

7.2 Sour Beer, Mixed-Culture Fermentation, and Barrel Aging

Mixed-culture and spontaneously fermented beers present a compositional problem that conventional analysis handles poorly, because the organisms involved produce metabolites that a Saccharomyces-oriented assay panel was never designed to look for. Figure 21 shows the effect of Brettanomyces and bacterial activity on a series of sour beers across the aliphatic and anomeric regions. Several features distinguish these products from conventionally fermented beer, and each is directly interpretable.

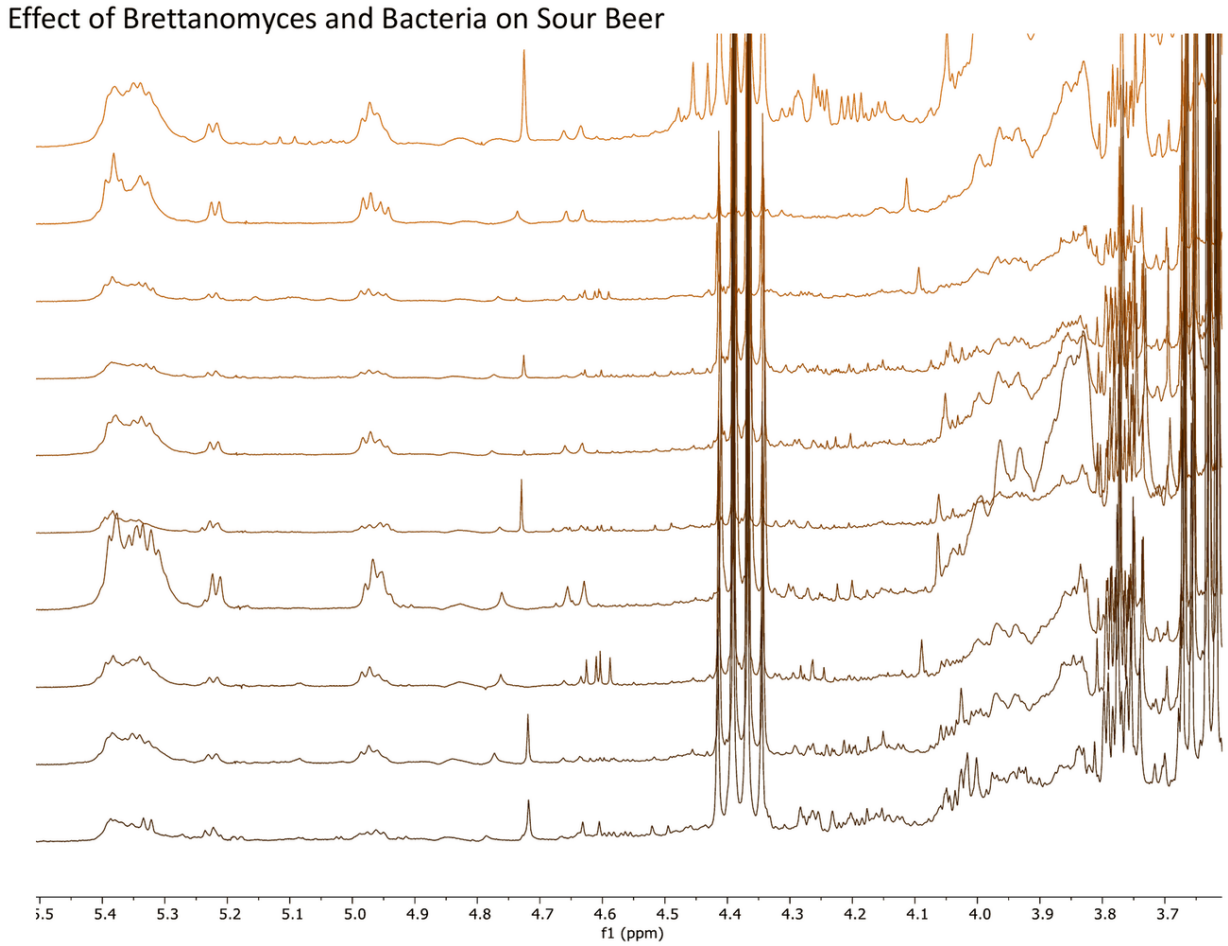


Figure 21. Stacked 300 MHz ^{1}H NMR spectra showing the effect of Brettanomyces and bacterial activity on sour beer composition, δ 3.6 to 5.6. Progressive consumption of the residual dextrin envelope, elevated organic acid content, and the appearance of metabolites absent from conventional Saccharomyces fermentations distinguish these products. Process NMR Associates data.

The most consequential is attenuation of the dextrin pool. Several Brettanomyces strains carry extracellular α-glucosidase and glucoamylase activity and can therefore utilize maltooligosaccharides and dextrins that Saccharomyces cannot, so a long-conditioned mixed-culture beer shows progressive erosion of the α-(1→4) envelope over months in barrel. The extracellular β-glucosidase for which the genus is better known acts on glycosidically bound aroma precursors and on β-linked substrates and has no bearing on the α-glucan envelope; the two activities should not be conflated. The measurement of Section 6 therefore becomes a time-resolved record of secondary attenuation, and its practical application is the prediction of package stability: a beer whose dextrin envelope is still declining at the point of packaging will continue to attenuate in the bottle and to generate carbon dioxide.[61]

The organic acid profile separates the organisms. Homofermentative lactobacilli yield lactate with little else; heterofermentative organisms yield lactate together with acetate and ethanol in characteristic proportion; acetic acid bacteria, which require oxygen and therefore appear in barrel-aged and open-fermented products, yield acetate at the expense of ethanol. The ratio of lactate to acetate, read directly from the spectrum, therefore reports on the microbial population and on oxygen ingress without a plating step. Elevated γ-aminobutyric acid accompanies lactic activity through glutamate decarboxylation, and succinate rises in mixed cultures relative to clean fermentations.

The trajectory of a spontaneous fermentation maps onto the spectrum phase by phase. The microbiology of traditional lambic production is well characterized: an enterobacterial phase occupies roughly the first month, the principal alcoholic fermentation by Saccharomyces follows and runs for several months, and a long maturation phase dominated by Pediococcus and Brettanomyces completes the cycle over one to three years in wood.[69] Each phase writes its own signature. The enterobacterial period contributes mixed-acid metabolites — acetate, lactate, succinate, and, distinctively, formate from pyruvate–formate lyase — at a stage when ethanol is still low; the main fermentation is read from the ethanol and glycerol curves and the collapse of the fermentable sugar signals; and maturation is read from the slow rise of lactate against a declining dextrin envelope as Pediococcus acidifies and Brettanomyces consumes the oligosaccharides that Saccharomyces left behind. A monthly spectrum through that cycle is a complete process record from a single experiment, and the panel maps directly onto the blending problem: traditional gueuze is composed from one-, two-, and three-year lambics, and the organic acid, ethanol, and residual carbohydrate profiles of the candidate casks — profiles of exactly the kind shown in Figure 8 — constitute a quantitative blending sheet in place of taste memory alone.

A metabolite that deserves more attention in sour beer work than it customarily receives is mannitol. Heterofermentative lactic acid bacteria reduce fructose to mannitol, using the ketose as an external electron acceptor to regenerate oxidized cofactor, and the redox arithmetic has a directly observable consequence: with an external acceptor available, the acetyl phosphate branch of the phosphoketolase pathway is discharged as acetate, with an extra substrate-level phosphorylation, rather than being reduced to ethanol.[68] Mannitol formation is therefore accompanied by a shift of the lactate-to-acetate ratio toward acetate, and the pairing — fructose falling, mannitol rising, acetate rising together — identifies heterofermentative activity on a fructose-bearing substrate, which in practice means a fruited or back-sweetened sour. The mannitol multiplets lie between δ 3.6 and 3.9 within the carbohydrate massif and require deconvolution or a heteronuclear experiment for clean quantitation, but their presence is not subtle at the gram-per-liter levels a stalled fruit refermentation can generate.

Two blind spots of the proton spectrum in this application should be stated. Lactate chirality is invisible: the D- and L-enantiomers, which report on the producing organism and which matter for the biogenic load

of heavily soured products, give identical spectra in an achiral solvent, and their resolution requires a chiral shift reagent or an enzymatic assay. And gluconic acid — a signature metabolite of Gluconobacter oxidation of glucose in lambic and in kombucha-style fermentations — resonates entirely within the crowded δ 3.6 to 4.2 window, so its identification rests on two-dimensional confirmation rather than on a clean one-dimensional reporter.

Barrel aging adds a second reactor on top of the microbiology, and its chemistry is legible in the same spectra. Oak is oxygen-permeable: dissolved oxygen ingress through the staves and the bung of a beer-filled barrel proceeds at tens of milligrams per liter per year, and that flux is what sustains the acetic acid bacteria — obligate aerobes — whose acetate and ethyl acetate distinguish barrel-soured from steel-soured beer. A controlled study of finished beers aged in oak documented exactly this coupled trajectory of microbial community and chemistry over months of maturation, with acetate, lactate, and ester concentrations evolving together as the community turned over.[70] The ester chemistry carries its own clock: at beer pH the Fischer esterification of lactate and acetate with ethanol is slow, uncatalyzed by any enzyme, and runs toward equilibrium over months, so ethyl lactate — observed through its coupled quartets between δ 4.2 and 4.35 alongside ethyl acetate, as annotated in the sidra spectra of Figure 23 — accumulates in rough proportion to the product of acid content and time in wood, and functions as an internal maturation timer that no fresh-soured beer can counterfeit.

The wood itself contributes substrate as well as flavor. Hydrolysis and toasting chemistry release pentoses and hexoses from the oak hemicellulose, together with cellobiose from cellulose, and it is here — rather than on the malt dextrins — that the celebrated β-glucosidase of Brettanomyces earns its keep, since cellobiose is a β-linked disaccharide that Saccharomyces cannot touch. Wood-sugar refermentation is slow and small, but over a year in cask it contributes measurably to attenuation and carbonation, and the appearance of transient cellobiose and pentose signals in the anomeric region of a barrel-aged beer is direct evidence of it. The oak extractives that dominate sensory discussion — vanillin, the cis- and trans-oak lactones, ellagitannins — lie at or below the one-dimensional detection limit at the tens-of-micrograms-to-low-milligrams-per-liter levels found in beer, and claims about them belong to chromatography; what the proton spectrum contributes is a broad polyphenolic hump in the aromatic region whose growth tracks extraction. Figure 22 illustrates the compositional reach of the same measurement across the cider cellar, where barrel-aged, malolactic, dry, and back-sweetened products separate at a glance on exactly the axes discussed here.

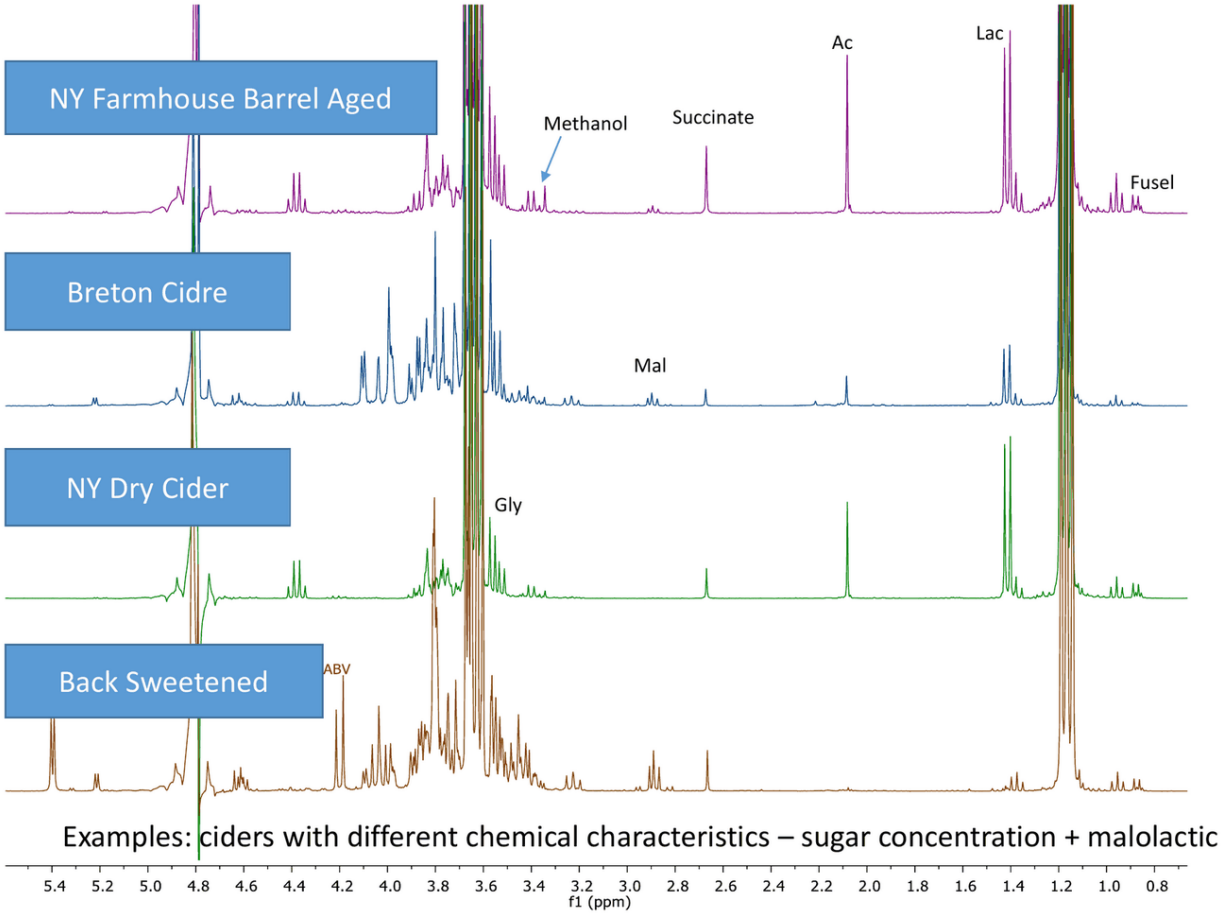


Figure 22. Stacked 300 MHz ^{1}H NMR spectra of four ciders illustrating the compositional axes of barrel and mixed-culture maturation: a New York farmhouse barrel-aged cider carrying elevated acetate, lactate, succinate, and methanol; a Breton cidre with retained malic acid; a New York dry cider with glycerol prominent and sugars exhausted; and a back-sweetened cider in which the sugar signals dominate. Ac, acetate; Lac, lactate; Mal, malic acid; Gly, glycerol. Process NMR Associates data.

7.3 The Glycerol Conversion Pathway: 1,3-Propanediol, 3-Hydroxypropionic Acid, and the Acrolein Question

One observation from this laboratory's broader work on fermented beverages deserves specific mention here because it generalizes to beer and because it is not widely appreciated. In spontaneously fermented and wild-cultured products that have been taken to complete sugar exhaustion, glycerol — normally a stable end product present at one to two and a half grams per liter — is found to have been substantially or entirely consumed, and in its place appear 1,3-propanediol, 3-hydroxypropionic acid, and propionic acid. The characteristic 1,3-propanediol signature is a clean two-proton quintet at δ 1.76 with the flanking methylene triplet at δ 3.68, and it is unmistakable.

The chemistry is well established and rewards being set out in full, because every branch of the pathway is separately observable. Certain lactic acid bacteria — Lactobacillus collinoides and Lactobacillus diolivorans are the type cases — express a coenzyme-B_{12}-dependent glycerol dehydratase that converts glycerol to 3-hydroxypropionaldehyde. That aldehyde sits at a metabolic branch point. Reduction by an NADH-linked oxidoreductase yields 1,3-propanediol and regenerates oxidized cofactor, which is the point of the exercise; oxidation by an aldehyde dehydrogenase yields 3-hydroxypropionic acid; and the aldehyde

itself, when it accumulates, exists in aqueous solution as an equilibrium system of the free monomer, its hydrate, and a cyclic dimer — the antimicrobial complex known in the food-microbiology literature as reuterin.[62,67]

The redox bookkeeping explains why the pathway runs and predicts what accompanies it. A heterofermentative organism that has exhausted its sugars faces a cofactor problem: without an electron acceptor, the acetyl phosphate produced by the phosphoketolase route must be reduced to ethanol merely to balance the books. Glycerol dehydration followed by reduction to 1,3-propanediol supplies that acceptor externally, exactly as fructose reduction to mannitol does in Section 7.2, and the organism is thereby freed to discharge acetyl phosphate as acetate with an additional substrate-level phosphorylation. The diagnostic consequence is a pairing, not a single marker: glycerol falls, 1,3-propanediol rises, and acetate rises with them. Propionic acid frequently completes the profile in wild ciders and sidra, arising from lactate or diol metabolism by other members of the consortium, and is read, at the fully protonated limit that the working pH imposes on every acid in the panel, from its methyl triplet near δ 1.08 and its methylene quartet near δ 2.39 — where it must be distinguished from the pyruvate singlet at δ 2.38 by its multiplicity.

The aldehyde branch is the one with consequences beyond flavor. 3-Hydroxypropionaldehyde dehydrates readily under heat or strong acid to acrolein, and acrolein condenses with polyphenols to produce the intense, persistent bitterness known in the cider literature as amertume and recorded historically in spoiled beer.[62] For a producer the practical exposure is twofold. In the beverage itself, a glycerol-degrading contamination announces a latent bitterness defect that develops as the product ages. In distillation the stakes are higher, because 3-hydroxypropionaldehyde carried into the still dehydrates quantitatively in the boiler and acrolein, boiling at 53 °C, concentrates in the heads: a cider brandy or pomace spirit distilled from glycerol-degraded substrate carries a lachrymatory, acrid distillate defect that no cut can fully remove. A pre-distillation ^{1}H spectrum showing glycerol intact — or showing the diol and acid already present — settles before the boiler is fired whether the charge is sound, and this is among the most directly monetizable single observations the beverage qNMR panel offers a distilling client.[67]

The reporter signals are collected in Figure 23, where the three sidra traces are accompanied by the spectrum of a lot-numbered 1,3-propanediol certified standard acquired under matched conditions — the identification practice applied throughout this laboratory, in which no new assignment enters the routine panel until it has been confirmed against an authentic standard in the same matrix and on the same instrument. For a brewer the diagnostic value is high and the measurement is free, since the signal appears in the same spectrum that supplied everything else. The disappearance of glycerol alongside the appearance of 1,3-propanediol identifies a specific organism class and a specific metabolic state — sugars exhausted, glycerol under attack — and does so before the associated flavor defect is necessarily apparent on the palate. It is, in the author's experience, among the most reliable early warnings of unintended bacterial activity that the technique provides. The beer-side relevance is not hypothetical: glycerol in a conventional beer stands at one to two and a half grams per liter, higher still in high-gravity products, and constitutes a reservoir of latent substrate in any package that acquires a heterofermentative population; the pathway metabolites have been reported in beer by ^{1}H NMR, and their appearance in a packaged product is grounds for a recall-scale conversation rather than a routine flavor note.[8]

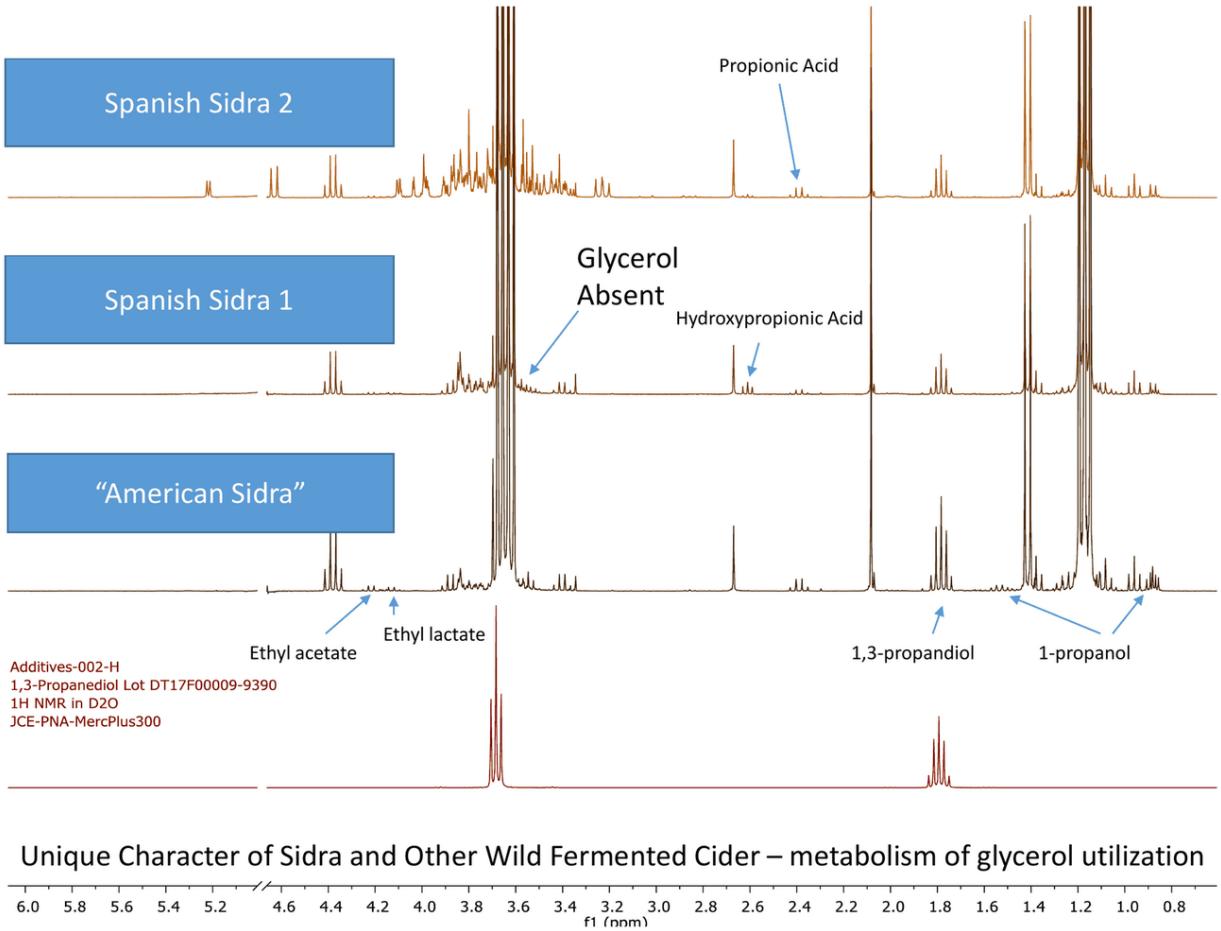


Figure 23. The glycerol conversion pathway read directly from the spectrum: stacked 300 MHz ^{1}H NMR spectra of two Spanish sidras and an American-made sidra-style cider, δ 0.7 to 6.1. In the Spanish products glycerol is absent and the pathway products are annotated — 1,3-propanediol (quintet, δ 1.76), 3-hydroxypropionic acid, propionic acid, ethyl acetate, ethyl lactate, and 1-propanol. The bottom trace is a lot-numbered 1,3-propanediol certified reference standard acquired in D_2O under matched conditions, against which the assignment was confirmed. Process NMR Associates data.

7.4 Non-Alcoholic and Low-Alcohol Products

The non-alcoholic and low-alcohol category poses two analytical problems simultaneously: an alcohol determination near the legal boundary of 0.5 % by volume, where the required accuracy is high and the analyte concentration is low, and a nutritional declaration for a product whose carbohydrate content is proportionally much larger than that of a conventional beer. Both are answered by the same experiment.

Figure 24 shows the analysis of a commercial non-alcoholic malt beverage. The declared values were 41 kcal, 8 g of carbohydrate, and an alcoholic strength below 0.5 % by volume per twelve-ounce serving; the NMR analysis returned 40.1 kcal, 7.6 g of carbohydrate, and 0.47 % by volume. Figure 25 extends the comparison to a set of six non-alcoholic and low-alcohol products, and Table 16 collects the results against the declarations.

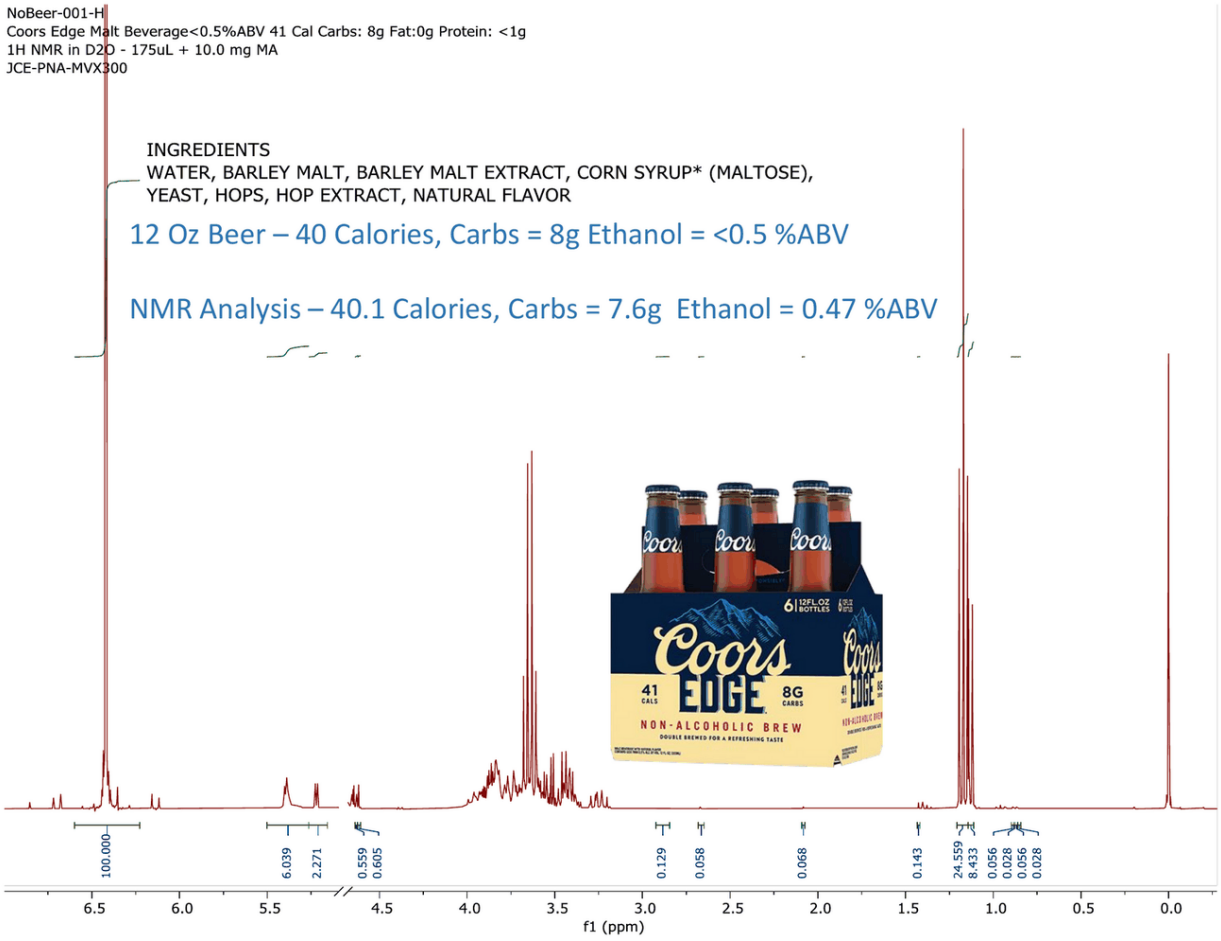


Figure 24. 300 MHz ^{1}H NMR spectrum of a commercial non-alcoholic malt beverage prepared from 175 µL of degassed product with 10.0 mg of maleic acid. Against declared values of 41 kcal, 8 g of carbohydrate, and less than 0.5 % v/v alcohol per twelve-ounce serving, the analysis returned 40.1 kcal, 7.6 g of carbohydrate, and 0.47 % v/v. The declared ingredient list — water, barley malt, barley malt extract, corn syrup (maltose), yeast, hops, hop extract, natural flavor — is reflected in the carbohydrate distribution. Process NMR Associates data.

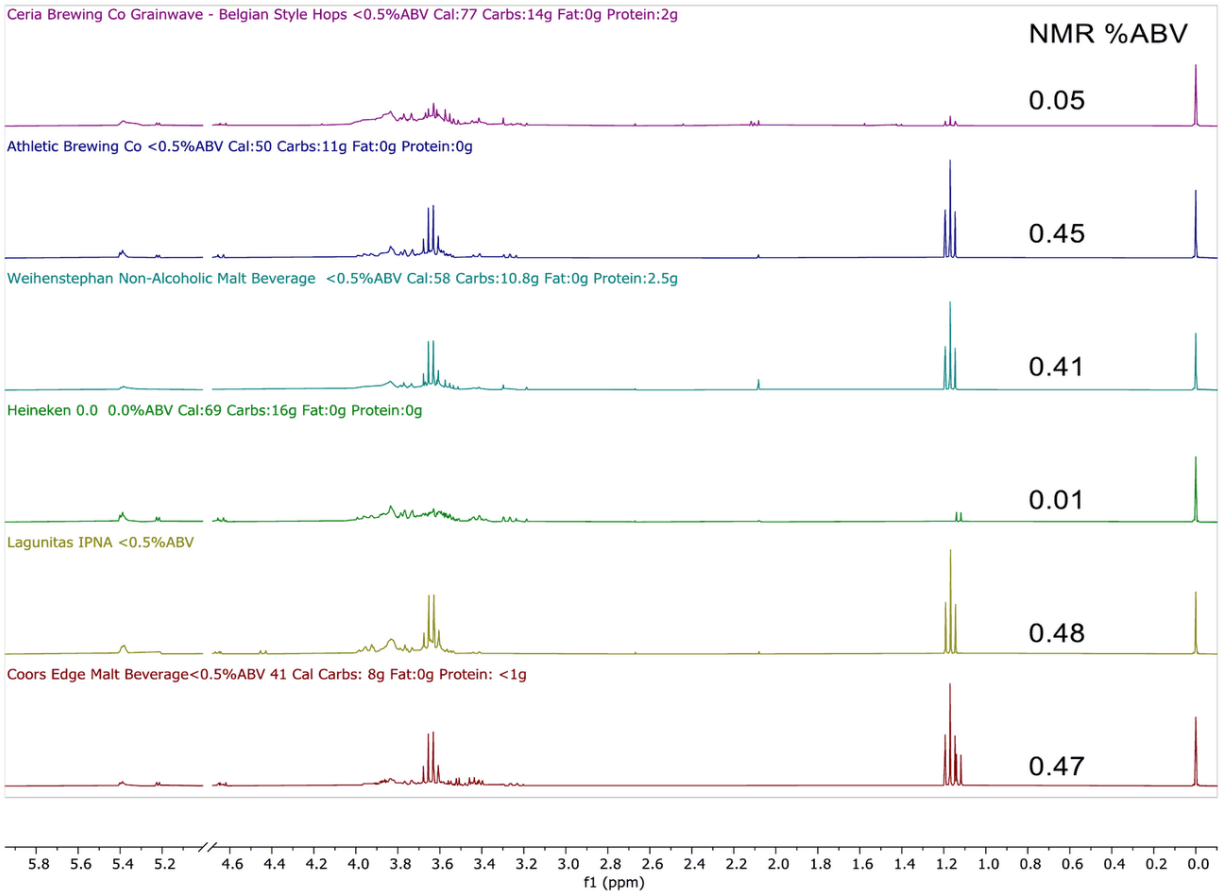


Figure 25. Stacked 300 MHz ^{1}H NMR spectra of six commercial non-alcoholic and low-alcohol products with the NMR-determined alcoholic strength annotated for each. Values span 0.01 % v/v for a product declared at 0.0 % to 0.48 % v/v for products declared below 0.5 %. The residual ethanol triplet near δ 1.18 is the reporter in every case. Process NMR Associates data.

Table 16. Non-alcoholic and low-alcohol products: qNMR alcoholic strength against declaration.

Product	Declared ABV	NMR ABV (% v/v)	Declared kcal	Declared carbohydrate (g)	Declared protein (g)
Ceria Brewing Grainwave, Belgian-style	<0.5 %	0.05	77	14	2
Athletic Brewing Co.	<0.5 %	0.45	50	11	0
Weihenstephan non-alcoholic malt beverage	<0.5 %	0.41	58	10.8	2.5
Heineken 0.0	0.0 %	0.01	69	16	0
Lagunitas IPNA	<0.5 %	0.48	—	—	—
Coors Edge malt beverage	<0.5 %	0.47	41	8	<1

Declared values are per twelve fluid ounce serving as printed on the package. The Coors Edge product was additionally subjected to the full nutritional calculation of Section 5.5, returning 40.1 kcal and 7.6 g of carbohydrate against the declared 41 kcal and 8 g. Process NMR Associates data.

Three points follow. The first concerns sensitivity: ethanol was measured at 0.01 % v/v, which is 79 mg L^{-1} or 1.7 mmol L^{-1}, in a sixteen-minute acquisition at 300 MHz, without concentration, extraction, or

distillation. That figure should be described as a measured value rather than as a validated limit of quantitation, because no blank, no replicate standard deviation, and no spike recovery accompany it, and at that level the ethanol triplet sits on the flank of the 2,3-butanediol doublet at δ 1.14 in a matrix that is chemically close to unfermented wort. A limit of quantitation established from replicate blanks and a spiked series is a short experiment and is required before the number is offered in a compliance context. The second is that the products cluster into two groups that the declaration does not distinguish: those made by restricted or arrested fermentation, which retain 0.4 to 0.5 % alcohol together with a substantial fermentation metabolite profile, and those made by dealcoholization or by essentially unfermented processes, which show one to five hundredths of a percent and a carbohydrate profile close to that of the starting wort. Both are lawfully described as containing less than 0.5 % alcohol by volume, and only the spectrum tells them apart. The chemistry of dealcoholized beer distillates and residual phases has been examined by NMR in exactly this spirit.[23,22]

The third is the observation that a product declared at 0.0 % returned 0.01 % v/v. This is not a compliance finding. It is well within any reasonable interpretation of a zero declaration and reflects the fact that dealcoholization is an equilibrium process rather than an absolute one. It does, however, illustrate the sensitivity available, and it is the kind of number that requires careful framing when it is reported to a client.

7.5 Preservatives, Additives, Sweeteners, and Label Chemistry

Because the analysis is untargeted, adjunct additions announce themselves without being sought. Lactose in a milk stout appears as the three-signal pattern of Section 6.2 and is quantified against the interference-free galactose doublet at δ 4.45. Cocoa nibs contribute theobromine, coffee contributes caffeine, and both are quantified from their methyl singlets in an otherwise clear region between δ 3.2 and 4.0. Fruit and fruit-juice additions contribute malic acid, and grape must contributes tartaric acid near δ 4.74, a signal visible in Figure 13 for the products in the survey that contain it, although its proximity to the suppression zone means the assignment should be confirmed against a spiked standard before it is offered as forensic evidence. Rice and maize adjuncts alter the dextrin distribution in ways the four-window scheme records. Preservatives, where present in a mixed beverage, are directly observable, sorbate through its conjugated diene resonances and benzoate through its aromatic pattern.

The forensic and label-compliance applications follow directly and require no additional method development. A beer claimed to contain wine must can be confirmed by tartrate; an all-malt claim can be tested against the dextrin and adjunct signature; a lactose declaration can be verified quantitatively; and a caffeine or theobromine content can be reported for a coffee or chocolate beer where a nutritional or allergen statement requires it. The broader authentication literature for beer, which uses the same spectra as the input to multivariate classifiers, is reviewed in Section 8.[17,21,24,26]

Preservatives deserve a systematic treatment, because their presence or absence encodes the entire production logic of a product. Conventionally fermented and packaged beer carries no added preservative and needs none: the matrix is intrinsically hostile, with a pH of 3.9 to 4.6, several percent of ethanol, dissolved carbon dioxide, near-anaerobiosis, and the iso-α-acids, which are themselves antimicrobial toward the Gram-positive organisms that would otherwise be the principal spoilers — and formulation practice under the Reinheitsgebot tradition and United States formula requirements reinforces the chemistry. The flavored malt beverage, hard seltzer, hard tea, and hard kombucha category inverts every one of those protections: bitterness is absent, flavor systems and fruit juices are added after fermentation, and many products are back-sweetened, so sorbate and benzoate preservation is routine there, and the

analytical question shifts from whether fermentation went right to whether the formulation is what the label says it is.

Both principal preservatives are excellent NMR analytes. Sorbic acid presents its conjugated diene multiplets between δ 5.8 and 7.3, a region of the flavored-beverage spectrum that is otherwise nearly empty, together with a methyl doublet near δ 1.85; benzoate presents its ortho-proton doublet near δ 7.9 with the meta and para protons near δ 7.5. Both are quantified against the maleic acid standard exactly as any other analyte, with no separate calibration, and the levels found in the Process NMR Associates survey — 182 to 222 mg/L of potassium sorbate and 234 to 688 mg/L of sodium benzoate across the products that contained them — sit comfortably within customary permitted-use ranges. Figure 26 makes the complementary point that the negative finding is equally certifiable: across a nine-product screening stack, the benzoate and sorbate windows are highlighted, the products that carry each preservative declare themselves at a glance, and the product labeled as preservative-free is confirmed to be so by the same spectrum. A screening of this kind, run as one experiment per product with no method development, is a label-compliance service in itself.[20,71]

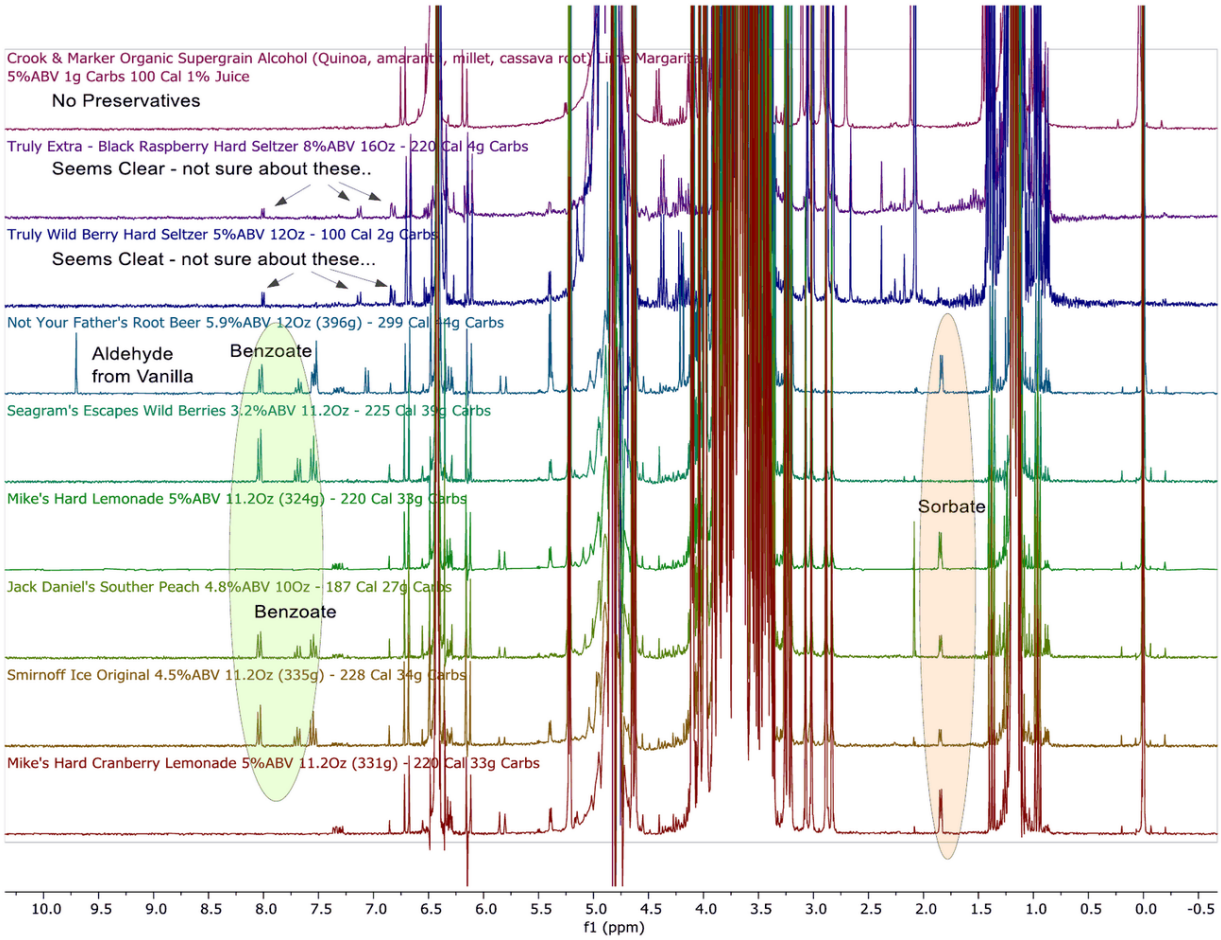


Figure 26. Preservative and additive screening across nine commercial flavored malt beverages and hard seltzers by 300 MHz ^{1}H NMR, δ 10.0 to −0.5. The benzoate aromatic window (highlighted, left) and the sorbate methyl window (highlighted, right) identify the preserved products directly; the vanillin aldehyde of a root-beer-flavored product is flagged in the aldehyde region; and the topmost product, declared free of preservatives, is confirmed clean in both windows. Process NMR Associates data.

The remainder of a flavored-beverage formulation reads out with equal directness, and Figure 27 annotates a single hard seltzer as a worked example. Citric acid at 1.4 to 4.3 g/L in the six acidulant-charged products of the survey — an order of magnitude above any fermentation citrate, and absent or at trace level in the remaining two — identifies the formulation acid. Propylene glycol at 1.5 to 2.3 g/L identifies the flavor-system carrier, and carries an integration trap worth recording: its methyl doublet at δ 1.13 falls almost exactly on the 2,3-butanediol doublet at δ 1.14, and the two are separated by deconvolution anchored on the propylene glycol methine multiplet near δ 3.9. Ethyl lactate and ethyl acetate appear as flavor-system components in products whose fermentation history could not have produced them. And the fermentation provenance of the alcohol base itself is legible: 2,3-butanediol and fusel alcohols at tens to hundreds of milligrams per liter mark a base that retains its fermentation congeners, whereas their absence marks a base stripped by distillation or aggressive carbon treatment.

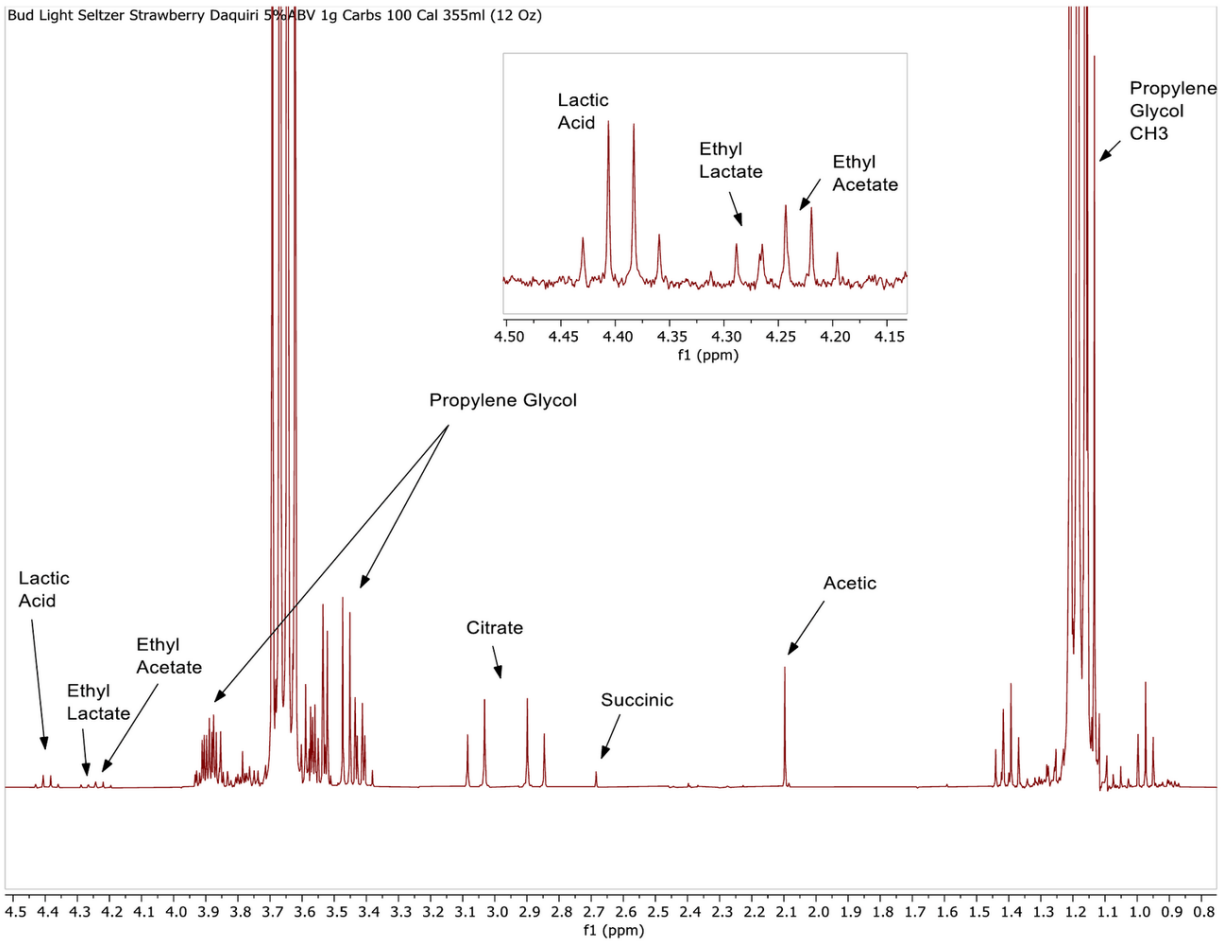


Figure 27. Fully annotated 300 MHz ^{1}H NMR spectrum of a commercial hard seltzer (declared 5 % ABV, 1 g carbohydrate, 100 kcal per 355 mL), δ 0.8 to 4.5, with the inset expanding δ 4.15 to 4.50. Labeled components: propylene glycol (methyl doublet δ 1.13, methine and methylene envelope δ 3.4–3.9), lactic acid, ethyl lactate and ethyl acetate (inset), citrate, succinate, and acetate. The additive inventory of the flavor system and the residual fermentation metabolites of the sugar base are read from a single acquisition. Process NMR Associates data.

Sweetener chemistry completes the formulation story, and it is here that the internal consistency of a label can actually be tested. Intact sucrose in a finished alcoholic product is a statement about process order: sucrose survives only if it was added after the yeast was removed or inactivated, so a back-sweetened

product must be pasteurized, sterile-filtered, or chemically preserved, and the spectrum shows whether the formulation is coherent. The ginger beer of Table 17, carrying 32.8 g/L of intact sucrose alongside potassium sorbate, is a coherent formulation; a hypothetical product showing the same sucrose with no preservative and a live-yeast sediment would be a refermentation incident in waiting, by exactly the logic of Section 7.7. The monosaccharide ratio is a second fingerprint: fructose-to-glucose near unity indicates invert sugar or hydrolyzed sucrose, a ratio near 1.3 matches high-fructose syrup of the HFCS-55 type, and a strongly inverted ratio — 3.3 in the hard kombucha of the survey — indicates selective microbial consumption of glucose, as the acetic acid bacteria of a kombucha culture oxidize glucose toward gluconate while leaving fructose behind. Steviol glycosides are directly observed in the products that declare them; sucralose and acesulfame at the tens-of-milligrams-per-liter levels of diet formulations sit at the margin of one-dimensional quantitation and are claimed here only as detectable, not as routinely quantifiable.

Two additive classes remain honest gaps, and one indirect observation partially closes a third. Propylene glycol alginate, the foam stabilizer, is a polymer whose broad resonances disappear into the baseline; caramel colorant contributes bulk carbohydrate-like intensity with no clean reporter beyond an elevated hydroxymethylfurfural marker; and the reduced iso-α-acid extracts used for light-stable products share the sensitivity limit of the native bitter acids. Sulfite, the third case, carries no proton and is formally invisible, but it betrays itself chemically: bisulfite adds across the acetaldehyde carbonyl to form the α-hydroxyethanesulfonate, whose methyl doublet appears near δ 1.5, so a product in which free acetaldehyde is absent while the adduct doublet is present is carrying sulfite — with the caution that the adduct falls close to the alanine doublet at δ 1.48 and must be resolved by coupling-constant inspection or deconvolution before it is reported.

Table 17 collects the full additive and sweetener inventory for eight commercial flavored malt beverages, seltzers, and related products analyzed by this method, and the interpretive reading in its final column shows how far a formulation can be reconstructed from one spectrum per product.

Table 17. Additive, preservative, and sweetener inventory of eight commercial flavored malt beverages and hard seltzers by ^{1}H qNMR. Concentrations in mg/L; alcoholic strength in % v/v. Declared strengths, in order: 4.8, 4.5, 5.0, 4.5, 5.0, 5.0, 4.8, and 4.5 % v/v.

Product	ABV (NMR)	Sucrose	Glucose	Fructose	Citric	Sorbate	Benzoate	Propylene glycol	Formulation reading
Crabbie's Ginger Beer	4.86	32 817	30 570	24 564	1379	222	0	0	Heavily back-sweetened after fermentation; sorbate-preserved; trace acetaldehyde consistent with ginger flavor system
Cape-Line Hard Strawberry Lemonade	4.68	0	10 526	10 150	2094	0	0	2258	Inverted-sugar sweetening; propylene glycol flavor carrier; citrate acidulant
White Claw Hard Seltzer, Natural Lime	5.10	2193	1608	1388	1524	0	0	0	Fermented near dryness; minimal sweetening; citrate acidulant only
Corona Guava-Lime Spiked Refresher	4.77	7722	31 281	30 509	4318	0	688	1453	Invert-sugar-type sweetening at f:g ≈ 1.0 with residual sucrose; benzoate-preserved; propylene glycol carrier
Mighty Swell Cherry Lime Spritzer	4.90	0	6482	7245	2388	0	0	0	Reduced-sugar formulation; steviol glycosides observed

Product	ABV (NMR)	Sucrose	Glucose	Fructose	Citric	Sorbate	Benzoate	Propylene glycol	Formulation reading
After Glow Hard Kombucha, Hops + Rose	4.90	0	6025	20 148	146	0	0	0	Kombucha signature: lactate 1298 and acetate 1146 mg/L; f:g = 3.3 from glucose-selective oxidation
Jack Daniel's Country Cocktail, Southern Citrus	4.86	0	39 566	51 044	3581	182	234	0	HFCS-55-type sweetening at f:g ≈ 1.3; dual sorbate–benzoate preservation
Wild Leaf Hard Tea, Green Tea + Apple + Honey	4.52	6266	14 248	13 547	0	0	0	0	Honey and apple sugar profile; malic acid 797 mg/L from apple; unpreserved

Concentrations transcribed from the Process NMR Associates flavored-malt-beverage survey (UC Davis Master Brewers presentation, 2022). Zero entries denote below the working quantitation limit of approximately 5–10 mg/L. 2,3-Butanediol was additionally observed at 85 to 648 mg/L in six of the eight products, marking fermented alcohol bases that retain their congeners.

7.6 Hops: α-Acids, β-Acids, and Terpenes

Hop analysis stands apart from the rest of this document in that the sample is not aqueous. Hop cones, pellets, and extracts are analyzed by ^{1}H NMR in deuterated chloroform after a solvent extraction adapted from the American Society of Brewing Chemists Hops-6 procedure, with NMR detection replacing the spectrophotometric or conductometric finish, and it is benchmarked against the chromatographic international method of the same body.[53] The approach follows the improved NMR method for α-acid quantification established by Hoek and co-workers,[54] and it sits alongside a body of work using NMR and chemometrics on lupulin gland material for hop breeding.[55]

Figure 28 shows the ^{1}H spectra of a hop series comprising Cascade harvested in two seasons and stored frozen and refrigerated, an Alpha Aroma variety, and a wild hop, with the myrcene and humulene olefinic resonances marked. Figure 29 shows the results of the analysis alongside a chromatogram acquired by the reference chromatographic method, and Table 18 collects the compositions.

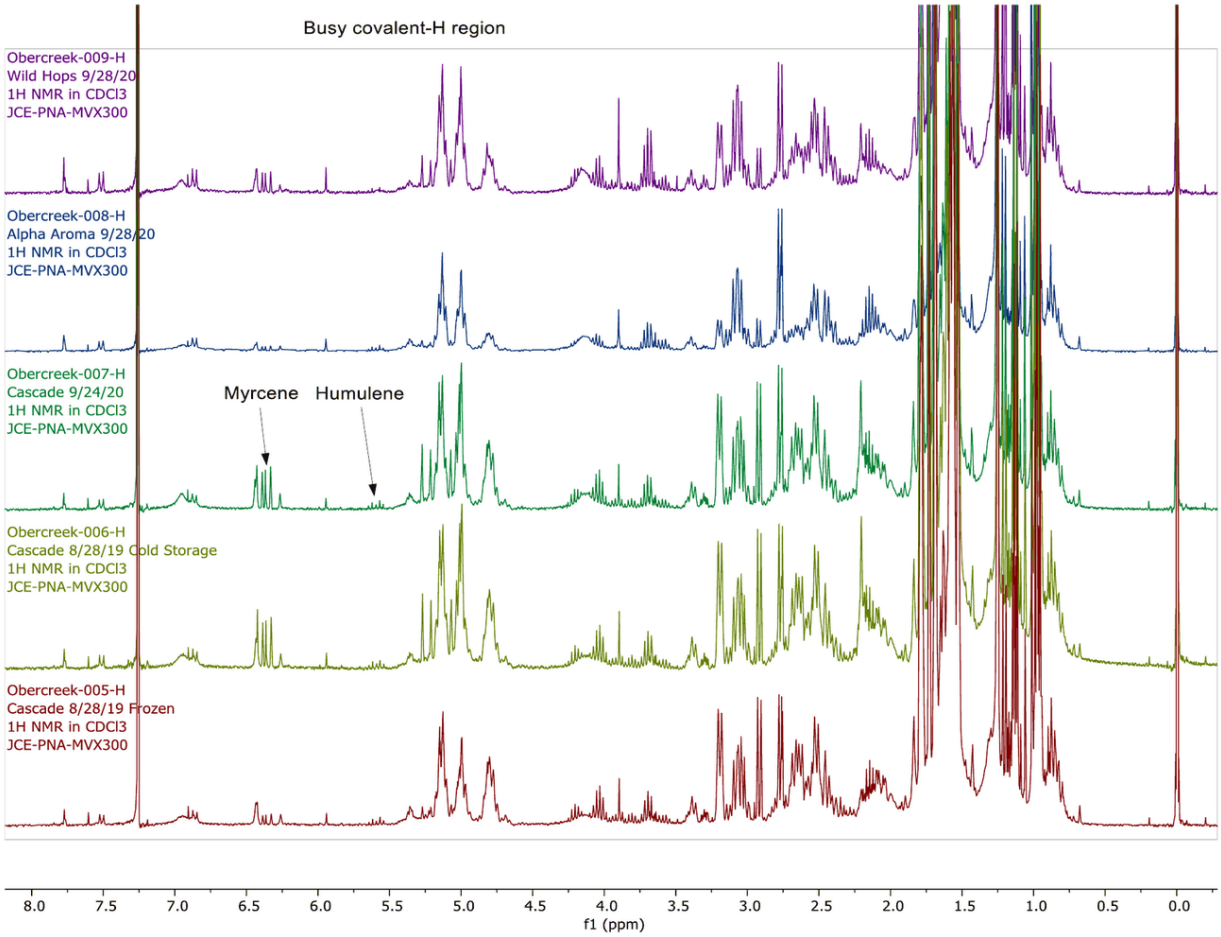
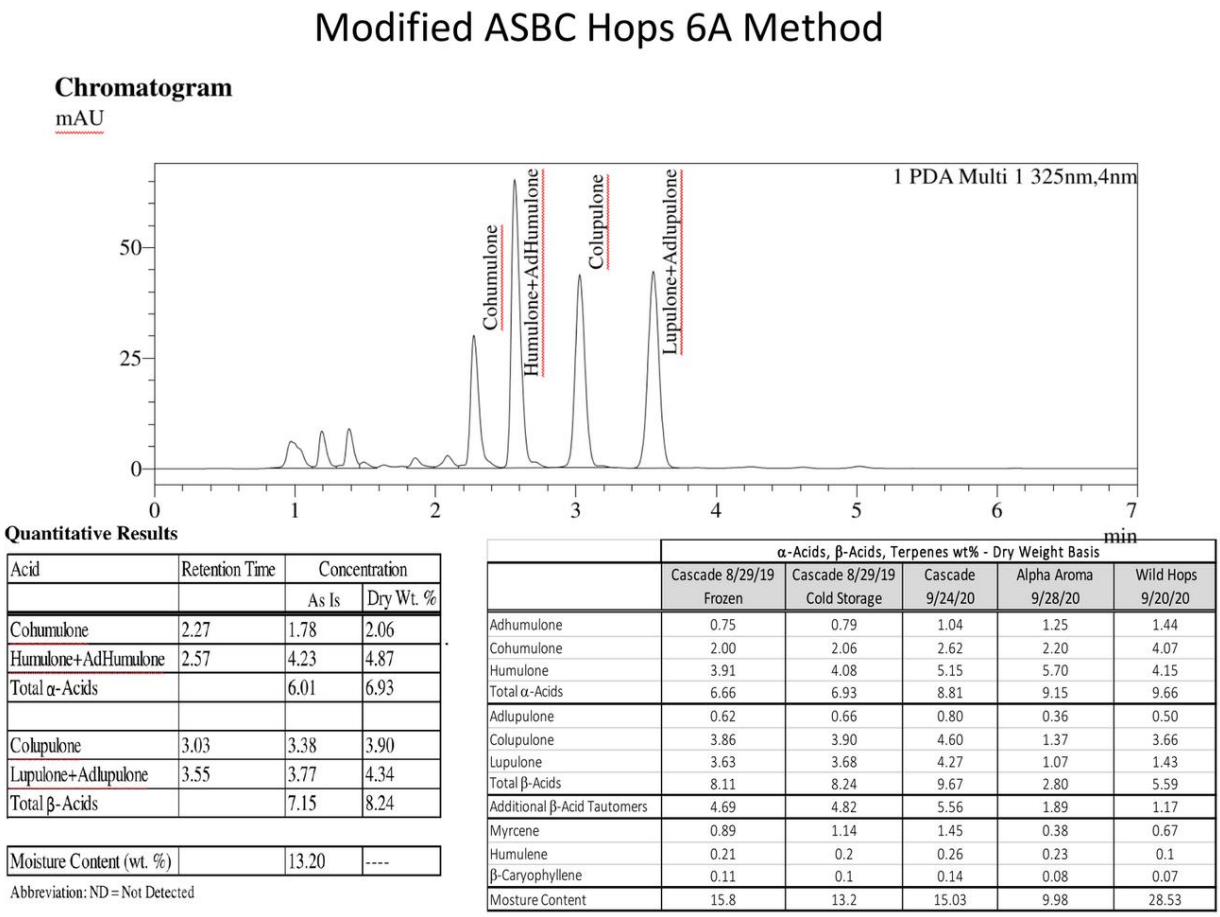


Figure 28. Stacked 300 MHz ^{1}H NMR spectra in $CDCl_3$ of five hop samples: Cascade harvested 29 August 2019 and held frozen and in cold storage, Cascade harvested 24 September 2020, an Alpha Aroma variety harvested 28 September 2020, and a wild hop harvested 20 September 2020. Myrcene and humulene olefinic resonances are marked; the congested region between δ 1.0 and 3.0 carries the aliphatic protons of the bitter acids and the terpene fraction. Process NMR Associates data.



Acid	Retention Time	Concentration	
		As Is	Dry Wt. %
Cohumulone	2.27	1.78	2.06
Humulone+AdHumulone	2.57	4.23	4.87
Total α-Acids		6.01	6.93
Colupulone	3.03	3.38	3.90
Lupulone+Adlupulone	3.55	3.77	4.34
Total β-Acids		7.15	8.24
Moisture Content (wt. %)		13.20	----

	α-Acids, β-Acids, Terpenes wt% - Dry Weight Basis				
	Cascade 8/29/19 Frozen	Cascade 8/29/19 Cold Storage	Cascade 9/24/20	Alpha Aroma 9/28/20	Wild Hops 9/20/20
Adhumulone	0.75	0.79	1.04	1.25	1.44
Cohumulone	2.00	2.06	2.62	2.20	4.07
Humulone	3.91	4.08	5.15	5.70	4.15
Total α-Acids	6.66	6.93	8.81	9.15	9.66
Adlupulone	0.62	0.66	0.80	0.36	0.50
Colupulone	3.86	3.90	4.60	1.37	3.66
Lupulone	3.63	3.68	4.27	1.07	1.43
Total β-Acids	8.11	8.24	9.67	2.80	5.59
Additional β-Acid Tautomers	4.69	4.82	5.56	1.89	1.17
Myrcene	0.89	1.14	1.45	0.38	0.67
Humulene	0.21	0.2	0.26	0.23	0.1
β-Caryophyllene	0.11	0.1	0.14	0.08	0.07
Mosture Content	15.8	13.2	15.03	9.98	28.53

Figure 29. Hop bitter acid analysis. Upper panel: chromatogram recorded at 325 nm as displayed, with cohumulone, humulone plus adhumulone, colupulone, and lupulone plus adlupulone resolved, together with the quantitative results on an as-is and dry-weight basis. Lower right: ^{1}H NMR compositional results for the five-sample hop series on a dry-weight basis, including the α-acid and β-acid congeners individually, additional β-acid tautomers, and the principal terpenes. Process NMR Associates data.

Table 18. Hop composition by ^{1}H NMR, mass percent on a dry-weight basis, with moisture content determined in the same analysis.

Component	Cascade 8/29/19 frozen	Cascade 8/29/19 cold storage	Cascade 9/24/20	Alpha Aroma 9/28/20	Wild hop 9/20/20
Adhumulone	0.75	0.79	1.04	1.25	1.44
Cohumulone	2.00	2.06	2.62	2.20	4.07
Humulone	3.91	4.08	5.15	5.70	4.15
Total α-acids	6.66	6.93	8.81	9.15	9.66
Adlupulone	0.62	0.66	0.80	0.36	0.50
Colupulone	3.86	3.90	4.60	1.37	3.66
Lupulone	3.63	3.68	4.27	1.07	1.43
Total β-acids	8.11	8.24	9.67	2.80	5.59
Additional β-acid tautomers	4.69	4.82	5.56	1.89	1.17

Component	Cascade 8/29/19 frozen	Cascade 8/29/19 cold storage	Cascade 9/24/20	Alpha Aroma 9/28/20	Wild hop 9/20/20
Myrcene	0.89	1.14	1.45	0.38	0.67
Humulene	0.21	0.20	0.26	0.23	0.10
β-Caryophyllene	0.11	0.10	0.14	0.08	0.07
Moisture content (%)	15.8	13.2	15.03	9.98	28.53

Process NMR Associates data. The reference chromatographic determination for the Cascade cold-storage lot shown in Figure 29 returned total α-acids of 6.93 % and total β-acids of 8.24 % on a dry-weight basis at 13.20 % moisture.

Two observations should be recorded, one favorable to the method and one cautionary. In favor: the NMR analysis resolves the individual α- and β-acid congeners, whereas the chromatographic method as run co-elutes humulone with adhumulone and lupulone with adlupulone, so that the NMR result carries structural detail the reference method does not. The cohumulone fraction of total α-acids is a variety- and quality-relevant parameter — 0.30 for the 2019 Cascade, 0.24 for the Alpha Aroma, and 0.42 for the wild hop in this set — and it is obtained here without a separate determination. The additional β-acid tautomer row, which has no counterpart in the chromatographic result, is potentially a further advantage, since tautomeric and oxidized forms of the β-acids are chemically distinct and are directly observable by NMR while being either invisible to or lumped within the chromatographic peaks. Whether that row is included in the stated β-acid total or is additional to it must, however, be recorded explicitly. If it is additional, the NMR total β-acid content of the cold-storage Cascade lot is 13.1 percent rather than 8.24, which is outside the published varietal range for Cascade and would remove the apparent agreement with the chromatographic figure altogether. The row should also be relabeled, since hulupones are oxidation products rather than tautomers and the two chemistries do not belong under one heading.

The caution concerns the comparison itself. For the cold-storage Cascade lot the tabulated NMR totals agree with the chromatographic totals to three significant figures in both α- and β-acids, and the congener sums reproduce the chromatographic co-eluting pairs exactly. Two independent determinations performed on a heterogeneous plant material do not agree to that precision. Either the tabulated column for that lot is the chromatographic result rather than an independent NMR determination, or the NMR integration was anchored to it. In either case the figure as presented cannot serve as evidence of agreement between methods, and it should not be offered to a client or a reviewer as such. A proper method comparison — twenty or more lots spanning the α-acid range, both methods run blind, results assessed by Bland–Altman analysis rather than by correlation coefficient — is straightforward to perform and would convert an illustrative table into a defensible validation. That study should be part of the accreditation package.

A second remark concerns the moisture content on which the whole dry-weight basis depends. Moisture cannot be obtained from the water resonance of a deuterochloroform extract, because water is soluble in chloroform only to some eight hundred milligrams per liter and the signal reports that solubility limit rather than the water content of the cone; the moisture values in Table 18 are therefore gravimetric or must be made so. The wild hop at 28.5 percent moisture was clearly incompletely dried, and the dry-weight correction it requires is correspondingly large and correspondingly uncertain. Where a dry-weight basis is reported, the moisture determination is part of the measurement chain and deserves the same scrutiny as the bitter acid determination itself. The identity, mass, and certified purity of the internal standard used for the deuterochloroform work are not recorded in the source material and must be entered in the method file: maleic acid is not soluble in chloroform and is not the standard here.

7.7 Diastatic Contamination and Package Stability

Among the most costly microbiological failures in modern craft brewing is contamination by Saccharomyces cerevisiae variety diastaticus, a strain group possessing an extracellular glucoamylase encoded by the STA1 gene that hydrolyzes α-(1→4) linkages from the non-reducing ends of dextrins and thereby ferments material that a conventional brewing strain cannot touch. The consequences appear after packaging: super-attenuation, loss of body, phenolic off-flavor where the strain also carries the POF1 phenotype, and, in the worst case, overpressurized and occasionally bursting packages. The organism is difficult to detect by conventional plating, and polymerase chain reaction assays targeting STA1 have been shown to give variable results because a promoter deletion determines whether the gene is expressed at a level sufficient to matter.[58,60]

The dextrin measurement of Section 6 addresses the problem from the opposite direction: rather than detecting the organism, it detects what the organism does. The signature is more specific than it might first appear, and getting it right matters. Glucoamylase acts exolytically from the non-reducing end, removing one glucose unit at a time; shortening a chain in that way destroys an α-(1→4) linkage but neither creates nor destroys a reducing terminus. Nor does the liberated glucose accumulate, since live yeast in the package ferments it as fast as it is released. The expected expression of diastatic activity is therefore a progressive decline in the α-(1→4) envelope at an essentially constant reducing-end integral, accompanied by rising ethanol and carbon dioxide — a distinctive pattern that no other spoilage route produces, and a cleaner diagnostic than a simple rise in free sugar would have been. Two spectra of the same package taken a fortnight apart at conditioning temperature therefore constitute a functional test for diastatic activity that is independent of the strain's genetics, that does not require the organism to be culturable, and that reports the magnitude of the risk rather than merely its presence. A stable dextrin envelope over a fortnight is evidence of package stability and a declining one is evidence against it, but the strength of that evidence is bounded by the repeatability of the α-(1→4) integral, which has not yet been measured in this laboratory; until it has been, the test detects gross activity reliably and marginal activity not at all.

> *Author data placeholder — diastaticus challenge study. A time-course experiment in which a clean beer is deliberately inoculated with a characterized STA1⁺ isolate and sampled at intervals, with the four-window integrals tracked against an uninoculated control, would establish the sensitivity and the time-to-detection of this test. It is a straightforward experiment with an obvious commercial application, and it would differentiate the laboratory's offering.*

7.8 Benchtop and At-Line Implementation

Nothing in the quantitation argument of Section 2 depends on high field. The ratio of Equation (2) holds at 43 MHz as it does at 800, and the components that matter most to a brewhouse — ethanol, the major organic acids, glycerol, the total carbohydrate envelope — have well-separated reporter signals that survive the loss of dispersion. Alcoholic strength has been determined in alcoholic beverages on a 45 MHz benchtop instrument,[63] fermentation has been followed by benchtop NMR in a teaching context with quantitation and process monitoring performed on the same data,[64] and non-invasive low-field monitoring of fermentation has been demonstrated on-line in a bioreactor.[65] What is lost at low field is precisely the material treated in Section 6: the anomeric region collapses, the four windows are no longer separable, and the structural argument disappears.

The realistic division of labor follows from that asymmetric loss. A benchtop instrument in the brewery answers the high-frequency questions — has this fermentation finished, is the alcohol on target, has lactate appeared where it should not have — at a cadence and a cost that a service laboratory cannot match. A high-field instrument in a specialist laboratory answers the questions that require resolution: what is the dextrin architecture, what is the branch distribution, what is the unidentified signal in the aromatic region. To position the two as competitors is to misread both.

8. From Spectra to Models: the Chemometric and Machine-Learning Roadmap

The material assembled in this document is intended to become the input to multivariate and machine-learning treatment, and the design decisions that determine whether that treatment succeeds are made at the point of data collection rather than at the point of modeling. This section sets out those decisions. The general framework — spectral preprocessing, latent-variable modeling, and validation — is the one set out for nutritional metabolomics by Savorani and co-workers, and the beer literature is a specialization of it.[29]

8.1 Two Data Matrices, Not One

Two distinct representations of the same spectra are available and they answer different questions. The targeted matrix has samples in rows and quantified concentrations in columns — ethanol, each organic acid, each amino acid, glycerol, the four dextrin windows, the branch and reducing-end integrals, and the derived structural parameters. It is compact, typically thirty to sixty columns, every column is interpretable without reference to a spectrum, and a model built on it can be explained to a brewer. Its weakness is that it discards everything that was not quantified, including the unassigned intensity that often carries the discriminating information.

The untargeted matrix has samples in rows and spectral intensities in columns, either at full digital resolution or binned. It preserves everything, including compounds not yet identified, and it is the representation in which style discrimination and authentication work is almost universally performed.[13,14,15,16,21,24,26] Its weakness is dimensionality: a 64k spectrum against a few dozen samples is a regime in which almost any classifier will find a perfect separation, and in which almost none of those separations will generalize. Binning to 0.01 or 0.04 ppm buckets reduces the column count to a few hundred and simultaneously absorbs small shift variations, at the cost of resolution.

The recommendation is to build both, from the same processed spectra, and to require that any conclusion drawn from one be visible in the other. A style separation that appears in the untargeted model and cannot be traced to any quantified component is a warning that the model has found a batch effect, an instrument drift, or a preparation artifact rather than a chemical difference.

8.2 Preprocessing

Preprocessing determines the outcome of a multivariate analysis more often than the choice of algorithm does, and each step embeds an assumption that should be stated. Table 19 sets out the chain recommended for this data set.

Table 19. Recommended preprocessing chain for the beer spectral matrix, with the assumption embedded in each step.

Step	Method	Assumption embedded	Failure mode if omitted or misapplied
Phase correction	Automated zeroth and first order with bounded PH1, reviewed manually	Absorption-mode lineshape is recoverable	Dispersive residue biases integrals asymmetrically and mimics concentration change
Baseline correction	Polynomial or penalized-least-squares over signal-free regions	Baseline is smooth relative to linewidth	Broad macromolecular signal is either removed as baseline or retained as analyte — decide explicitly
Referencing	TSP-d_4 at δ 0.00, or maleic acid at δ 6.40	Reference does not shift with matrix	Global shift offsets between samples appear as chemical differences
Solvent region excision	Remove δ 4.72–4.88 only, or the measured suppression profile	Suppression profile is constant between samples	A generously drawn window removes the β-reducing-end doublet at δ 4.65 and the α-(1→6) branch envelope at δ 4.95–5.00 — the chain count and branch count on which Section 6 depends
Alignment	icoshift, interval-wise[37]	Peaks correspond between samples	pH-driven shift of the acid resonances splits one variable into several
Binning	0.01–0.04 ppm buckets, or adaptive binning	Within-bin composition is homogeneous	Too coarse destroys resolution; too fine reinstates the alignment problem
Normalization	Total area, or probabilistic quotient, or to the internal standard	A common scale exists between samples	Total-area normalization makes every variable compositional and induces spurious negative correlations
Scaling	Pareto or unit variance	Low-intensity variables carry real information	Unit variance inflates noise regions to the status of major components
Transformation	Optional log or generalized-log	Multiplicative error structure	Untransformed data let the largest signals dominate the covariance

Two of these entries deserve emphasis. Normalization to total area is the default in metabolomics and is actively dangerous here, because beers differ enormously in total dissolved solids and because closing the data to a constant sum makes every variable dependent on every other. Where absolute concentrations are available — and in this method they are, which is unusual — the correct choice is to model the concentrations directly and to let the total vary. The second is the treatment of the suppression region: because water suppression profiles differ between samples and between sessions, the region must be excised on a common, generously drawn window rather than trimmed to whatever looks clean in each spectrum.

8.3 Unsupervised Structure First

Principal component analysis on the preprocessed matrix should be the first model built and should be examined before any class label is introduced. Its purpose is not classification but diagnosis: to reveal whether the dominant variance in the data set is chemical or procedural. Where samples separate by acquisition date, by analyst, or by which of two spectrometers was used, that separation will appear in the first two components and will contaminate every supervised model built afterward. Detecting it early is worth more than any subsequent modeling refinement. Hierarchical clustering on the same matrix provides a complementary view that does not impose orthogonality.

8.4 Supervised Models and the Validation Discipline

Partial least squares discriminant analysis and its orthogonal variant are the standard tools for style and origin discrimination and have been applied to beer repeatedly and successfully — to brewing site and production date,[2] to Trappist origin,[14] to Brazilian lagers,[15] to craft against industrial production,[13] to wheat beer sub-styles,[16] and to the starch-fragment composition that is the subject of Section 6.[42] Partial least squares regression against a continuous response has been used for alcoholic strength and for organic acid content.[5,42]

These methods share a well-documented failure mode: they will separate randomly labeled classes with apparent confidence if the number of variables exceeds the number of samples, which in spectroscopic work it invariably does. The safeguards are not optional and should be treated as part of the method rather than as a reporting nicety. Cross-validation must be applied to the entire modeling chain including variable selection and scaling, not to the final fit alone, since selecting variables on the full data set and then cross-validating the fit is a standard route to an optimistic result. Permutation testing, in which the class labels are randomized and the model rebuilt many times, establishes the null distribution against which the real model must be judged; the forty-five-beer starch study cited above used one hundred permutations for exactly this purpose.[42] A genuinely held-out test set, never seen during model development, is the only fully persuasive validation. And the sample counts must be honestly reported: a twenty-three-beer survey supports exploratory structure and hypothesis generation; it does not support a classification claim with a quoted accuracy.

The last point applies directly to the data set described in this document. The commercial survey was assembled for breadth of chemistry rather than by any sampling design, contains one or two examples of most styles, and includes two entries for the same product. It is an excellent demonstration set and a poor inference set, and any model built on it should be described as such.

8.5 Where Machine Learning Earns Its Place — and Where It Does Not

The case for methods beyond the linear latent-variable family rests on specific properties of the data rather than on the general attractiveness of the techniques. Three situations genuinely favor them. Where the relationship between spectrum and property is non-linear — and the relationship between the dextrin distribution and a sensory descriptor almost certainly is — tree ensembles and support vector regression will outperform partial least squares. Where the task is peak detection, deconvolution, or automated assignment in congested regions, convolutional models trained on simulated spectra have a real and demonstrated advantage, and automated profiling platforms for beer already operate on this principle.[6] And where the objective is anomaly detection rather than classification — flagging a production batch that departs from its own history — one-class methods trained on a single product's spectra are both appropriate and robust, and they sidestep the sample-count problem entirely because the training set is a hundred spectra of one beer rather than one spectrum each of a hundred beers.

Against this, three cautions. Interpretability is not a luxury in this application: a brewer will not change a process on the strength of a model that cannot say which part of the spectrum drove the prediction, and variable-importance measures from tree ensembles are a poor substitute for a loading plot that points at a chemical shift. Data volume is the binding constraint, and no architecture compensates for a data set of eighty spectra. And the temptation to fit an end-to-end model from raw spectrum to sensory score should be resisted until the intermediate quantities — the concentrations, the structural parameters — have been shown to correlate with the outcome, because a model that fails at that stage is informative about the chemistry, whereas one that fails end-to-end is not.

8.6 Designing the Library

A spectral library assembled for modeling has requirements that a library assembled as a by-product of client work does not meet, and the difference is worth planning for. Acquisition parameters must be frozen and recorded, since a change in recycle delay, transient count, or suppression scheme introduces a systematic difference that no preprocessing removes. Sample preparation must be identical, and the residual-ethanol process control proposed in Section 3.10 should be recorded for every lyophilized preparation. Metadata must be captured at the time of analysis rather than reconstructed later: style, original and final gravity, declared alcohol, mash regime, yeast strain, hopping schedule, packaging date, and analysis date. A control beer should be run at a defined interval and its results charted, so that instrument drift is documented rather than inferred. And the raw free induction decays should be retained alongside the processed spectra, because processing choices that seem settled today will be revisited, and reprocessing from the time-domain data is the only way to apply a new decision uniformly to historical samples.

> *Author data placeholder — the modeling data set. The assembled targeted and untargeted matrices, together with the metadata table and the control-chart history, are the deliverables that will carry this work into its chemometric phase. In accordance with standing practice, both matrices and all model inputs and outputs should be retained as spreadsheets and delivered alongside any modeling report.*

9. Limitations and What the Method Does Not See

A method description that lists only capabilities is of limited use to the person who has to decide whether to rely on it. The following limitations are real, are not fully removable by refinement of the present protocol, and should be stated to clients at the outset.

Sensitivity sets the floor. Components present below approximately five to ten milligrams per liter are difficult to observe and quantify in a one-dimensional spectrum acquired under the conditions of Section 3.5, and this is the boundary stated in the laboratory's own published summary of the method. The consequences are specific. The vicinal diketones — diacetyl and 2,3-pentanedione — occur in beer at ten to one hundred and fifty micrograms per liter, two to three orders of magnitude below the threshold, and although diacetyl appears in the nominal analytical panel it is in practice observable only in a grossly defective sample or in a deliberately spiked matrix; the methyl singlet near δ 2.36 cannot be relied upon for a diketone rest decision, sitting as it does within six hertz of the pyruvate singlet at δ 2.38 that the panel does quantify, and headspace gas chromatography with electron-capture detection remains the appropriate method. The sulfur volatiles, dimethyl sulfide above all, are likewise inaccessible and require sulfur-selective chromatographic detection. Isoamyl acetate and the other trace esters that dominate ester aroma are at or below the limit. The individual iso-α-acids in finished beer, at ten to one hundred milligrams per liter distributed across six congeners and multiple ring protons, cannot be resolved and quantified in one dimension, and the extensive NMR literature on their structures and storage chemistry was built on isolated material rather than on beer itself.[56,57]

Signal overlap sets a second limit that is independent of sensitivity. The carbohydrate ring-proton region between δ 3.2 and 4.4 is not resolvable at 300 MHz and is only partially resolvable at 600 MHz; compound-specific quantitation there is not attempted and should not be claimed. The branched-chain amino acids and fusel alcohols are a composite at 300 MHz. Where these matter, higher field, two-dimensional acquisition, or a chromatographic method is required.

Non-hydrogen-bearing and exchange-averaged species are invisible in principle. Carbon dioxide, the inorganic ions, and sulfate and phosphate are not observed in the proton spectrum, although the latter two are accessible by ^{31}P and the cations by their own nuclei. Exchangeable protons — hydroxyl, carboxyl, and amine — are exchanged into the deuterium reservoir and do not appear, which is a simplification for the carbohydrate work and a loss for anything that would have been reported by them.

Protein and peptide nitrogen is under-reported. The method quantifies free amino acids; it does not quantify peptide-bound nitrogen, and beers with appreciable soluble protein will return a protein figure well below a Kjeldahl or Dumas result. Where a regulatory protein declaration is required, a nitrogen determination remains necessary.

Finally, two systematic errors documented earlier in this paper remain uncorrected in the protocol as it stands: the relaxation bias of Section 3.8, whose magnitude is of the order of a few percent and is common to all analytes, and the volatile losses during degassing and lyophilization of Section 3.10, whose magnitude has not been measured. Both are straightforward to quantify and both should be quantified before the method is submitted for accreditation.

10. Conclusions

10.1 What the Method Delivers

A single sixteen-minute proton acquisition on a degassed beer, taken together with a second acquisition on a lyophilized aliquot of the same sample, returns a quantitative inventory spanning the alcohols, the fermentation-derived organic acids, the free amino acids and nucleosides, the polyols and diols, the free sugars, the residual dextrins resolved by chain length and by linkage, the aromatic and Maillard fraction, and the added adjuncts, together with the nutritional declaration values that follow arithmetically from them. No compound-specific calibration is required at any point, the response is linear across the full observable range, and the archived spectrum remains available for questions that had not been asked when the sample was run. Against a conventional analytical panel the technique replaces the majority of the routine composition determinations, complements rather than displaces chromatography for the trace volatiles, and supplies structural information about the dextrin fraction that no other routine method provides at all. The same composition, passed through the Balling mass balance, returns the traditional brewing parameters — original extract, apparent and real extract, and the apparent and real degrees of fermentation — in the vocabulary the brewhouse actually uses, and the same spectrum quantifies the preservatives, acidulants, carriers, and sweeteners of the flavored-beverage category, where formulation verification rather than fermentation control is the analytical question.

10.2 What This Study Adds

Three contributions of this document are worth restating. The quantitation scheme has been reduced from two multi-factor expressions to a pair of scalar response factors, tabulated in Table 9, which removes arithmetic from the routine analysis and makes the integration template auditable. The dominant uncorrected systematic error has been identified as the interaction between the 60° flip angle, the 15 s recycle period, and the spin–lattice relaxation of the maleic acid standard, and has been quantified in Table 3 so that the correction can be computed as soon as a relaxation survey has been performed. And an internal quality-control statistic has been introduced — the α-anomer fraction at the reducing end, which must lie

near the mutarotation equilibrium value — which detected an integration fault in one of the four mash samples reported here that would otherwise have propagated undetected into the derived structural parameters.

On the dextrin chemistry that motivated the study, the four-window integration scheme in use at Process NMR Associates has been compared point by point against degrees of polymerization determined independently by diffusion-ordered spectroscopy in the published literature and found consistent in ordering and at its high-frequency anchor, though not yet calibrated throughout, its structural parameters have been given in closed form with worked numerical examples, and a new compact descriptor — the branch-proximal fraction φ_NB of equation (18) — has been proposed and shown to vary from approximately 0.29 to 0.46 across the commercial survey independently of total dextrin content. The limits of what the present data can support have been stated explicitly in Section 6.12.

10.3 The Immediate Experimental Priorities

Four experiments would materially strengthen everything above and none of them is difficult. An inversion-recovery relaxation survey of the internal standard and the principal reporter signals would remove the largest uncorrected bias in the method. A degassing and lyophilization recovery study would replace an unknown with a measured figure. A calibration of the four α-(1→4) windows against high-performance anion-exchange chromatography or mass spectrometry on the same samples would convert the degree-of-polymerization labels from working annotations into validated assignments. And a proper blind method comparison for the hop bitter acid determination, assessed by difference analysis rather than correlation, would convert an illustrative table into accreditation evidence. Beyond these, the application of broadband homonuclear decoupling to the α-(1→6) branch envelope is the single most promising extension of the dextrin work, since it would convert one branch number into a branch-type distribution.

10.4 Corrections to Reference Material

Every reference cited in this document was resolved against the CrossRef registry before drafting. Three digital object identifiers carried in earlier Process NMR Associates material were found to be incorrect and are corrected here. The DiCaprio and Edwards sour-mash paper is registered under 10.1002/jib.138, not 10.1002/jib.144, the latter belonging to an unrelated paper on malt storage in the same journal. The Walther study of nineteenth-century beers is registered under 10.1016/j.foodchem.2015.03.051, not 10.1016/j.foodchem.2015.03.049, the latter belonging to an unrelated food-allergen paper. The Hoek method for α-acid quantification in hops is registered under an article code ending PCA550 with the check suffix 2-E, not PCA553 with suffix 2-8. Two further points of citation hygiene are noted: the Gidley starch branching paper carries two CrossRef registrations, of which 10.1016/0008-6215(85)90009-6 is the record served by the publisher and should be preferred over the legacy duplicate; and the American Society of Brewing Chemists chromatographic method for hop bitter acids is Hops-14, not Hops-6, the latter being the spectrophotometric and conductometric determination.

References

Every entry below was resolved against the CrossRef registry before drafting; author lists, titles, journals, volumes, pages, and years are as registered. Corrections to digital object identifiers carried in earlier Process NMR Associates material are itemized in Section 10.4.

1. Duarte, I.; Barros, A.; Belton, P. S.; Righelato, R.; Spraul, M.; Humpfer, E.; Gil, A. M. High-Resolution Nuclear Magnetic Resonance Spectroscopy and Multivariate Analysis for the Characterization of Beer. *J. Agric. Food Chem.* 2002, 50, 2475–2481. DOI: 10.1021/jf011345j.

2. Almeida, C.; Duarte, I. F.; Barros, A.; Rodrigues, J.; Spraul, M.; Gil, A. M. Composition of Beer by ^{1}H NMR Spectroscopy: Effects of Brewing Site and Date of Production. *J. Agric. Food Chem.* 2006, 54, 700–706. DOI: 10.1021/jf0526947.

3. Nord, L. I.; Vaag, P.; Duus, J. Ø. Quantification of Organic and Amino Acids in Beer by ^{1}H NMR Spectroscopy. *Anal. Chem.* 2004, 76, 4790–4798. DOI: 10.1021/ac0496852.

4. Duarte, I. F.; Godejohann, M.; Braumann, U.; Spraul, M.; Gil, A. M. Application of NMR Spectroscopy and LC-NMR/MS to the Identification of Carbohydrates in Beer. *J. Agric. Food Chem.* 2003, 51, 4847–4852. DOI: 10.1021/jf030097j.

5. Rodrigues, J. E. A.; Erny, G. L.; Barros, A. S.; Esteves, V. I.; Brandão, T.; Ferreira, A. A.; Cabrita, E.; Gil, A. M. Quantification of Organic Acids in Beer by Nuclear Magnetic Resonance (NMR)-Based Methods. *Anal. Chim. Acta* 2010, 674, 166–175. DOI: 10.1016/j.aca.2010.06.029.

6. Lee, B. L.; Shahin, F.; Selim, A.; Berjanskii, M.; Torres-Calzada, C.; Kovur, P.; Mandal, R.; Wishart, D. S. Automated Beer Analysis by NMR Spectroscopy. *ACS Food Sci. Technol.* 2025, 5, 378–388. DOI: 10.1021/acsfoodscitech.4c00896.

7. Lachenmeier, D. W.; Frank, W.; Humpfer, E.; Schäfer, H.; Keller, S.; Märtter, M.; Spraul, M. Quality Control of Beer Using High-Resolution Nuclear Magnetic Resonance Spectroscopy and Multivariate Analysis. *Eur. Food Res. Technol.* 2005, 220, 215–221. DOI: 10.1007/s00217-004-1070-7.

8. Kaufmann, M.; Schwarz, K. J.; Dallmann, A.; Kuballa, T.; Bergmann, M. ^{1}H NMR Spectroscopic Discrimination of Different Beer Styles Combined with a Chemical Shift-Based Quantification Approach. *Eur. Food Res. Technol.* 2022, 248, 635–645. DOI: 10.1007/s00217-021-03914-8.

9. Khatib, A.; Wilson, E. G.; Kim, H. K.; Lefeber, A. W. M.; Erkelens, C.; Choi, Y. H.; Verpoorte, R. Application of Two-Dimensional J-Resolved Nuclear Magnetic Resonance Spectroscopy to Differentiation of Beer. *Anal. Chim. Acta* 2006, 559, 264–270. DOI: 10.1016/j.aca.2005.11.064.

10. Spevacek, A. R.; Benson, K. H.; Bamforth, C. W.; Slupsky, C. M. Beer Metabolomics: Molecular Details of the Brewing Process and the Differential Effects of Late and Dry Hopping on Yeast Purine Metabolism. *J. Inst. Brew.* 2016, 122, 21–28. DOI: 10.1002/jib.291.

11. Rodrigues, J. A.; Barros, A. S.; Carvalho, B.; Brandão, T.; Gil, A. M. Probing Beer Aging Chemistry by Nuclear Magnetic Resonance and Multivariate Analysis. *Anal. Chim. Acta* 2011, 702, 178–187. DOI: 10.1016/j.aca.2011.06.042.

12. Duarte, I. F.; Barros, A.; Almeida, C.; Spraul, M.; Gil, A. M. Multivariate Analysis of NMR and FTIR Data as a Potential Tool for the Quality Control of Beer. *J. Agric. Food Chem.* 2004, 52, 1031–1038. DOI: 10.1021/jf030659z.

13. Palmioli, A.; Alberici, D.; Ciaramelli, C.; Airoldi, C. Metabolomic Profiling of Beers: Combining ^{1}H NMR Spectroscopy and Chemometric Approaches to Discriminate Craft and Industrial Products. *Food Chem.* 2020, 327, 127025. DOI: 10.1016/j.foodchem.2020.127025.

14. Mannina, L.; Marini, F.; Antiochia, R.; Cesa, S.; Magrì, A.; Capitani, D.; Sobolev, A. P. Tracing the Origin of Beer Samples by NMR and Chemometrics: Trappist Beers as a Case Study. *Electrophoresis* 2016, 37, 2710–2719. DOI: 10.1002/elps.201600082.

15. da Silva, L. A.; Flumignan, D. L.; Tininis, A. G.; Pezza, H. R.; Pezza, L. Discrimination of Brazilian Lager Beer by ^{1}H NMR Spectroscopy Combined with Chemometrics. *Food Chem.* 2019, 272, 488–493. DOI: 10.1016/j.foodchem.2018.08.077.

16. Chorbadzhiev, P.; Gerginova, D.; Simova, S. Weiss or Wit: Chemical Profiling of Wheat Beers via NMR-Based Metabolomics. *Foods* 2025, 14, 1621. DOI: 10.3390/foods14091621.

17. Kuballa, T.; Brunner, T. S.; Thongpanchang, T.; Walch, S. G.; Lachenmeier, D. W. Application of NMR for Authentication of Honey, Beer and Spices. *Curr. Opin. Food Sci.* 2018, 19, 57–62. DOI: 10.1016/j.cofs.2018.01.007.

18. Hatzakis, E. Nuclear Magnetic Resonance (NMR) Spectroscopy in Food Science: A Comprehensive Review. *Compr. Rev. Food Sci. Food Saf.* 2019, 18, 189–220. DOI: 10.1111/1541-4337.12408.

19. Anderson, H. E.; Santos, I. C.; Hildenbrand, Z. L.; Schug, K. A. A Review of the Analytical Methods Used for Beer Ingredient and Finished Product Analysis and Quality Control. *Anal. Chim. Acta* 2019, 1085, 1–20. DOI: 10.1016/j.aca.2019.07.061.

20. Milbert, S.; Laumeyer, J. T.; Müller, T. M.; Krenz, O.; Fuchs, J.; Lehmann, L.; Seifert, S. T. Quantification of Ingredients and Additives of Beer and Beer-Based Mixed Beverages by ^{1}H NMR Spectroscopy and Automated PULCON Analysis. *Anal. Chem.* 2026, 98, 12351–12361. DOI: 10.1021/acs.analchem.5c07171.

21. Jeong, J.-H.; Cho, S.-J.; Kim, Y. High-Resolution NMR Spectroscopy for the Classification of Beer. *Bull. Korean Chem. Soc.* 2017, 38, 466–470. DOI: 10.1002/bkcs.11113.

22. Sánchez-Estébanez, C.; Ferrero, S.; Alvarez, C. M.; Villafañe, F.; Caballero, I.; Blanco, C. A. Nuclear Magnetic Resonance Methodology for the Analysis of Regular and Non-Alcoholic Lager Beers. *Food Anal. Methods* 2018, 11, 11–22. DOI: 10.1007/s12161-017-0953-8.

23. Labrado, D.; Ferrero, S.; Caballero, I.; Alvarez, C. M.; Villafañe, F.; Blanco, C. A. Identification by NMR of Key Compounds Present in Beer Distillates and Residual Phases after Dealcoholization by Vacuum Distillation. *J. Sci. Food Agric.* 2020, 100, 3971–3978. DOI: 10.1002/jsfa.10441.

24. Biancolillo, A.; Bucci, R.; Magrì, A. L.; Magrì, A. D.; Marini, F. Data-Fusion for Multiplatform Characterization of an Italian Craft Beer Aimed at Its Authentication. *Anal. Chim. Acta* 2014, 820, 23–31. DOI: 10.1016/j.aca.2014.02.024.

25. Carisma, N. A. S.; Calingacion, M. N. Metabolomics and (Craft) Beers – Recent Advances. *Food Res. Int.* 2025, 205, 116010. DOI: 10.1016/j.foodres.2025.116010.

26. Cavallini, N.; Savorani, F.; Bro, R.; Cocchi, M. A Metabolomic Approach to Beer Characterization. *Molecules* 2021, 26, 1472. DOI: 10.3390/molecules26051472.

27. Walther, A.; Ravasio, D.; Qin, F.; Wendland, J.; Meier, S. Development of Brewing Science in (and since) the Late 19th Century: Molecular Profiles of 110–130 Year Old Beers. *Food Chem.* 2015, 183, 227–234. DOI: 10.1016/j.foodchem.2015.03.051.

28. DiCaprio, A.; Edwards, J. Application of Quantitative Nuclear Magnetic Resonance Spectroscopy to Biological Acidification of Barley Mashes. *J. Inst. Brew.* 2014, 120, 207–211. DOI: 10.1002/jib.138.

29. Savorani, F.; Rasmussen, M. A.; Mikkelsen, M. S.; Engelsen, S. B. A Primer to Nutritional Metabolomics by NMR Spectroscopy and Chemometrics. *Food Res. Int.* 2013, 54, 1131–1145. DOI: 10.1016/j.foodres.2012.12.025.

30. Bharti, S. K.; Roy, R. Quantitative ^{1}H NMR Spectroscopy. *TrAC, Trends Anal. Chem.* 2012, 35, 5–26. DOI: 10.1016/j.trac.2012.02.007.

31. Wider, G.; Dreier, L. Measuring Protein Concentrations by NMR Spectroscopy. *J. Am. Chem. Soc.* 2006, 128, 2571–2576. DOI: 10.1021/ja055336t.

32. Akoka, S.; Barantin, L.; Trierweiler, M. Concentration Measurement by Proton NMR Using the ERETIC Method. *Anal. Chem.* 1999, 71, 2554–2557. DOI: 10.1021/ac981422i.

33. Ernst, R. R.; Anderson, W. A. Application of Fourier Transform Spectroscopy to Magnetic Resonance. *Rev. Sci. Instrum.* 1966, 37, 93–102. DOI: 10.1063/1.1719961.

34. McKay, R. T. How the 1D-NOESY Suppresses Solvent Signal in Metabonomics NMR Spectroscopy: An Examination of the Pulse Sequence Components and Evolution. *Concepts Magn. Reson., Part A* 2011, 38A, 197–220. DOI: 10.1002/cmr.a.20223.

35. Smallcombe, S. H.; Patt, S. L.; Keifer, P. A. WET Solvent Suppression and Its Applications to LC NMR and High-Resolution NMR Spectroscopy. *J. Magn. Reson., Ser. A* 1995, 117, 295–303. DOI: 10.1006/jmra.1995.0759.

36. Hwang, T. L.; Shaka, A. J. Water Suppression That Works. Excitation Sculpting Using Arbitrary Wave-Forms and Pulsed-Field Gradients. *J. Magn. Reson., Ser. A* 1995, 112, 275–279. DOI: 10.1006/jmra.1995.1047.

37. Savorani, F.; Tomasi, G.; Engelsen, S. B. icoshift: A Versatile Tool for the Rapid Alignment of 1D NMR Spectra. *J. Magn. Reson.* 2010, 202, 190–202. DOI: 10.1016/j.jmr.2009.11.012.

38. Petersen, B. O.; Nilsson, M.; Bøjstrup, M.; Hindsgaul, O.; Meier, S. ^{1}H NMR Spectroscopy for Profiling Complex Carbohydrate Mixtures in Non-Fractionated Beer. *Food Chem.* 2014, 150, 65–72. DOI: 10.1016/j.foodchem.2013.10.136.

39. Petersen, B. O.; Hindsgaul, O.; Meier, S. Profiling of Carbohydrate Mixtures at Unprecedented Resolution Using High-Precision ^{1}H–^{13}C Chemical Shift Measurements and a Reference Library. *Analyst* 2014, 139, 401–406. DOI: 10.1039/C3AN01922E.

40. Petersen, B. O.; Motawie, M. S.; Møller, B. L.; Hindsgaul, O.; Meier, S. NMR Characterization of Chemically Synthesized Branched α-Dextrin Model Compounds. *Carbohydr. Res.* 2015, 403, 149–156. DOI: 10.1016/j.carres.2014.05.011.

41. Bøjstrup, M.; Petersen, B. O.; Beeren, S. R.; Hindsgaul, O.; Meier, S. Fast and Accurate Quantitation of Glucans in Complex Mixtures by Optimized Heteronuclear NMR Spectroscopy. *Anal. Chem.* 2013, 85, 8802–8808. DOI: 10.1021/ac401980m.

42. Sundekilde, U. K.; Meier, S. ^{1}H–^{13}C NMR-Based Profiling of Biotechnological Starch Utilization. *Anal. Chem.* 2016, 88, 9685–9690. DOI: 10.1021/acs.analchem.6b02555.

43. Beeren, S. R.; Petersen, B. O.; Bøjstrup, M.; Hindsgaul, O.; Meier, S. Time-Resolved in-Situ Observation of Starch Polysaccharide Degradation Pathways. *ChemBioChem* 2013, 14, 2506–2511. DOI: 10.1002/cbic.201300461.

44. Petersen, B. O.; Olsen, O.; Beeren, S. R.; Hindsgaul, O.; Meier, S. Monitoring Pathways of β-Glucan Degradation by Enzyme Mixtures in Situ. *Carbohydr. Res.* 2013, 368, 47–51. DOI: 10.1016/j.carres.2012.12.006.

45. Gidley, M. J. Quantification of the Structural Features of Starch Polysaccharides by N.M.R. Spectroscopy. *Carbohydr. Res.* 1985, 139, 85–93. DOI: 10.1016/0008-6215(85)90009-6.

46. Nilsson, G. S.; Gorton, L.; Bergquist, K.-E.; Nilsson, U. Determination of the Degree of Branching in Normal and Amylopectin Type Potato Starch with ^{1}H-NMR Spectroscopy: Improved Resolution and Two-Dimensional Spectroscopy. *Starch/Stärke* 1996, 48, 352–357. DOI: 10.1002/star.19960481003.

47. Enevoldsen, B. S.; Bathgate, G. N. Structural Analysis of Wort Dextrins by Means of β-Amylase and the Debranching Enzyme, Pullulanase. *J. Inst. Brew.* 1969, 75, 433–443. DOI: 10.1002/j.2050-0416.1969.tb06377.x.

48. Enevoldsen, B. S.; Schmidt, F. Dextrins in Brewing: Studies on the Singly-Branched and Multiply-Branched Dextrins in Brewing. *J. Inst. Brew.* 1974, 80, 520–533. DOI: 10.1002/j.2050-0416.1974.tb03643.x.

49. Viel, S.; Capitani, D.; Mannina, L.; Segre, A. Diffusion-Ordered NMR Spectroscopy: A Versatile Tool for the Molecular Weight Determination of Uncharged Polysaccharides. *Biomacromolecules* 2003, 4, 1843–1847. DOI: 10.1021/bm0342638.

50. Nilsson, M.; Duarte, I. F.; Almeida, C.; Delgadillo, I.; Goodfellow, B. J.; Gil, A. M.; Morris, G. A. High-Resolution NMR and Diffusion-Ordered Spectroscopy of Port Wine. *J. Agric. Food Chem.* 2004, 52, 3736–3743. DOI: 10.1021/jf049797u.

51. Maple, S. R.; Allerhand, A. Detailed Tautomeric Equilibrium of Aqueous D-Glucose. Observation of Six Tautomers by Ultrahigh Resolution Carbon-13 NMR. *J. Am. Chem. Soc.* 1987, 109, 3168–3169. DOI: 10.1021/ja00244a063.

52. Maebayashi, M.; Ohba, M.; Takeuchi, T. Anomeric Proportions of D-Glucopyranose at the Equilibrium Determined from ^{1}H-NMR Spectra I. Investigation of Experimental Conditions and Concentration Dependence at 25.0 °C. *J. Mol. Liq.* 2017, 232, 408–415. DOI: 10.1016/j.molliq.2017.02.062.

53. American Society of Brewing Chemists. *Methods of Analysis*, 14th ed.; Method Hops-14: α-Acids and β-Acids in Hops and Hop Extracts by HPLC (International Method); ASBC: St. Paul, MN, 2011. DOI: 10.1094/ASBCMOA-Hops-14.

54. Hoek, A. C.; Hermans-Lokkerbol, A. C. J.; Verpoorte, R. An Improved NMR Method for the Quantification of α-Acids in Hops and Hop Products. *Phytochem. Anal.* 2001, 12, 53–57. DOI: 10.1002/1099-1565(200101/02)12:1<53::AID-PCA550>3.0.CO;2-E.

55. Killeen, D. P.; Watkins, O. C.; Sansom, C. E.; Andersen, D. H.; Gordon, K. C.; Perry, N. B. Fast Sampling, Analyses and Chemometrics for Plant Breeding: Bitter Acids, Xanthohumol and Terpenes in Lupulin Glands of Hops (*Humulus lupulus*). *Phytochem. Anal.* 2017, 28, 50–57. DOI: 10.1002/pca.2642.

56. Intelmann, D.; Kummerlöwe, G.; Haseleu, G.; Desmer, N.; Schulze, K.; Fröhlich, R.; Frank, O.; Luy, B.; Hofmann, T. Structures of Storage-Induced Transformation Products of the Beer's Bitter Principles, Revealed by Sophisticated NMR Spectroscopic and LC–MS Techniques. *Chem. – Eur. J.* 2009, 15, 13047–13058. DOI: 10.1002/chem.200902058.

57. Intelmann, D.; Hofmann, T. On the Autoxidation of Bitter-Tasting Iso-α-acids in Beer. *J. Agric. Food Chem.* 2010, 58, 5059–5067. DOI: 10.1021/jf100083e.

58. Meier-Dörnberg, T.; Kory, O. I.; Jacob, F.; Michel, M.; Hutzler, M. *Saccharomyces cerevisiae* Variety *diastaticus* Friend or Foe? — Spoilage Potential and Brewing Ability of Different *Saccharomyces cerevisiae* Variety *diastaticus* Yeast Isolates by Genetic, Phenotypic and Physiological Characterization. *FEMS Yeast Res.* 2018, 18, foy023. DOI: 10.1093/femsyr/foy023.

59. Hill, A. E.; Stewart, G. G. Free Amino Nitrogen in Brewing. *Fermentation* 2019, 5, 22. DOI: 10.3390/fermentation5010022.

60. Krogerus, K.; Magalhães, F.; Kuivanen, J.; Gibson, B. A Deletion in the STA1 Promoter Determines Maltotriose and Starch Utilization in STA1^{+} *Saccharomyces cerevisiae* Strains. *Appl. Microbiol. Biotechnol.* 2019, 103, 7597–7615. DOI: 10.1007/s00253-019-10021-y.

61. Steensels, J.; Daenen, L.; Malcorps, P.; Derdelinckx, G.; Verachtert, H.; Verstrepen, K. J. *Brettanomyces* Yeasts — From Spoilage Organisms to Valuable Contributors to Industrial Fermentations. *Int. J. Food Microbiol.* 2015, 206, 24–38. DOI: 10.1016/j.ijfoodmicro.2015.04.005.

62. Garai-Ibabe, G.; Ibarburu, I.; Berregi, I.; Claisse, O.; Lonvaud-Funel, A.; Irastorza, A.; Dueñas, M. T. Glycerol Metabolism and Bitterness Producing Lactic Acid Bacteria in Cidermaking. *Int. J. Food Microbiol.* 2008, 121, 253–261. DOI: 10.1016/j.ijfoodmicro.2007.11.004.

63. Isaac-Lam, M. F. Determination of Alcohol Content in Alcoholic Beverages Using 45 MHz Benchtop NMR Spectrometer. *Int. J. Spectrosc.* 2016, 2016, 2526946. DOI: 10.1155/2016/2526946.

64. Jenne, A.; Soong, R.; Downey, K.; Biswas, R. G.; Decker, V.; Busse, F.; Goerling, B.; Haber, A.; Simpson, M. J.; Simpson, A. J. Brewing Alcohol 101: An Undergraduate Experiment Utilizing Benchtop NMR for Quantification and Process Monitoring. *Magn. Reson. Chem.* 2024, 62, 429–438. DOI: 10.1002/mrc.5428.

65. Kreyenschulte, D.; Paciok, E.; Regestein, L.; Blümich, B.; Büchs, J. Online Monitoring of Fermentation Processes via Non-Invasive Low-Field NMR. *Biotechnol. Bioeng.* 2015, 112, 1810–1821. DOI: 10.1002/bit.25599.

66. Cutaia, A. J.; Reid, A.-J.; Speers, R. A. Examination of the Relationships Between Original, Real and Apparent Extracts, and Alcohol in Pilot Plant and Commercially Produced Beers. *J. Inst. Brew.* 2009, 115, 318–327. DOI: 10.1002/j.2050-0416.2009.tb00387.x.

67. Vollenweider, S.; Lacroix, C. 3-Hydroxypropionaldehyde: Applications and Perspectives of Biotechnological Production. *Appl. Microbiol. Biotechnol.* 2004, 64, 16–27. DOI: 10.1007/s00253-003-1497-y.

68. Wisselink, H. W.; Weusthuis, R. A.; Eggink, G.; Hugenholtz, J.; Grobben, G. J. Mannitol Production by Lactic Acid Bacteria: A Review. *Int. Dairy J.* 2002, 12, 151–161. DOI: 10.1016/S0958-6946(01)00153-4.

69. Spitaels, F.; Wieme, A. D.; Janssens, M.; Aerts, M.; Daniel, H.-M.; Van Landschoot, A.; De Vuyst, L.; Vandamme, P. The Microbial Diversity of Traditional Spontaneously Fermented Lambic Beer. *PLoS ONE* 2014, 9, e95384. DOI: 10.1371/journal.pone.0095384.

70. Bossaert, S.; Winne, V.; Van Opstaele, F.; Buyse, J.; Verreth, C.; Herrera-Malaver, B.; Van Geel, M.; Verstrepen, K. J.; Crauwels, S.; De Rouck, G.; Lievens, B. Description of the Temporal Dynamics in Microbial Community Composition and Beer Chemistry in Sour Beer Production via Barrel Ageing of Finished Beers. *Int. J. Food Microbiol.* 2021, 339, 109030. DOI: 10.1016/j.ijfoodmicro.2020.109030.

71. Ackermann, S. M.; Dolsophon, K.; Monakhova, Y. B.; Kuballa, T.; Reusch, H.; Thongpanchang, T.; Bunzel, M.; Lachenmeier, D. W. Automated Multicomponent Analysis of Soft Drinks Using 1D ^{1}H and 2D ^{1}H–^{1}H J-resolved NMR Spectroscopy. *Food Anal. Methods* 2017, 10, 827–836. DOI: 10.1007/s12161-016-0643-y.

Summary

This white paper has set out the full scope of what quantitative proton nuclear magnetic resonance spectroscopy can be made to report on in beer, and how each observation is converted into a number that a brewer can act on. The argument opened with the primary-ratio character of the measurement: because integrated signal area is proportional to the number of resonant nuclei with a constant that carries no molecular parameter, a single weighed reference compound calibrates every analyte in the spectrum at once, the response is linear over the entire observable range, and a compound is quantifiable as soon as its structure is recognized. Against that stands an honest sensitivity floor of roughly five to ten milligrams per liter for one-dimensional work, which places the vicinal diketones, the sulfur volatiles, the trace esters, and the individual iso-α-acids of finished beer outside the reach of the technique and leaves them to gas chromatography with mass-selective or sulfur-selective detection.

The Process NMR Associates method was described in complete detail, including the dual-aliquot design in which a 175 µL native sample carries the volatile inventory while a lyophilized 1000 µL aliquot carries the non-volatile inventory, and including a consequence of the standard mass that had not previously been recognized: ten milligrams of maleic acid is 133 millimolar in the analytical solution and fixes every preparation near pH 1.5, so that the organic acids are observed at their fully protonated limits and at style-independent positions. The stronger justification for that division was developed here for the first time: lyophilization removes the water and most of the ethanol, and with them the residual water line that renders the anomeric region unusable and the ethanol carbon-13 satellite at δ 1.39 that is three times the size of the lactate signal it sits upon. The two quantitation expressions were reduced to a single scalar response factor per analyte, tabulated for the full panel, and verified against an independent first-principles calculation that returned 4.98 % v/v for a beer declared at 5.0 %. A relaxation analysis quantified the dominant uncorrected systematic error in the protocol, showing that the interaction of the 60° flip angle, the 15 s recycle period, and the spin–lattice relaxation of the maleic acid standard produces a multiplicative bias of the order of a few percent common to all analytes, with slowly relaxing species such as formate under-reported by considerably more, and an inversion-recovery survey was identified as the single highest-value experiment available for improving the accuracy of the method.

The spectrum was then read region by region, with tabulated chemical shifts, multiplicities, coupling constants, proton counts, and response factors supplied in a form suitable for direct transcription into a laboratory integration template, and with the pH dependence of the organic acid resonances treated both as an integration hazard and as an independent route to concentration. Results across a survey of twenty-three to thirty commercial beers were presented for alcoholic strength against label declaration, for the organic acid distribution and its forensic reading, for the free amino acid pool and the proline partition that reports on nitrogen utilization, for the aromatic and Maillard fraction, and for the nutritional bookkeeping that follows arithmetically from the composition and that reproduced a declared forty-one calorie value as 40.1.

A section new to this revision translated the composition into the vocabulary of the brewhouse: through the Balling mass balance, the measured ethanol and dissolved solids return the original extract, the apparent and real extract, the original and final gravities, and the apparent and real degrees of fermentation, worked through to 11.94 °P, 77.1 %, and 63.2 % for a representative lager, together with a wort-side fermentability prediction that replaces the two-day forced-fermentation test and a free-amino-nitrogen analogue computed from the amino acid panel; bitterness, color, and pH were stated plainly to remain outside the technique’s reach. The residual dextrin section formed the core. The anomeric window was dissected into the α-(1→4)

linear and branch-proximal envelopes, the α-(1→6) branch-point signal, the reducing-end α and β pair, and the free-glucose anomers; one annotation on the working figure was corrected on chemical grounds; and the four-window integral scheme in routine use was compared point by point against degrees of polymerization determined independently by diffusion-ordered spectroscopy in the published literature and found consistent in ordering and at its high-frequency anchor, while remaining uncalibrated at its branch-proximal end. Closed-form expressions were derived for number-average degree of polymerization, α-(1→6) branch fraction, dextrose equivalent, and a newly proposed branch-proximal fraction, and were carried through numerically for four mash samples and discussed for the commercial survey. Two internal consistency checks were introduced. The α-anomer fraction at the reducing end and at free glucose is fixed by mutarotation equilibrium, and its application detected a systematic bias in the free-glucose determination across all four mash samples and an outright integration fault in one of them, neither of which would have been visible on inspection; a mass-balance closure requiring the residue count to equal the chain count plus the linkage count supplies a second, independent test on the same integrals. The limits of what the present data can support were stated explicitly.

Process case studies followed. The temperature dependence of biological mash acidification was shown to vindicate the traditional 49 °C hold not because it maximizes lactic acid, which it does not, but because it maximizes the lactic-to-acetic ratio while suppressing wild yeast — a conclusion available only because the measurement is untargeted. The sour beer treatment was extended through the phase structure of spontaneous fermentation, in which the enterobacterial, principal, and Pediococcus–Brettanomyces maturation phases each write a distinct metabolite signature; through the redox chemistry that couples mannitol formation from fructose to the lactate-to-acetate balance; and into the barrel, where oxygen ingress through the staves sustains acetic acid bacteria, ethyl lactate accumulates as a slow esterification clock, and wood-derived cellobiose gives the β-glucosidase of Brettanomyces its genuine substrate. The glycerol conversion pathway was set out in full — the coenzyme-B_{12}-dependent dehydration to 3-hydroxypropionaldehyde, the reduction to 1,3-propanediol that regenerates cofactor, the oxidation to 3-hydroxypropionic acid, and the dehydration of the accumulated aldehyde to acrolein that underlies the amertume bitterness defect and the heads contamination of spirits distilled from degraded substrate — with every stable branch product identified in the spectra against a lot-numbered authentic standard. Turbid mashing for a New England India pale ale was shown to raise the intermediate linear dextrin fraction more than threefold and the number-average chain length by roughly half, with the sensory inference explicitly withheld for want of a panel. Preservatives and additives were treated systematically: sorbate and benzoate were quantified at 182 to 688 mg/L across a flavored-malt-beverage survey through reporter signals in otherwise empty spectral windows, negative findings were shown to be equally certifiable, citrate acidulant, propylene glycol carrier, steviol glycosides, and back-sweetening sucrose were read as a formulation logic whose internal consistency the spectrum can test, and sulfite — itself proton-invisible — was shown to betray its presence through the acetaldehyde bisulfite adduct. Diastatic contamination monitored through the decline of the dextrin envelope, non-alcoholic products quantified to 0.01 % v/v ethanol, and hop bitter acid assay against the chromatographic reference were each treated in turn. The hop method comparison was flagged as not yet constituting evidence of agreement between techniques, and the design of the study that would make it so was specified.

The document closes with the design of the spectral library, the preprocessing chain, and the validation discipline required to carry this data set into the chemometric and machine-learning phase for which it is intended, together with a candid statement of what the method does not see and a set of four immediate experimental priorities. Seventy-one CrossRef-verified references anchor the text, and three incorrect

digital object identifiers carried in earlier Process NMR Associates material have been corrected. The paper is delivered as an AI-assisted framework built on the author's own experimental data, awaiting the primary concentration tables, replicate statistics, and additional residual dextrin measurements that will convert it into a complete account.